



UNIVERSITÀ
DEGLI STUDI
DI PADOVA

Sede amministrativa: Università degli Studi di Padova
Dipartimento di Scienze Cardiologiche, Toraciche e Vascolari

SCUOLA DI DOTTORATO DI RICERCA IN SCIENZE MEDICHE,
CLINICHE E SPERIMENTALI
INDIRIZZO "SCIENZE CARDIOVASCOLARI"
25° CICLO

Expression and functional role of Ccdc80 in normal heart and cardiomyopathies

Direttore della Scuola: Ch.mo Prof. Gaetano Thiene

Coordinatore d'indirizzo: Ch.mo Prof. Gaetano Thiene

Supervisore: Ch.ma Prof.ssa Annalisa Angelini

Dottorando: Daniele Iaccarino

Index

1. Summary	page 4
2. Riassunto	page 5
3. Aim of the study	page 7
4. Introduction	page 7
4.1 Cardiomyopathies, definition and classification	page 7
4.2 Dilated cardiomyopathy and heart failure	page 8
4.3 Other cardiomyopathies	page 13
4.4 Ccdc80 gene/protein	page 16
4.5 Ccdc80 and morphogenesis	page 21
4.6 Ccdc80 and tumors	page 22
4.7 Ccdc80 and metabolic regulation	page 25
4.8 Ccdc80 in cardiac and skeletal muscle	page 32
5. Materials and methods	page 36
5.1 Rat model of heart failure	page 36
5.2 Zebrafish	page 37
5.2.1 RNA extraction and purification	page 38
5.2.2 Semi-quantitative PCR analysis	page 40
5.2.3 Morpholino knocking-down	page 41
5.2.4 Whole-Mount In Situ Hybridization (WISH)	page 42

5.2.5 Histological analysis	page 43
5.3 Immunohistochemistry and immunofluorescence	page 45
5.4 Northern Blot	page 46
5.5 Western Blot	page 47
6. Results	page 48
6.1 Functional role in Zebrafish	page 48
6.2 Expression in normal heart	page 56
6.3 Expression in failing heart	page 63
6.4 Skeletal muscle	page 68
7. Discussion	page 71
8. Conclusions	page 77
9. References	page 78
10. Acknowledgments	page 91

1. Summary

Background: The gene Coiled Coil Domain Containing 80 (Cc dc80) is widely expressed in normal human tissues, at particularly high levels in heart, skeletal muscle and adipose tissue. Its role is well defined in tumor suppression, axon path finding, glucose homeostasis, bone marrow stromal cells and adipocyte differentiation. Moreover, it plays a role in embryonic development of lens and muscle, but no clear-cut data are available about the role of Cc dc80 in heart development and in heart disease.

Aims: To define if Cc dc80 is expressed during embryonic development of zebrafish heart and if its functional block causes alterations of heart structure or contractility; to define the expression pattern of Cc dc80 protein in normal heart vs cardiomyopathies in humans (samples taken from patients with dilated cardiomyopathy – DCM) and rodents (samples taken from right ventricle heart failure induced by monocrotaline – MCT).

Results: In zebrafish Cc dc80 is widely expressed in the forming heart, during all the developmental stages; Cc dc80-morphants show defects in the developing heart, with impaired cardiac looping, atrium enlargement, blood stasis and peripheral congestion. These phenotypical alterations, similar to heart failure, are due to a disorder of the late phase of cardiac development, after myocyte differentiation.

In normal human and rats, Cc dc80 mRNA, analyzed by Northern blot technique, showed a higher expression in atria compared to ventricles, while the Cc dc80 protein (108 Kd), analyzed by Western blot, showed similar expression levels in atria and ventricles. Cc dc80 protein showed different expression patterns, in atria and ventricles with a cytoplasmic localization and co-localization with sarcomeric proteins at immunofluorescence analysis.

In pathological samples (DCM and MCT rats) Cc d80 protein showed evident overexpression and different isoforms, related to protein phosphorylation and secreted protein isoform, suggesting a different feature in pathological conditions compared to normal.

Conclusions: Our results demonstrated that Ccdc80 has an indispensable role for correct heart development. In complete developed heart, Ccdc80 showed an adaptive function to stress conditions, such as pressure overload, and in cardiomyopathies showed increased expression and different isoforms.

2. Riassunto

Introduzione: Il gene Coiled Coil Domain Containing 80 (Ccdc80) è ampiamente espresso in tessuti umani normali, a livelli particolarmente elevati nel cuore, muscolo scheletrico e tessuto adiposo. E' ben definito il suo ruolo come oncosoppressore, nella innervazione degli assoni, nella omeostasi glicemica, e nel differenziamento delle cellule stromali del midollo osseo e degli adipociti. Inoltre, svolge un ruolo nello sviluppo embrionale muscolare e della lente del cristallino, ma non sono disponibili dati sul ruolo di Ccdc80 nello sviluppo del cuore e nelle malattie cardiache.

Obiettivi : Definire se Ccdc80 è espresso durante lo sviluppo embrionale del cuore zebrafish e se il suo blocco funzionale provoca alterazioni della struttura o della contrattilità; definire il pattern di espressione della proteina Ccdc80 nel cuore normale vs cardiomiopatie nell'uomo (campioni prelevati da pazienti con cardiomiopatia dilatativa - DCM) e roditori (campioni prelevati da ratti con insufficienza ventricolare destra indotta da monocrotalina - MCT).

Risultati: In zebrafish Ccdc80 è ampiamente espresso nel cuore in formazione, durante tutte le fasi di sviluppo; i morfanti per Ccdc80 mostrano difetti nello sviluppo cardiaco, con alterato looping, dilatazione atriale, stasi ematica e congestione periferica. Queste alterazioni fenotipiche, simili ad uno scompenso cardiaco, sono dovuti ad un disturbo della fase tardiva dello sviluppo cardiaco, dopo che la differenziazione dei miociti è già stata completata.

Nei campioni normali di uomo e ratto, l'RNA messaggero di Ccdc80, analizzato con tecnica di Northern blot, è risultato maggiormente espresso negli atri rispetto ai ventricoli, il mentre

l'espressione della proteina Ccdc80 (108 Kd), analizzata con tecnica Western blot, è risultata simile negli atri e nei ventricoli. La proteina Ccdc80 ha mostrato pattern di espressione diversi in atri e ventricoli, con localizzazione citoplasmatica e chiara co-localizzazione con le proteine sarcomeriche all'immunofluorescenza. Nei campioni patologici (DCM ed MCT ratti) la proteina Ccd80 ha mostrato una netta iper-espressione sia negli atri che nei ventricoli, e la presenza di diverse isoforme, suggerendo diverse funzioni in condizioni patologiche rispetto al normale .

Conclusioni: I nostri risultati hanno dimostrato che Ccdc80 ha un ruolo indispensabile nello sviluppo cardiaco. Nel cuore adulto, Ccdc80 si manifesta con diverse isoforme e maggiore espressione, rivestendo una funzione adattativa in condizioni di stress, come il sovraccarico di pressione, e nelle cardiomiopatie.

3. Aim of the study

Aims of our investigation are:

1. Define the functional role of Ccdc80 in embryonic development of zebrafish heart, in particular evaluate if the gene is expressed during heart formation and if its functional block causes alterations of heart structure or contractility;
2. Define the expression pattern of Ccdc80 protein in normal heart and muscle of rodents and humans;
3. Define the expression pattern of Ccdc80 protein in cardiomyopathies both in rodents and humans.

4. Introduction

4.1 Cardiomyopathies, definition and classification

Cardiomyopathies are a broad spectrum of diseases that affect the muscle or myocardium of the heart. The official definition of cardiomyopathy by the American Heart Association (AHA) in 2006 is as: “Cardiomyopathies are a heterogeneous group of diseases of the myocardium associated with mechanical and/or electrical dysfunction that usually (but not invariably) exhibit inappropriate ventricular hypertrophy or dilatation and are due to a variety of causes that frequently are genetic. Cardiomyopathies either are confined to the heart or are part of generalized systemic disorders, which may lead to cardiovascular death or progressive heart failure-related disability [1].” Otherwise, the working group of the European Society of Cardiology (ESC) in 2008 defined cardiomyopathy as: “A myocardial disorder in which the heart muscle is structurally and functionally abnormal, in the absence of coronary artery disease, hypertension, valvular disease and congenital heart disease sufficient to cause the observed myocardial abnormality [2].” A complete classification based on the above AHA

definition divides cardiomyopathies into (1) primary cardiomyopathies, which affect the heart alone, and (2) secondary cardiomyopathies, which are the result of a systemic illness affecting many other parts of the body. These are then further broken down into subgroups within these two broad categories incorporating new genetic and molecular insights (Figure 1). Historically, most cardiomyopathies have been defined by the absence of particular features or associated disorders, but it is increasingly apparent that many patients with unexplained heart muscle disease in fact have rare, but well described diseases that can involve the myocardium.

Primary cardiomyopathies	Secondary cardiomyopathies
Genetic (hypertrophic cardiomyopathy; conduction abnormalities: prolonged QT syndrome; Brugada syndrome)	Infiltrative (amyloidosis and Gaucher disease)
Mixed (dilated cardiomyopathy; restrictive cardiomyopathy)	Storage (haemochromatosis and Fabry's disease)
Acquired (inflammatory myocarditis, peripartum, stress cardiomyopathy—"broken heart syndrome" or tako-tsubo)	Toxicity (drugs, alcohol, heavy metals, and chemicals/chemotherapy)
	Inflammatory (sarcoidosis) endocrine (diabetes mellitus; thyroid disorders; hyperparathyroidism), cardiofacial (Noonan syndrome, lentiginosis) neuromuscular/neurological, nutritional deficiencies, and autoimmune and collagen disorders

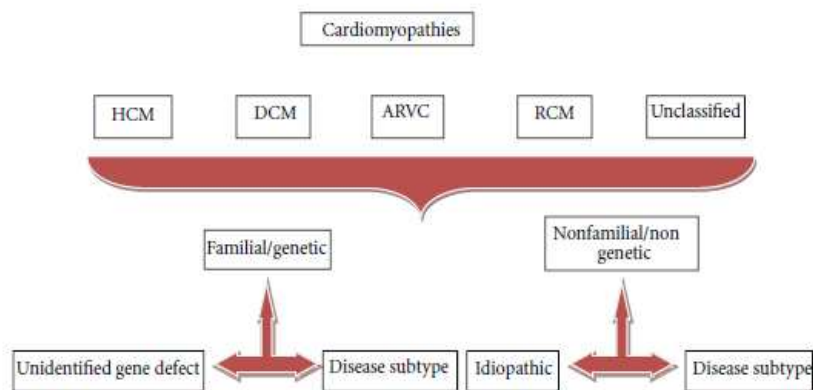


Figure 1
Summary of AHA 2006 and ESC 2008 Classification. DCM: dilated cardiomyopathy; HCM: hypertrophic cardiomyopathy; ARVC: arrhythmogenic right ventricular cardiomyopathy; RCM: restrictive cardiomyopathy.

4.2 Dilated cardiomyopathy and heart failure

Dilated Cardiomyopathy (DCM) is a common cause of congestive cardiac failure and is defined by the presence of left ventricular dilatation and systolic dysfunction in absence of coronary artery disease or other causes such as hypertension or valvular pathology [2]. The

right ventricle may be involved but is not necessary for the diagnosis. The exact prevalence of DCM in the general population is unknown, but it clearly varies with age and geography; [3] DCM has an incidence of more than 36.5 cases per 100,000 persons and it accounts for nearly 50,000 hospitalizations and 10,000 deaths each year in the United States. For now, dilated cardiomyopathy remains the primary indication for heart transplantation in the Western countries [4]. As aforementioned, DCM is one of the most common cause of Heart Failure (HF), as well as ischemic heart disease, valvular heart disease, viral myocarditis. The onset and progression of HF is closely associated with several molecular and cellular alterations [5], including abnormal calcium handling, neurohumoral activation, increased oxidative stress, and abnormal cytokine signalling. The left ventricle dysfunction and low cardiac output lead to compensatory activation of the sympathetic nervous system and the renin–angiotensin and vasopressin system. However, these compensatory mechanisms throughout years can worsen the cardiac dysfunction and exacerbate the pathophysiology of HF. This is the major reason that medications for HF include angiotensin-converting enzyme inhibitors and β -blockers.

Drug treatment has advanced markedly over the past 20 years and the employ of cardiac implantable defibrillators and electric resynchronization therapy has improved the prognosis of patients with HF. However, despite an optimal cardiovascular treatment, chronic HF is still a progressive disorder with high morbidity and mortality, suggesting that important pathogenic mechanisms remain unmodified by the present treatment modalities as immune activation and persistent inflammation.

Beside humoral and cell-mediated immune responses, familial forms have been implicated in idiopathic dilated cardiomyopathy.

Indeed, around 30–50% of cases have a familial component [6], and more than 30 genes have been identified, to date, that cause DCM. Most are inherited in an autosomal dominant fashion although some can be autosomal recessive, X-linked or mitochondrial. The actual frequency of familial DCM is probably underestimated.

Peripartum cardiomyopathy is a specific subgroup of dilated cardiomyopathy defined as the development of heart failure with evidence of left ventricular dysfunction, within the last month of pregnancy to within 5 months of delivery, without other identifiable cause or underlying cardiac condition [7, 8]. Groups of women presenting during the earlier stages of pregnancy have been identified and with similar epidemiological characteristics and with similar disease progression and outcomes. The earlier time frame of presentation has been postulated to represent part of a spectrum of peripartum cardiomyopathy [9].

Peripartum cardiomyopathy affects approximately 1 : 4000 women across the US and Europe each year, with higher rates noted across the African continent [10]. The aetiology of peripartum cardiomyopathy has been unclear for many years; however, new research into an inflammatory or immunological basis, and the role of prolactin in the development of the disease has shed new light on the causative mechanisms that may be behind this condition. Familial clustering of peripartum cardiomyopathy has been identified; however, on screening other family members and with further genetic testing, this clustering may represent a subset of undiagnosed familial dilated cardiomyopathy. TNF alpha, and other proinflammatory cytokines have been shown to be elevated in a large number of peripartum cardiomyopathy cases and similarly some studies have suggested a role for autoantibodies against normal human cardiac tissues proteins and further research is required in this area [11]. Higher levels of CRP, Fas/Apo-1, TNF alpha and IL-6 have been demonstrated in some population groups with peripartum cardiomyopathy and have implicated a role for inflammatory mediator in the disease process [12, 13].

Mutations in relevant genes can cause DCM. [14-20] (Figure 2). It is estimated that myofibrillar protein mutations account for roughly 10% of familial DCM cases [21] but a recent finding suggests that 25% of idiopathic DCM cases are due to sarcomeric gene mutations [22]. Sarcomere proteins include heavy and light chain myosin and myosin binding proteins, cardiac actin, α -tropomyosin, troponin complexes, and others. Common sarcomere

gene mutations identified in DCM as a cause of familial and sporadic disease include β -myosin heavy chain (*MYH7*) missense mutations. Other disease-causal gene mutations include Troponin T (*TNNT2*) missense or deletion mutations; Troponin C (*TNNC1*) missense mutations [23-25]; Troponin I (*TNNI3*) missense mutations [26, 27]; α -tropomyosin (*TPMI*) missense mutations [28-30]; and cardiac actin (*ACTC*) missense mutations [31]. Concerning mutations, the *MYH7* gene is the most frequently mutated in the familial DCM population (approximately 10% of cases), although disease onset is delayed, with incomplete disease penetrance, compared with that for mutations of *TNNT2* and *TNNC1* genes. In addition to gene mutations that affect sarcomeric proteins, gene mutations of structural proteins such as the intermediate filament proteins and the dystrophin-associated glycoprotein complex are known as a cause of DCM. Intermediate filaments are important components of the cytoskeletal system that stabilize organelles by linking the Z-disc to the sarcolemma. Desmin (*des*) is a component of type III intermediate filaments, and missense mutation can cause DCM [32]. In addition, many missense and deletion mutations have been shown to cause myofibrillar myopathy (MFM; also called desmin-related myopathy) [33-34]. The MFM caused by desmin gene mutations, such as a putative 7-amino acid deletion and missense mutations, are heterogeneous myopathies characterized by abnormal intrasarcoplasmic desmin accumulation. Concerning sarcomere stability and force transmission to the extracellular matrix, the importance of protein interactions among dystrophin (*DMD*), actin (*ACTC1*), and the dystrophin-associated glycoprotein complex composed of α - and β -dystroglycans (*DAG1*), γ - and δ -sarcoglycans (*SGCG* and *SGCD*), caveolin-3 (*CAV3*), and dystrobrevin (*DTNA*) is well recognized [35-36]. Muscular dystrophy with associated DCM and heart failure is caused by many kinds of dystrophin mutation, such as deletion of the first muscle exon and the muscle-promoter region of the *DMD* gene, a splice donor site mutation in the first exon, or mutations in intron regions of the *DMD* gene that inactivate the universally conserved 5-prime splice site consensus sequence of the first intron [37-38].

Mutation of a dystrophin-associated protein, such as an S151A substitution in the SGCD gene, can also cause familial and sporadic dilated cardiomyopathy [39] Calcium regulating proteins and disturbed ion channel function have been identified as causative of DCM [40-41]. Phospholamban (*PLN*) is known as a regulator of calcium uptake into the sarcoplasmic reticulum (SR) *via* inhibition of SR Ca²⁺-ATPase (SERCA2) in cardiomyocytes. The *PLN* R9C mutation and arginine 14 deletion mutation (R14Del) in *PLN* lead to disease through cardiomyocyte calcium dysregulation. It is thought that *PLN* R9C protein can trap protein kinase A, which blocks PKA-mediated phosphorylation of wild-type *PLN*, and *PLN* R14Del protein can inhibit SR ATPase, despite phosphorylation by protein kinase A.

Sarcomere proteins
β-Myosin heavy chain (<i>MYH7</i>)
Troponin T (<i>TNNT2</i>)
Troponin C (<i>TNNC1</i>)
α-Tropomyosin (<i>TPM1</i>)
Cardiac actin (<i>ACTC</i>)
Structural proteins
Desmin (<i>des</i>)
Cypher/Z-band alternatively spliced PDZ-motif containing protein (<i>ZASP</i>) (<i>LDB3</i>)
Cystein- and glycin-rich protein 3 (also called muscle LIM protein) (<i>CSRP3</i>)
Titin (<i>TTN</i>)
Dystrophin (<i>DMD</i>)
α- and β-Dystroglycans (<i>DAG1</i>)
γ-Sarcoglycans (<i>SGCG</i>)
δ-Sarcoglycans (<i>SGCD</i>)
Caveolin-3 (<i>CAV3</i>)
Dystrobrevin (<i>DTNA</i>)
Fukutin (<i>FKTN</i>)
Fukutin-related protein (<i>FKRP</i>)
Nuclear envelope proteins
Lamin A/C (<i>LMNA</i>)
Calcium signaling proteins
Phospholamban (<i>PLN</i>)
Cardiac sodium channel (<i>SCN5A</i>)

Protein names (gene names) are shown.

Figure 2

Summary of Causal Genes of Dilated Cardiomyopathy (DCM)

4.3 Other cardiomyopathies

Hypertrophic cardiomyopathy (HCM) has been defined by the presence of myocardial hypertrophy incongruent with the haemodynamic stress required for the degree of hypertrophy and the exclusion of infiltrative diseases such as amyloidosis and storage diseases [42-43]. In the absence of hypertension and valve disease, left ventricular hypertrophy (LVH) occurs in approximately 1 : 500 of the general population [44]. In day-to-day clinical practice it is very difficult to differentiate between pathologies using minimally invasive techniques such as cardiac echo or cardiac magnetic resonance imaging (MRI). Histological demonstration (on myocardial biopsy) of myocyte hypertrophy in the definition of HCM is unreliable due to the patchy nature of the abnormality within the myocardium. The position statement from the ESC [2] contained the following “the presence of intramyocardial storage material is not an exclusion criterion for HCM. Instead, hypertrophic cardiomyopathies are simply defined by the presence of increased ventricular wall thickness or mass in the absence of loading conditions (hypertension, valve disease) sufficient to cause the observed abnormality.” The potential inaccuracy in not fully excluding infiltrative disease or demonstrating myocyte hypertrophy on biopsy is justified by leading to increased emphasis in the clinical picture and a promise of better minimally invasive diagnostic strategies. If the HCM is familial, then it is usually transmitted in an autosomal dominant pattern of inheritance caused by mutations within genes that encode for various proteins of the cardiac sarcomere (Figure 3). Currently, there are over 500 mutations in 13 genes that have been identified that cause HCM and 50% of these are familial [45-48]. Pathologically, left ventricular (LV) cavity size is normally reduced and this can progress to LV dilatation and heart failure, albeit in a minority of patients. There are many patterns of hypertrophy and all are consistent with a diagnosis of HCM but concentric hypertrophy is more suggestive of a systemic cause such as glycogen storage disease. Moreover, mutations in the genes encoding

for cardiac troponins can be associated with mild phenotypes but, conversely, a high incidence of cardiac death [49].

Gene	Protein	Function	Reference
β -MHC	β -Myosin heavy chain	Sarcomere protein	[5]
α -MHC	α -Myosin heavy chain	Sarcomere protein	[6, 7]
cMYBPC	Cardiac myosin-binding protein C	Sarcomere protein	[8, 9]
cTnI	Cardiac troponin I	Sarcomere protein	[10]
cTnT	Cardiac troponin T	Sarcomere protein	[11]
cTnC	Cardiac troponin C	Sarcomere protein	[12]
α -TM	α -Tropomyosin	Sarcomere protein	[11]
MLC-1	Myosin essential light chain	Sarcomere protein	[13]
MLC-2	Myosin regulatory light chain	Sarcomere protein	[7]
ACTC	Actin	Sarcomere protein	[14]
TTN	Titin	Sarcomere protein	[15, 16]
Metabolic phenocopies			
PRKAG2	AMP kinase		[17]
LAMP2	Lysosome membrane protein		[18]

Figure 3
Genes associated with hypertrophic cardiomyopathy.

Restrictive cardiomyopathies have a diverse range of aetiology; however, all are recognised as having distinct haemodynamic features separating them from other forms of cardiomyopathy.

Restrictive cardiomyopathies in general are defined as showing normal ventricular size (nondilated and non-hypertrophied) with impaired haemodynamic function, elevated filling pressures, and diastolic dysfunction, and in most cases normal systolic function [50-51].

Presentation can include symptoms of both right and left sided failure; decreased exercise tolerance, dyspnoea, peripheral oedema, and palpitations are the most common

symptoms. Due to the contrast in both aetiology and treatment options and the similarities in haemodynamics, it is important to recognise the difference between restrictive

cardiomyopathy and constrictive pericarditis. Usually, this is defined with a variety of investigatory modalities with both haemodynamic and morphological assessment and includes echocardiography and pericardial imaging [52]. Various aetiologies have been identified as causing restrictive cardiomyopathy and range from idiopathic (primary)

restrictive cardiomyopathy, to systemic conditions including infiltrative, noninfiltrative, and storage disorders, as well as endomyocardial disorders, various medications, and iatrogenic causes [53]. Familial restrictive cardiomyopathies are usually inherited in an autosomal

dominant fashion, the genetic basis of which remains to be identified, and are noted to be relatively rare [54]. Hereditary conditions known to cause a restrictive cardiomyopathy include haemochromatosis, glycogen storage diseases, Fabry's disease, Gaucher's disease, and Hurler syndrome.

Arrhythmogenic Right Ventricular Dysplasia (ARVD) is a heart muscle disease which, pathologically, consists of progressive fibrofatty replacement of the right ventricular musculature which may or may not involve the left ventricle. It predisposes towards malignant arrhythmias originating from the right ventricle and is a major cause of sudden death in young athletes [55]. Major and minor criteria of ARVD diagnosis have been compiled, and the diagnosis can be made if there are two major, one major and one minor or four minor criteria present [56]. Diagnosis and risk stratification are extremely important as there are proven life saving interventions which are available to the clinician [57].

It is a familial disease in around 50% of cases and is usually transmitted in an autosomal dominant fashion [58]. The first gene, ARVD1, coding for a desmosome protein, was discovered in 1994 [59], and since then multiple causative genes relating to the desmosome have been discovered, indicating that ARVD is a disease of the desmosome (Figure 4) [60-66].

Locus	Gene	Protein	Function	References
ARVD1	TGFB3	Transforming growth factor β 3	Cell signalling	[42, 43]
ARVD2	RYR2	Ryanodine receptor 2	Sarcoplasmic reticulum calcium channel	[44, 45]
ARVD3	Not known	[46]		
ARVD4	Not known	[47]		
ARVD5	LAMR1	Extracellular matrix glycoprotein	Cell signalling, adhesion, and migration	[48, 49]
ARVD6	PTPLA	Protein-tyrosine phosphatase-like member A	Fatty acid synthesis	[50, 51]
ARVD7	DES; ZASP	Desmosomal protein; PDZ domain protein	Dystrophin-associated glycoprotein complex, and Cytoskeletal assembly	[52, 53]
ARVD8	DSP	Desmoplakin	Anchoring of intermediate filaments	[53, 54]
ARVD9	PKP2	Plakophilin 2	Cell adhesion	[55, 56]
ARVD10	DSG2	Desmoglein 2	Calcium-binding transmembrane glycoprotein	[57, 58]
ARVD11	DSC2	Desmocollin 2	Calcium-dependent glycoprotein	[59, 60]

Figure 4
Genes associated with ARVD

4.4 Ccdc80 gene/protein

Ccdc80 (also known as CL2, DRO1, equarin, SSG1, and URB) was initially identified as an estrogen-induced gene in rat uterus and mammary gland [67] and in a rat model of thyroid carcinogenesis. Chicken [68], mouse [69], and human [70] orthologs have also been identified, but little is known about the function of Ccdc80. Ccdc80 mRNA has been found to be up-regulated in brown adipose tissue from old but not young bombesin receptor subtype-3 (BRS-3)-deficient mice. Moreover, Ccdc80 was found to be strongly upregulated in PC CL3 epithelial thyroid cells immortalized by the adenovirus E1A gene (PC E1A cells) [71-72] (Figure 5).

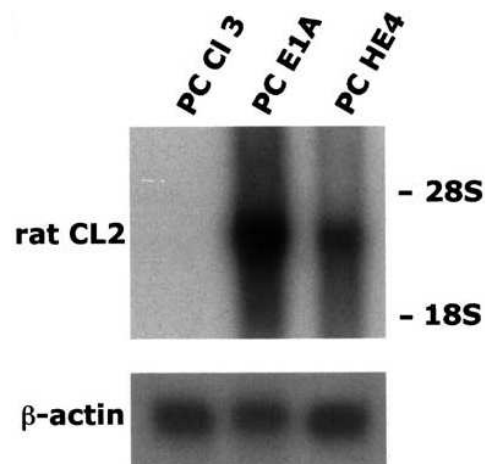


Figure 5

Analysis of the expression of the Ccdc80 gene in PC Cl 3, PC E1A and PC HE4 cells

10 micro-g of total RNA for each cell line was size-fractionated on a 1.2% denaturing formaldehyde agarose gel, blotted onto Nylon filters hybond-N and probed with a 1.1 kb EcoRI/HindIII fragment from the pGem3ZCcdc80 vector, b-actin was used as control for uniform RNA loading [71].

Ccdc80 cDNA analysis showed a single long Open Reading Frame (ORF), which has the potential to code for a 949 amino-acid protein, having a molecular mass of 107.7 kDa [71] (Figure 6).

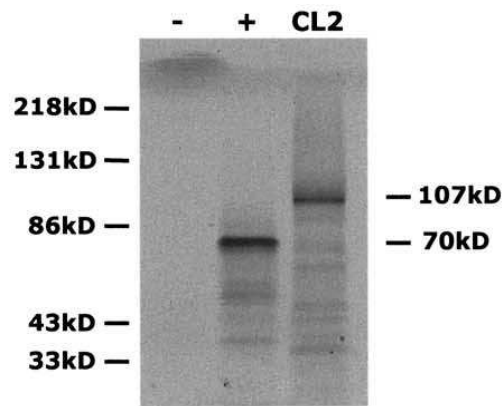


Figure 6

***In vitro* transcription–translation of the rat Ccdc80 protein**

In vitro transcription–translation was performed in the presence of [³⁵S]methionine using the TNT Promega kit. A total of 3 μ l of the reaction was loaded on a 10% SDS–PAGE and autoradiographed. As expected, the translation product migrates around 107 kDa. The construct pcDNA3–RET/PTC3 (lane +), encoding an unrelated protein of about 70 kDa, was used as positive control for the transcription–translation reaction [71].

The highly basic (pI 9.6) protein has multiple potential nuclear localization signals at amino-acid positions 420, 545, 549, 569, 573 and 583. Furthermore, it has a potential signal peptide (SP) ending at amino-acid 24. Taken together, these results suggest that the Ccdc80 gene encodes either nuclear or secreted proteins. This was confirmed by an *in vitro* experiment, in which COS7 cells were transfected with an expression vector containing the entire ORF of Ccdc80 fused in-frame with the EGFP (Enhanced Green Fluorescent Protein) gene. Expression of EGFP–Ccdc80 resulted in two different sub-cellular localization patterns: in most cells the fluorescent signal was juxtannuclear, indicating a Golgian localization, while in the 5–10% of them it was nucleo-cytoplasmic (Figure 7).

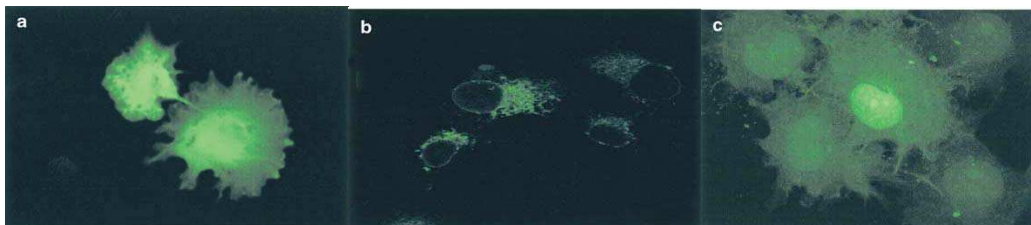


Figure 7

Cellular localization of EGFP–Ccdc80 in COS7 cells

COS7 cells were transiently transfected and monitored for EGFP–Ccdc80 expression 48 h post-transfection. Fluorescence was examined with a Zeiss LSM410 scanning confocal microscope. Panel (a) COS7 cells transfected with the EGFP control vector. Panel (b) Polar perinuclear accumulation of the EGFP–Ccdc80 signal, suggestive of a Golgian localization. Panel (c) The signal is spread throughout the cytoplasm, with some nuclear–nucleolar staining, heterogeneous in intensity depending on the cell [71].

Searching for common motifs in the Ccdc80-encoded protein, a cluster of subsequences was identified, which occur three times along the protein and identify three domains (D1, D2, D3), which show an overall identity of 27% and a similarity of 48% (Figure 8). The BLAST screening with the Ccdc80 domains as probes identified three proteins sharing 27% identity and 46% similarity with them. These proteins are encoded by the rat *drs* (down-regulated by *v-src*) gene [73], its human homologue *ETX1* (or *SRPX*, sushi-repeat containing protein chromosome X) gene [74], and the human *SRPUL* (sushi-repeat protein up-regulated in leukemia) gene [75].

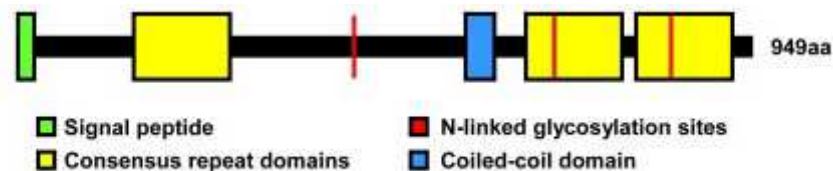


Figure 8
Schematic representation of mouse Ccdc80 protein

Screening of human sequences in the GenBank database with the rat Ccdc80 cDNA revealed a sequence containing the complete ORF of the human Ccdc80 gene, which is located between chromosomal bands 3q 13.2-3q 13.3 and in a tel-5'-3'-cen orientation. The predicted human Ccdc80 amino acid sequence was highly conserved (82% identity and 86% similarity) with respect to that of the rat, indicating an important role of Ccdc80 in higher eukaryotes. Northern blot analysis of poly(A)⁺ mRNA from adult human tissues showed that Ccdc80 is almost ubiquitously expressed in two alternative forms of the transcript, 4.2 and 3.8 kb, suggesting its role in the functioning of many organs. The highest expression was observed in heart, the lowest in brain, liver, spinal cord, and lymph node, while it was not detectable in bone marrow and peripheral blood leucocytes (Figure 9).

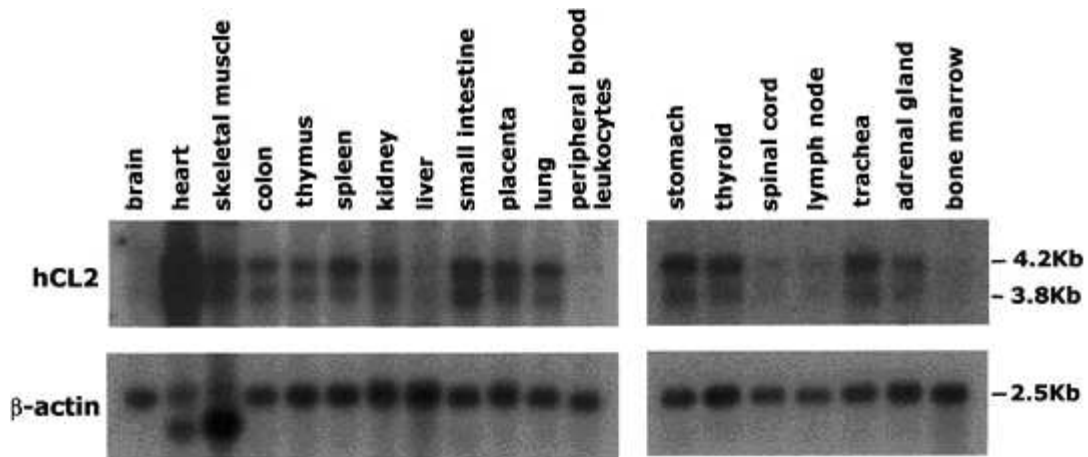


Figure 9

Expression pattern of Ccdc80 mRNA in human tissues

Human multiple tissue Northern blot was hybridized with a 1.1 kb EcoRV/HindIII fragment from the pGem3ZCcdc80 vector. Autoradiograms were exposed for 4 days [71].

During mouse embryonic development, northern blot results showed Ccdc80/URB expression starting from the lowest level at 7 days *post coitum* (dpc) up to the highest level at 17 dpc [71]. Liu *et al.* [76], described an abundant expression in rib, sternal cartilage, heart, kidney, and leg muscles in both embryos and newborn mice. Moreover, the authors performed an ISH analysis on developing embryos, detecting evident expression of the *URB* transcript in the developing cartilage of the developing skeleton until 14 dpc, and a bare expression in a ventricular zone of the central nervous system. In the same work, an immunohistochemical analysis at 17 dpc revealed the presence of the *URB* protein in the extracellular matrix of hypertrophic chondrocytes. This suggests for *URB* a role during embryogenesis, in particular in the development of skeleton. Liu *et al.*, further investigated the expression of *URB* gene in human differentiating bone marrow stromal cells (BMSC), which are a heterogeneous stem-cell-like population residing in the bone marrow cavity, which can differentiate in multiple mesenchymal lineages, such as chondrocytes, osteoblasts, and adipocytes. In this case, *URB* expression was strongly downregulated during *in vitro* osteoblastic differentiation.

Three human proteins, SRPX, SRPX2 and Ccdc80, possess a conserved region of similarity with repeated domains, and are all involved in tumor suppression and progression. Bommer *et al.* named these repeated regions as DUDES (DRO1-URB-DRS-Equarin-SRPUL) [70], but

were identified many prokaryotic homologs: so was decided to rename the domain to P-DUDES (Prokaryotes-DUDES) [77].

The vertebrate P-DUDES proteins are multidomain, possessing one (SRPX and SRPX2) or three (Ccdc80) P-DUDES domains (Figure 10). The similarity of the C-terminal regions of SRPX and SRPX2 proteins, referred to herein as P-DUDES domain, to the three repeat regions in Ccdc80 was noticed early [67, 68]. The three genes appear to be conserved in all vertebrates for which full genome information is available, although in fishes (e.g. *Danio rerio*, *Tetraodon nigroviridis*) there are three distinct paralogues of the Ccdc80 gene.

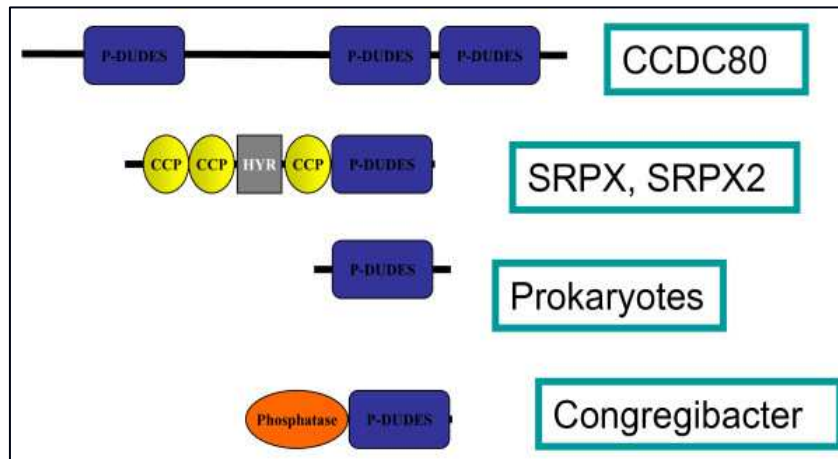


Figure 10
Diagram showing domain composition of representative P-DUDES proteins

The similarities of vertebrate P-DUDES domains suggest that the common ancestor of vertebrates had a duplicated SRPX-like gene and that the common ancestor of vertebrates had at least one Ccdc80-like gene. P-DUDES domains appear to be absent from nonvertebrate chordates, and all other metazoans. The sequence similarity of P-DUDES to peroxiredoxins and to bacterial comigratory proteins, in particular, may reflect only the general fold similarity because the cysteine residue, important for peroxiredoxin function, is not conserved in the P-DUDES domain.

4.5 Ccdc80 and morphogenesis

Another ortholog of the Ccdc80 gene, named Equarin [68], was found to be involved in the morphogenesis of the chicken lens (Figure 11). Two splicing variants (4.2 kb Equarin-L and 3.9 kb Equarin-S) of the gene were identified and they were demonstrated to be expressed in the isthmus, in the 4th and 6th rhombomers, and in the anterior pore of the neural tube beside the lens.

The ectopic injection of the transcripts in *Xenopus* embryos was found to impair normal retinal development. This evidence reveals that Equarin has a broader role during eye development. The same study also confirmed, by immunoblotting analysis, the secreted nature of the encoded protein, which is modified, cleaved, and secreted after translation.

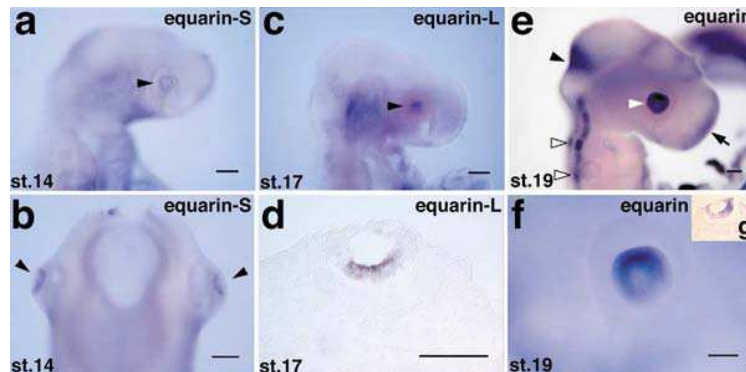


Figure 11

Localization of equarin-S and equarin-L mRNAs during early lens development

- (a) Equarin-S is first detected in the lens placode at stage 14 (arrowheads in a and b). (b) Dorsal view of (a). (c) Equarin-L is first detected in the lens vesicle at stage 17 (arrowhead). (d) Coronal section of the eye at stage 17 (proximal is downwards, dorsal towards the right). Note that equarin-L is localized on the proximal side of the lens vesicle. (e) Lateral view of stage 19 embryo. The distributions of equarin-S and equarin-L transcripts are identical. Note that equarin transcripts are strongly expressed in the lens (white arrowhead) with a high-dorsal-to-low-ventral gradient (e,f). Equarin transcripts are also expressed in the isthmus (arrowhead), the rhombomeres (particularly strongly at r4 and r6; open arrowhead), and the anterior pore of the neural tube (arrow). (f) High magnification of the eye shown in (e). (g) Coronal section of the eye in (e) with the same orientation as (d). Scale bars: 50 μ m [68].

In another study [78], the zebrafish homologues Ccdc80 and Ccdc80-like1 proteins (Ccdc80-11) are showed to be expressed in nervous and non-nervous tissues, in particular in territories correlated with axonal migration. Loss of Ccdc80 impaired somitogenesis and loss of Ccdc80-11 in zebrafish embryos induced motility issues suggesting that Ccdc80-11 is involved

in axon guidance of primary and secondary motoneurons populations. In particular, *Ccdc80-11* has a differential role as regards the development of ventral and dorsal motoneurons, and the axonal migration defects are similar to the phenotype of several mutants with altered Hedgehog activity. Indeed, it was reported that *Ccdc80-11* expression is positively regulated by the Hedgehog pathway in adaxial cells and muscle pioneers [79]. These findings strongly indicate *Ccdc80-11* as a down-stream effector of the Hedgehog pathway.

4.6 *Ccdc80* and tumors

In recent years, more reports on P-DUDES proteins appeared, bringing the attention to differential expression of *SRPX*, *SRPX2*, and *Ccdc80* genes in various developmental processes and in various tumors. In general, *SRPX2* was reported as overexpressed in cancer while *SRPX* and *Ccdc80* were identified as downregulated in malignant conditions [70]. The two latter genes were described as tumor suppressors, and some relevant tumor suppression mechanisms were proposed. The P-DUDES gene with links to cancer most broadly documented is *SRPX*. It was found to be downregulated in malignant pulmonary neuroendocrine tumors [80] whereas its downregulation was correlated with the malignancy of the tumor (most downregulation observed in tumors is related to shortest survival time). Of note, 30% of *SRPX* knock-out mice developed various tumors: lymphoma, lung cancer, hepatoma, sarcoma [81], while no tumors appeared in the control wild-type mice. The proposed mechanism of tumor suppression by *SRPX* is induction of apoptosis. Ectopic expression of the *SRPX* protein induced apoptosis in human cancer cell lines. Both the P-DUDES and the sushi repeat regions were necessary for apoptosis induction, and *SRPX* activated caspases-12, -9, and caspase-3 [82]. Reintroduction of *SRPX* into lung cancer cell line from *SRPX* knock-out mice led to the suppression of tumor formation, accompanied by enhanced apoptosis [81].

SRPX-mediated apoptosis was correlated with the suppression of tumor formation [81]. However, the tumor suppression mechanism mediated by SRPX is more complicated than solely that of apoptosis induction serum, as studied in SRPX knock-out mouse-derived fibroblast cultures [83]. Thus, P-DUDES, since a recent report shows that this gene is involved in the maturation process of autophagy induced by low proteins may mediate both apoptosis and autophagy which suggests for its broader function. In a manner somewhat reminiscent of SRPX, *Ccdc80* was found to suppress anchorage independent growth and sensitize cells to anoikis and CD95-induced apoptosis. Interestingly, *Ccdc80* protein is localised to endothelial cells of the vasculature of the tumors [67] which may suggest a role in angiogenesis for *Ccdc80*. Of implication to a role in cancer is the observation that mouse *Ccdc80* is involved in assembly of extracellular matrix and mediates cell adhesiveness [84].

Confirming its possible role in regulation of tumor growth, a RT-PCR analysis showed that *Ccdc80* expression was clearly detectable in normal human thyroid tissue while strongly down-regulated or absent in both human thyroid carcinoma cell lines and tumors [71]. Moreover, Bommer *et al.* [70] demonstrated that DRO1 (down-regulated by oncogene 1, the way they named human *Ccdc80*) gene is extremely downregulated in colon and pancreatic cancer cell lines, as well as in most colorectal cancer specimens with respect to the corresponding non tumor cell lines and tissues. Similar evidence have been obtained on liver specimens from patients affected by hepatocellular carcinoma (HCC), which showed a down-regulation of the gene in 80% of HCCs when compared to their surrounding cirrhotic tissue.

Furthermore, human *Ccdc80* ectopic expression in tumor cell lines, lacking endogenous *Ccdc80* expression, impaired their growth capabilities, making cancer cells susceptible to apoptotic stimuli [70].

Another study [85] confirms the *Ccdc80* down-regulation in thyroid carcinomas, supporting the concept that CL2/*Ccdc80* plays a role in human thyroid carcinogenesis by mediating the control of cell growth, invasion, and apoptosis. The reduction of CL2/*Ccdc80*mRNA was

greatest in the follicular variant with an average down-regulation of~51.3-fold. Interestingly, the CL2/ Ccdc80 protein was delocalized from the nucleus to the cytoplasm in those carcinoma samples that retained detectable levels of the protein, also shuttling from Golgi to the endoplasmic reticulum to exert its apoptotic function. Furthermore, the results of experiments on restoration of CL2/Ccdc80 gene expression in thyroid carcinoma cell lines indicate that loss of this gene expression plays a critical role in thyroid carcinogenesis. In fact, the growth rate of cells transfected with a CL2/Ccdc80 expression vector was significantly reduced. Moreover, flow cytometric analysis, confirmed by the TUNEL assay, showed a shift of the DNA profile of CL2/Ccdc80 transfected cells to a subG1 position, which is consistent with the concept that CL2/Ccdc80 expression exerts an apoptotic effect. This finding is also in line with the recent finding that CL2/Ccdc80 plays a crucial role in the apoptotic process [86]. Finally, the oncosuppressor function of the CL2/Ccdc80 gene was clearly indicated by the suppression of the neoplastic phenotype by the cells reexpressing CL2/Ccdc80. Indeed, these cells were no longer able to efficiently grow in semisolid medium and did not induce tumors when injected into athymic mice.

Ccdc80 is also repressed in AIB1 transgenic mice [86]. AIB1 is an oncogene that functions as a transcriptional coactivator in the nucleus [87-88]. Nuclear shuttling of AIB1 correlates with cell cycle progression in non-cancer cells [89], but this distribution is altered in cancer cell lines [88]. AIB1 overexpression occurs in many types of tumors and this is also the cause of cancer in animal models. In agreement, AIB1 represses DRO1 promoter and its expression levels inversely correlate with DRO1 in several cancer cell lines and in ectopic and silencing assays. Importantly, DRO1 shuttles from Golgi to the endoplasmic reticulum upon apoptotic stimuli, where it is predicted to facilitate the apoptosis cascade and DRO1 overexpression resulted in BCLAF1 upregulation. Therefore, DRO1 repression is an important factor for AIB1-mediated inhibition of apoptosis.

All these observations suggest that Ccdc80 may have a role as a tumor suppressor gene.

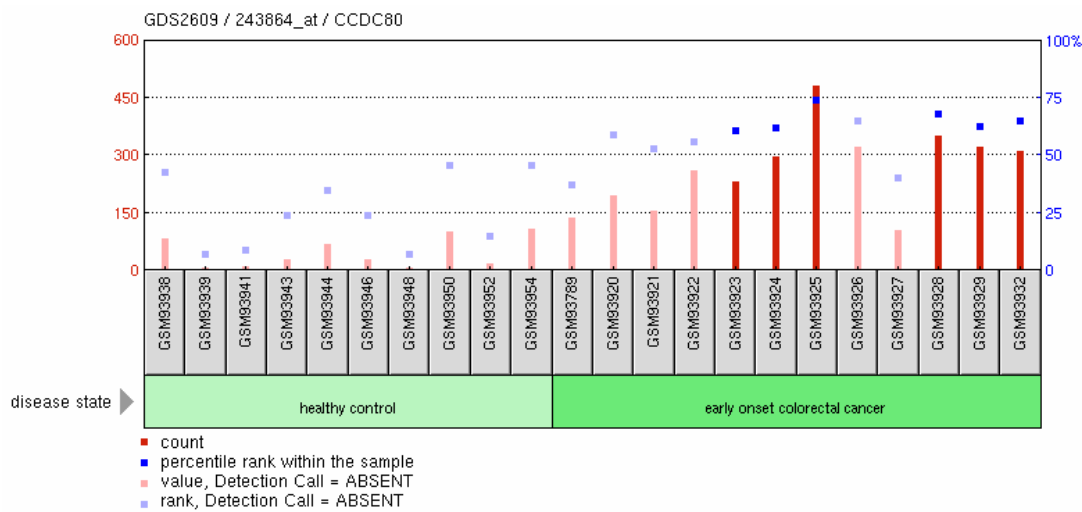


Figure 12
Comparison of Ccdc80-RNA expression in healthy controls and in patients with colorectal cancer, from NCBI GEO database

4.7 Ccdc80 and metabolic regulation

The function of both the human and mouse orthologs of Ccdc80 was also investigated in adipose tissues. Here the gene was named *URB* (upregulated in bombesin receptor subtype 3 knockout mouse) [69] and was demonstrated to be down-regulated in obese mice [90]. Was actually demonstrated that URB mRNA was predominantly expressed in human and mouse adipose tissues and was downregulated in obese mice; mRNA expression of URB in 3T3L1 adipocytes was downregulated by insulin, TNF- α , H₂O₂, and hypoxia; V5- tagged URB protein was secreted into culture media of Flp293 URB cells and endogenous URB protein was also detected in the media of human cultured adipocytes (ADSC-adipocytes). In the current study, like adiponectin, URB expression was reduced in with adipose tissue (WAT) of all three obese mouse models (*ob/ob*, *KKAy*, and *DIO*), while the expression levels of MCP-1 and TNF- α were increased as reported previously. These data suggest a role for URB in metabolic syndrome.

In another study [91] was shown that Ccdc80 is highly expressed in WAT and that its expression is regulated during adipocyte differentiation *in vitro*.

Using knockdown and overexpression studies, was found that Ccdc80 plays dual roles in adipogenesis by modulating C/EBP α and PPAR γ expression. To confirm that Ccdc80 is a secreted protein, human Ccdc80 containing an in-frame C-terminal FLAG epitope was expressed in HEK293T cells. Examination of HEK293T supernatants by Western blotting using an anti-FLAG antibody showed that Ccdc80 is not only secreted in its full-length form (~108 kDa) but also as cleaved fragments of ~95 and ~50 kDa. Was next examined the temporal regulation of Ccdc80 gene expression during the differentiation of 3T3-L1 cells into adipocytes. Although classical adipokines such as leptin or adiponectin are up-regulated only during the terminal phase of adipocyte differentiation [92-93], Ccdc80 was expressed in a biphasic manner. Ccdc80 mRNA was relatively low in proliferating 3T3-L1 preadipocytes but increased almost 10-fold when cells reached postconfluence before the initiation of differentiation. The addition of adipogenic inducers (dexamethasone, IBMX, and insulin) led to a dramatic reduction in Ccdc80 expression, an effect that was observed as early as 8 h after the addition of the mixture and was maximal after 24 h. Ccdc80 mRNA levels increased again during the late stage of adipocyte differentiation. To determine which component of the adipogenic mixture was able to induce down-regulation of Ccdc80, was assessed the individual and combined contribution of various adipogenic inducers during the early stages of differentiation. The biphasic expression of Ccdc80 during adipocyte differentiation raised the possibility that Ccdc80 regulates adipogenesis. Indeed, although Ccdc80 immunostaining was significantly reduced in Ccdc80 KD cells during both stages of adipocyte differentiation, the very few Ccdc80 KD cells that differentiate into adipocytes showed significant levels of Ccdc80. Furthermore, the addition of Ccdc80-containing medium to Ccdc80 KD cells was able to partially restore the ability of knockdown cells to differentiate into adipocytes. The authors also demonstrated that silencing of Ccdc80 was accompanied by decreased expression of genes involved in fatty acid uptake (*e.g.* lipoprotein lipase), triglyceride formation (*e.g.* diacylglycerol acyltransferase 1/2, lipin 1), and lipid metabolism. Expression of the

insulinsensitive glucose transporter GLUT4, a gene known to be upregulated during adipocyte differentiation [94], was also decreased in Ccdc80 KD cells, whereas expression of the basal glucose transporter GLUT1 was unchanged after Ccdc80 gene silencing. Interestingly, expression of several transcription factors that function early in adipogenesis, such as C/EBP β , C/EBP δ , and cAMP-responsive element-binding protein 1, was unchanged, and expression of KLF5, a positive regulator of PPAR γ gene expression [95], was increased in Ccdc80KD cells. These data suggest that Ccdc80 acts downstream of C/EBP β/δ and KLF5, but upstream of C/EBP α and PPAR γ . Since thiazolidinediones are potent inducers of adipogenesis [96], the addition of rosiglitazone (100 nM) to the adipogenic mixture increased differentiation in both control and Ccdc80 KD cells but did not restore differentiation of Ccdc80 KD cells to the same level as control cells. Given that increased expression of C/EBP α and PPAR γ during adipogenesis requires down-regulation of Wnt/ β -catenin signalling, the authors measured TOPFLASH activity as an index of β -catenin-mediated transcriptional activity via TCF, to determine whether modulation of canonical Wnt signaling might be involved in the phenotype of Ccdc80 KD cells. Moreover, Wnt10b, a secreted protein that has been shown to negatively affect adipocyte differentiation [97], is also expressed in a biphasic manner similar to Ccdc80 during adipogenesis.

Upon reaching postconfluence, cells expressing a non-silencing or Ccdc80 shRNA displayed similar TOPFLASH activity. After induction of differentiation, TOPFLASH activity in control cells declined slowly, reaching ~50% of its initial activity after 4 days. In contrast, Ccdc80 KD cells showed a significant, ~2-fold increase in TOPFLASH activity compared with control cells as early as 1 day after induction of differentiation and maintained this difference throughout the 4-day period examined. In agreement with these observations, was found that several target genes of the Wnt/ β -catenin signaling pathway (Axin-2, cyclin D1, Frizzled-7) were not significantly decreased after induction of differentiation in Ccdc80 KD cells, suggesting a failure to down-regulate Wnt/ β -catenin signaling in these cells upon

induction of differentiation. Other data also suggest that Ccdc80 modulates the activity of the TCF transcriptional complex in a manner independent of Wnt10b and β -catenin and that endogenous Ccdc80 is both necessary and sufficient for repression of Wnt/ β -catenin signalling during adipocyte differentiation.

Because the effects of Ccdc80 are observed in the absence of any changes in β -catenin protein levels (in 3T3-L1 cells) as well as in cells expressing a constitutively active form of β -catenin (HepG2 cells), it is unlikely that Ccdc80 modulates TCF-mediated transcription by affecting upstream components of the Wnt/ β -catenin signalling cascade. Taken together, these data suggest a model (Figure 13) in which Ccdc80 positively modulates adipocyte differentiation by repressing the activity of the TCF transcriptional complex after induction of adipocyte differentiation. Ccdc80 also appears to play a negative role in adipogenesis by a mechanism that does not involve Wnt signalling repression. Achieving a balanced and timely expression of Ccdc80 throughout differentiation is essential for the induction and activation of C/EBP α and PPAR γ and the acquisition of the adipocyte phenotype in 3T3-L1 cells.

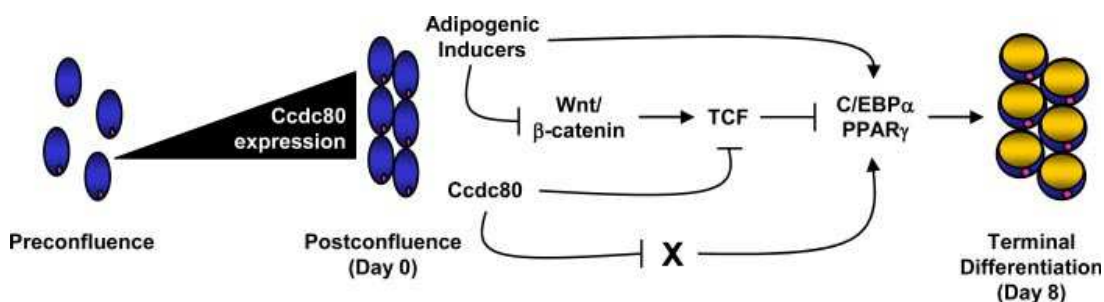


Figure 13
Proposed mechanism by which Ccdc80 bidirectionally regulates adipogenesis

A key finding of this study is that Ccdc80 is required for adipocyte differentiation and is regulated in a biphasic manner during adipocyte differentiation. This pattern of expression is distinct from classical secreted adipokines, such as adiponectin or leptin, but reminiscent of that of Wnt10b, a known adipocyte-secreted protein with an important role in adipogenesis.

In another study [98], a whole-body *Ccdc80* knockout (KO) mouse was generated to investigate the function of *Ccdc80* in glycaemic balance. Was found that mice lacking *Ccdc80* are hyperglycemic and glucose intolerant and display impaired insulin secretion *in vivo* when fed a high fat diet. Transcriptional analysis revealed that some components of the molecular clock were altered in muscle, WAT, and pancreas of *Ccdc80*^{-/-} mice. Furthermore, gene expression changes in the KO mice were associated with altered feeding behaviour, greater caloric intake, reduced energy expenditure, and obesity.

In contrast to previous finding in 3T3-L1 cells [91], *Ccdc80* does not appear to be required for normal WAT development as assessed by histology, as well as expression of PPAR γ and adipocyte protein 2. Was also found no evidence that *Ccdc80* was an important regulator of Wnt/ β -catenin signaling *in vivo* as evidenced by unchanged expression of Cyclin D1 and Axin-2 between WT and *Ccdc80*^{-/-} mice. Morphometrical analysis of WAT sections further revealed that adipocyte size was slightly larger upon HF feeding but was unaffected by the absence of *Ccdc80*.

Furthermore, *Ccdc80*^{-/-} mice fed a HF diet had reduced insulin levels upon glucose administration that was associated with slightly albeit not significantly higher glucose levels. This impairment in glucose-induced insulin secretion *in vivo* led to marked glucose intolerance in *Ccdc80*^{-/-} mice fed a HF diet for 30 wk. In addition, *Ccdc80*^{-/-} mice were found to be hyperglycemic at the end of the study. In contrast, glucose tolerance and glucose-induced insulin secretion *in vivo* in *Ccdc80*^{-/-} mice fed a LF diet were virtually indistinguishable from their WT counterparts. Insulin tolerance tests further showed that peripheral insulin sensitivity was similar between WT and *Ccdc80*^{-/-} mice, suggesting that defective *in vivo* insulin secretion was responsible for the glucose intolerance observed in HF-fed *Ccdc80*^{-/-} mice. In an attempt to determine the mechanisms underlying the metabolic abnormalities associated with *Ccdc80* deletion in mice, was performed a transcriptional profiling analysis by microarray of skeletal muscle, pancreas, and WAT from WT and

Ccdc80^{-/-} mice fed either a LF or HF diet. Although numerous unique transcripts were regulated by Ccdc80 in each of the tissues examined, only 10 were simultaneously regulated by the deletion of Ccdc80 in all three tissues. Initial examination of these transcripts revealed that four of them, representing three different genes, were components of the circadian clock. Because of the prominent role of circadian rhythms in metabolic control, it is possible that altered expression of Arntl (also known as Bmal1), Dbp, and Tef contributes to the metabolic phenotype of Ccdc80^{-/-} mice. Although the exact mechanism by which disruption of Ccdc80 affects the expression of Arntl, Dbp, and Tef is not known, our study in 3T3-L1 cells provide evidence that Dbp biphasic expression is regulated, at least to some extent, in a cell-autonomous manner by Ccdc80. Importantly, silencing of Ccdc80 led to a reduction in Dbp and, to a lesser extent, Tef expression before induction of adipocyte differentiation, suggesting that these changes were not due to the impaired adipogenesis phenotype of the knockdown cells.

As above mentioned, this study shows that Ccdc80 is not required for normal WAT development *in vivo* as evidenced by unchanged adipocyte morphology and size, as well as PPAR γ and adipocyte protein 2 expression in Ccdc80^{-/-} mice. Was also not find evidence that Ccdc80 was an important modulator of canonical Wnt signaling and expression of Wnt target genes, at least in WAT, skeletal muscle, and pancreas. This is in contrast to previous findings in 3T3-L1 adipocytes in which Ccdc80 was shown to act as a repressor of Wnt/ β -catenin signaling during differentiation [91] as well as findings in cancer cell lines that established a connection between Ccdc80 expression and Wnt signalling [69-71]. The reason for this discrepancy is not clear but might indicate that Ccdc80 regulates Wnt signaling during development and neoplastic transformation but not in terminally differentiated cells from adult mouse tissues. Furthermore, was show that absence of Ccdc80 exacerbates diet-induced glucose intolerance and hyperglycemia in mice fed a high fat (HF) diet. The inability of KO mice to maintain normal glucose homeostasis appeared to be due to defective glucose-

induced insulin secretion. However, no major morphological and biochemical changes were detected in pancreas from *Ccdc80*^{-/-} mice. Furthermore, pancreatic islet hypertrophy in response to HF feeding was similar between WT and *Ccdc80*^{-/-} mice, suggesting that other mechanisms underlie the defective insulin secretion that is observed upon glucose challenge in the KO mice.

Moreover, in another study [99], using a yeast 2-hybrid screen of an adipocyte cDNA library, *Ccdc80* was identified as a novel JAK2-binding protein. The Janus family of tyrosine kinases, which includes Janus kinase 1 (JAK1), JAK2, JAK3, and Tyk2, plays a critical role in signaling by members of the cytokine superfamily of receptors. JAK2 is activated by more than two-thirds of these receptors, including the receptor for GH, prolactin, erythropoietin, leptin, leukemia inhibitory factor, interferon- γ , and multiple interleukines (ILs). JAK2 promotes the growth, proliferation, and/or differentiation of many cell types, and dysregulation of JAK2 has been linked to various forms of cancer [100-101].

Despite the fact that JAK2 is necessary for signalling by multiple cytokines, hormones, and growth factors [102] and is the most studied of the JAKs, only a handful of proteins have been identified that bind directly to JAK2. The authors in this paper show that *Ccdc80* binds to the active tyrosylphosphorylated form of JAK2 but not the inactive form of JAK2 and that in the presence of active JAK2, *Ccdc80* is also phosphorylated. Binding to JAK2 requires the regions in *Ccdc80* that are homologous to domain 5 of the sushirepeat-containing protein, X-linked (SRPX) and in mammalian systems also SRPX2 binds preferentially to activated JAK2. These results suggest that the DUES protein interaction domain characterizes a novel class of proteins that bind activated JAK2. Regarding function, *Ccdc80* does not enhance JAK2 kinase activity, however *Ccdc80* stimulates the phosphorylation of Stat5b on Tyr699, which is required for Stat5b activation, and enhances Stat3 phosphorylation. Finally, was shown that *Ccdc80* has a functional signal peptide and that a portion of *Ccdc80* is secreted

into the extracellular compartment where it both associates with the extracellular matrix and is released into the medium.

Importantly, in this article the authors provide a different size and sequence of Ccdc80 as a protein of 949 aa (110 kDa) that resulted identical to rat DRO1 [70] and rat CL2 [71]. Because Ccdc80 has a wide tissue distribution, and JAK2 is activated by nearly two-thirds of the cytokine receptors, it seems likely that Ccdc80 plays a role in not only GH signalling but also signalling by other ligands that bind to members of the cytokine receptor family. Consistent with this hypothesis, in the bombesin-receptor-subtype (BRS)-3-deficient model of obesity, the brown adipose tissue is characterized by elevated Ccdc80 levels, suppressed GH levels, and dramatically elevated leptin levels [69, 103]. An inhibitory role for Ccdc80 on leptin signaling would be consistent with the apparent leptin resistance detected in these mice. Moreover, because Ccdc80 binds JAK2 and coexpression of Ccdc80 with JAK2 elevates phosphorylation of Stat3 and Stat5, suggest that Ccdc80 functions in the intracellular compartment. Ccdc80 contains a putative signal peptide, the hallmark of a protein destined for processing by the endoplasmic reticulum/Golgi and secretion. Indeed, was observed that Ccdc80 localizes to the perinuclear region of the cell and comigrates with markers for the endoplasmic reticulum and Golgi [70, 86], is secreted from the cell [76, 90], binds to the extracellular matrix [68, 76, 84], and, once secreted, is cleaved into several fragments [68, 70, 90, 91]. However, not all cells that express Ccdc80 secrete Ccdc80.

4.8 Ccdc80 in cardiac and skeletal muscle

As abovementioned, it is demonstrated that Ccdc80 is abundantly expressed in heart and skeletal muscle and it is also proved that Ccdc80 is highly expressed in skeletal myotubes during differentiation [104]. Moreover, microarray data demonstrate the suppression of its expression in starved myotubes (Figure 14) and the increased expression in muscles from patients affected by Duchenne dystrophy [105] (Figure 15): taken together, these data suggest

a possible role of Ccdc80 as a cell differentiation protein both in cultured cells and muscle tissues undergoing regeneration or remodelling.

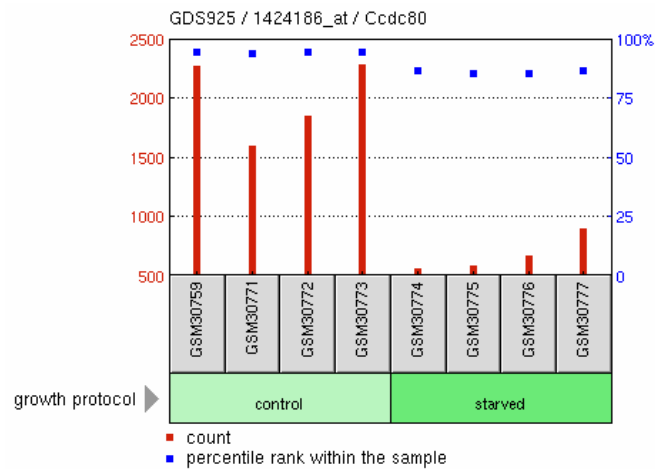


Figure 14
Comparison of Ccdc80-RNA expression in normal and starved myotubes, from NCBI GEO database.

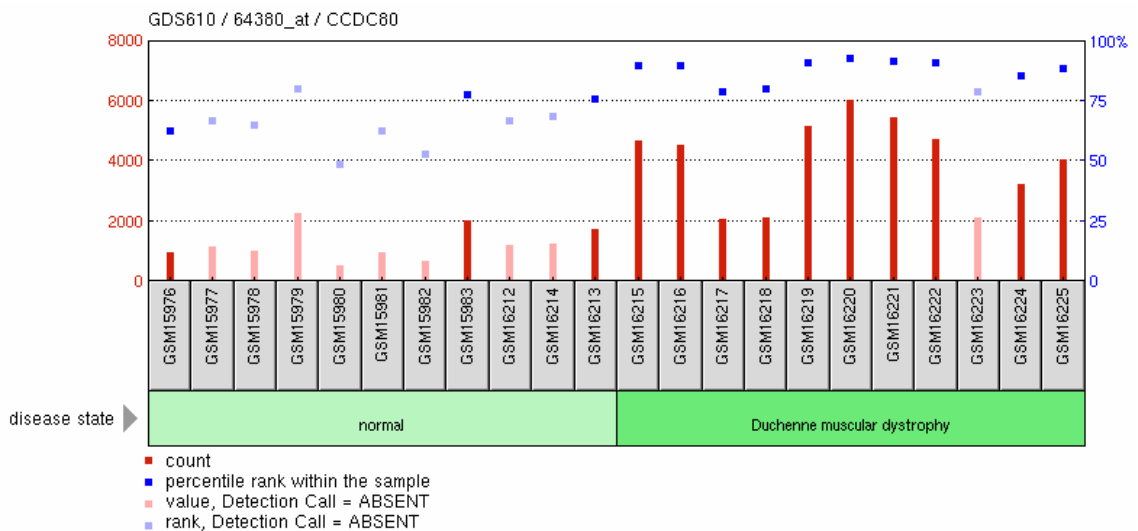


Figure 15
Comparison of Ccdc80-RNA expression in normal muscle and in patients with Duchenne muscular dystrophy, from NCBI GEO database [105].

On the other side, the only data available in literature, about normal cardiac expression of Ccdc80, have evaluated the expression profile of Ccdc80-RNA in atria and ventricles (Figure 16).

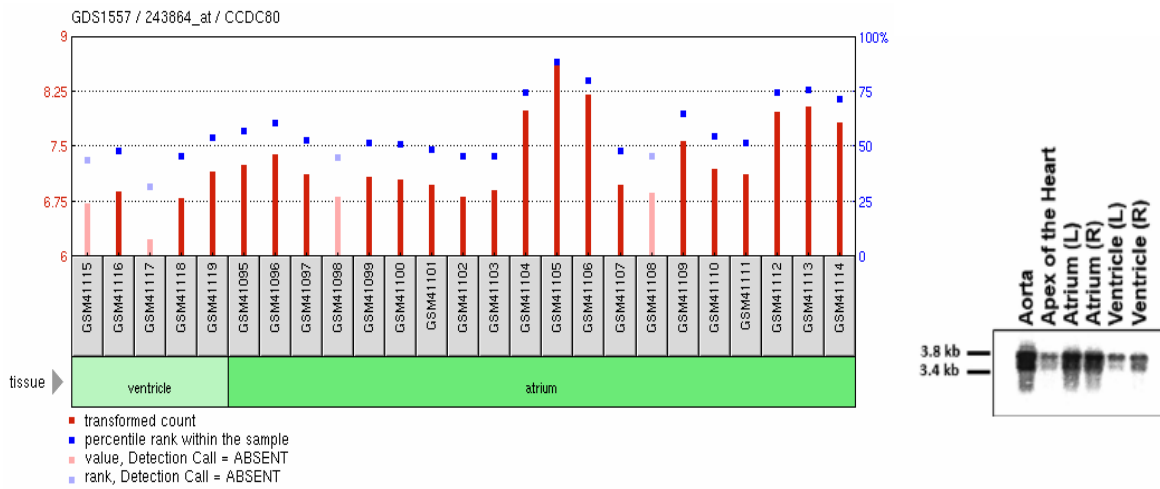
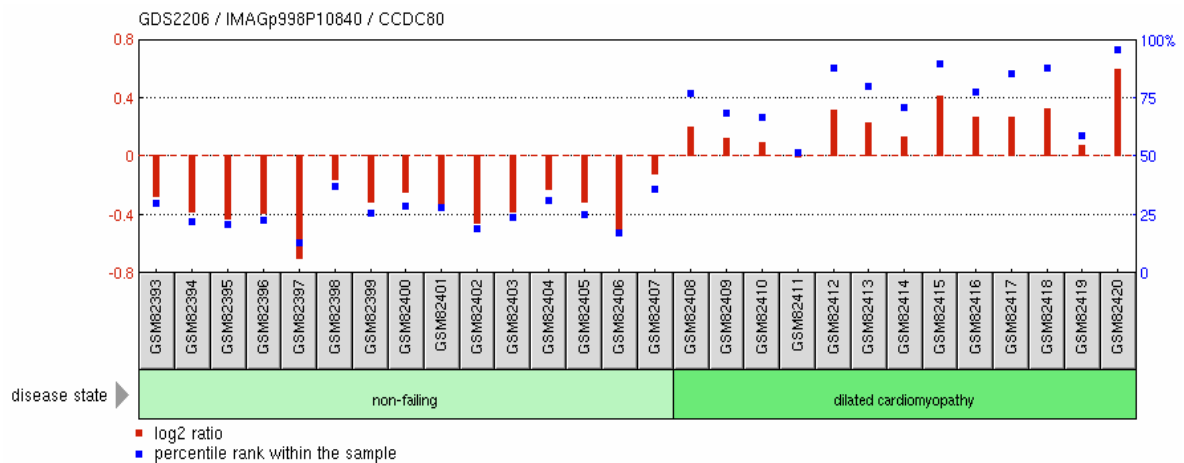


Figure 16
Ccdc80-RNA in heart of RNA from human cardiovascular tissues, from NCBI GEO database.
In the right part is shown Northern blot analysis [106].

Regarding a possible role of Ccdc80 in cardiomyopathies, are currently available only two gene expression profile studies, which compared samples from DCM to non-failing pairs, and to ischemic cardiopathy, identifying Ccdc80 as a clear-cut upregulated gene in diseased tissues (Figure 17).



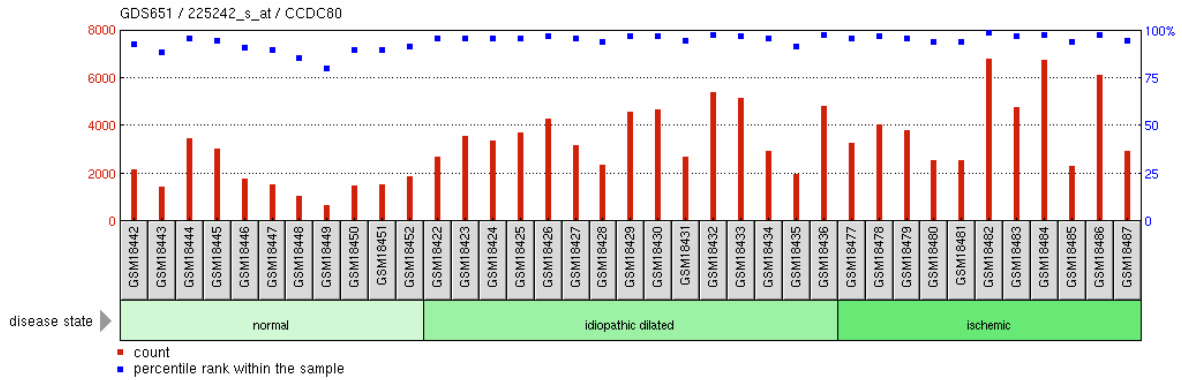


Figure 17
Comparison of Ccd80 RNA expression in normal heart and cardiomyopathies (DCM and ischemic), from NCBI GEO database

Another study [106] identified steroid-sensitive gene 1 (SSG1, an orthologue of Ccdc80) as a novel protein kinase G (PKGI) substrate: in vascular cells, a λ -phage coronary artery smooth muscle cell library was constructed and screened for phosphorylation by PKGI. The screen identified SSG1, which harbours several predicted PKGI phosphorylation sites. Was observed direct and cGMP-regulated interaction between PKGI and SSG1 and in vascular smooth muscle cells, both the NO donor *S*-nitrosocysteine and atrial natriuretic peptide induced SSG1 phosphorylation, and mutation of SSG1 at each of the two predicted PKGI phosphorylation sites completely abolished its basal phosphorylation by PKGI. This study confirmed the highest SSG1 expression in the heart, followed by skeletal muscle and colon. Lower expression levels were observed in the thymus, spleen, kidney, liver, small intestine, placenta, and lung. PKGI inhibits VSMC contractility by regulating signalling pathways that control myosin phosphorylation and by modulating the level of intracellular calcium and by altering the sensitivity of the contractile apparatus to calcium [107]. PKGI and cGMP inhibit left ventricular remodeling in response to pressure overload [108-109], although the downstream PKGI effectors in the myocardium remain incompletely understood. Interestingly, left ventricular pressure overload modulates cardiac SSG1 expression [110].

Overall, the abovementioned results suggest multiple roles of the Ccdc80 gene in the different species investigated, during embryonic development and adult life, for adipocyte

differentiation, metabolic regulation, cancer development as well in muscle tissues undergoing regeneration or remodelling; they also indicate that Ccdc80 exerts its function in different intracellular and extracellular compartments.

5. Materials and methods

Giving the aims of our investigation, we used different models:

1. Zebrafish model, to define the functional role of Ccdc80 in embryonic development: 24 controls and 42 zebrafish morphants, injected with the Ccdc80 antisense morpholino;
2. Rat model: 6 controls compared with 6 samples of right ventricle heart failure induced by intraperitoneal monocrotaline injection;
3. Human model: 2 controls (donor healthy hearts which were not transplanted for logistic problems), compared with 14 samples of patients affected by dilated cardiomyopathy.
4. Skeletal muscle: 2 samples of normal intercostals human skeletal muscle were compared to 2 samples of patients affected by Duchenne muscular dystrophy.

5.1 Rat model of heart failure

Right ventricular heart failure was induced in male Sprague-Dawley rats (90 to 100 g) by intraperitoneal injection of 30 mg/kg monocrotaline (MCT) according to Vescovo et al. [111] Our rat samples were derived from a previous study [112]: after 21 days, a time-point when pulmonary hypertension is present and right ventricular hypertrophy and failure begin to develop, the rats were sacrificed.

A second group of rats injected with Dulbecco's modified Eagle medium (DMEM), but without MCT, serving as a control without right ventricular heart failure.

MCT [113] is a pyrrolizidine alkaloid found in the foliage of *Crotalaria spectabilis*. Ingestion of MCT has been associated with hepatic and pulmonary disease in humans and many animal

species. In rats, a single administration of MCT results in pneumotoxic changes that are delayed in onset and progressive [114]. These include pulmonary vascular leak, pulmonary arterial vascular remodelling, and pulmonary hypertension. Pulmonary damage is not caused directly by MCT but by its metabolic products. Monocrotaline is converted to reactive pyrroles by the mixed function oxidase system of the liver, but not of the lungs [115-116]. It is presumed that small quantities of these pyrrolic metabolites escape binding in the liver and travel via the blood stream to the pulmonary vascular bed, where they bind covalently to cellular macromolecules [117]. Monocrotaline pyrrole (MCTP) is an unstable, electrophilic, putative metabolite of MCT. When a single injection of a low dose of chemically synthesized MCTP is injected into tail veins of rats, delayed and progressive pulmonary injury, pulmonary hypertension, and right heart hypertrophy results that is similar to that induced by MCT itself [118].

All these changes in pulmonary vascular bed leads to pulmonary hypertension, right ventricular hypertrophy and right ventricular failure. This kind of right ventricular heart failure induced by MCT is a well established model, which mimics the congestive heart failure syndrome in man. The paraffin-embedded tissue were analyzed with Haematoxylin and Eosin (H&E), immunohistochemistry and immunofluorescence staining.

5.2 Zebrafish

Besides the traditional rodent and invertebrate models, zebrafish (*Danio rerio*) has been used since the early last century as a classical developmental and embryological model. Zebrafish has emerged in the last past decades as an effective model organism for biomedical research due to the unique combination of the optical clarity of the embryos, allowing in vivo observation of cell-biological events and the rapid development in 24 hours of all the

differentiated tissues. In addition it is well known that the zebrafish homolog of human Ccdc80 shows a high similarity.

Given also that zebrafish is able to survive during embryonic development without a functional cardiovascular system, this model appears particularly useful for the study of functional role of proteins in heart development.

The Zebrafish strains used are obtained from ZIRC, Oregon US, and from Wilson lab, University College London.

Adult fish were maintained at 28.5 C, 14 hours light/10 hours dark cycle, in a recirculating fresh water system according to standard procedures.

Embryos were raised at the same temperature as adults in Petri dishes with a change of water twice / day. Fish were fed every day with brineshrimps, *Artemia salina*, (living or frozen) and Small Granular feed from Zebrafish Management Ltd., England.

Embryos were obtained from natural spawning and, starting from 24 hours post fertilization (hpf), were treated with 0,003 % 1-phenyl-2-thiourea (Sigma-Aldrich) for avoiding pigmentation. Embryos were staged in hours post fertilization and by counting somites numbers according to Kimmel et al. [119]. For a better observation embryos were anesthetized in 0,0016 % Tricaine (MS-222, Sigma-Aldrich).

5.2.1 RNA extraction and purification

The full-length sequence of the Ccdc80 mRNA was cloned as reported by Visconti et al. and the sequences at the 5' and 3' Untranslated Regions (UTR) of the Ccdc80-mRNA were identified, amplified and cloned.

For the 5' end identification and cloning the following oligonucleotides were used: forward

5' - GCGAATTCGATTTGTCTTTGTTAAAACTAT - 3',

and reverse 5' - GACGCCAGTAGTTTGGAGAACC - 3'. For the 3' end identification and cloning the following oligonucleotides were used: forward

5' - GGCCATCCAGCAGTCTCTAGG - 3',

and reverse 5' – TAAGGATCCGACCACGCGTATCGATGTCGAC -3'.

The UTR sequences obtained from the RACE have been analysed with the ABI PRISM® 310 Genetic Analyzer (Applied Biosystems), using the oligonucleotides indicated by the RACE kit manufacturer for the Cycle Sequencing reaction, which was performed according to manufacturer's instructions.

The analysis of all the possible reading frames of the amplified putative CDR sequence revealed that one single ORF was present. The starting codon was located in the first position of the amplified sequence (ATG) and the stop codon (TAG) in the last position of the amplified sequence, giving a coding region of 2604 bp. Also in the 5' ending sequence, identified using the RACE technique, were not found alternative starting codons located in frame with the putative CDR sequence. These results let us bona fide consider that the full-length sequence we have cloned, contains the full CDR sequence of the Ccdc80 gene, and that the 5' and 3' amplified sequences can be considered the UTR of the Ccdc80 gene.

Physico-chemical properties of the Ccdc80 protein were deduced *in silico* by the analysis of the amino acidic sequence with the software program Compute pI / Mw.

The putative sub-cellular localization of the Ccdc80 protein was predicted using the software program WoLF PSORT.

The presence of common motifs in the Ccdc80-encoded protein was analyzed with the software program MEME, and the software program Motif Alignment and Search Tool analysis (MAST).

Alignment of the three obtained domains was performed with the software program ClustalW2.

Samples were treated as follows:

Adult fish were quickly frozen in liquid nitrogen and stored at -80 C until further processing. Eggs were cleared from medium, snap frozen in liquid nitrogen and stored at -80 C until further processing. For the purification of total RNA from adults organs, adult fish were anesthetized in 0,0016 % Tricaine (MS-222, Sigma-Aldrich) until no opercula movement was reached. Organs were then rapidly dissected under a stereomicroscope, quickly frozen in liquid nitrogen and stored at -80 C until total RNA extraction. Frozen specimens were gently homogenized in TRIZOL®

(Invitrogen), a mono-phasic solution of phenol and guanidine isothiocyanate which maintains RNA integrity while allowing tissues and cells lysis during homogenization. After homogenization, addition of chloroform followed by centrifugation induced the separation between an organic phase and an aqueous phase, which contained the total RNA. It was then recovered by precipitation with isopropyl alcohol, then washed in 75 % ethanol and suspended in DEPC treated water.

It was purified from total RNA with the NucleoTrap mRNA Mini Purification kit (Macherey-Nagel) which allows the purification of mRNA by means of a spin-column filter combined with an oligo(dT)-latex bead suspension technology. Manufacturer's instructions were followed with minor modifications.

After purification total and poly A⁺ RNA were photometrically quantified and analyzed for purity.

5.2.2 Semi-quantitative PCR analysis

A semi-quantitative PCR analysis was performed in order to evaluate the temporal expression of the Ccdc80 gene during the embryo development, and in organs from adult fish.

At this purpose 0.5 µg of total RNA, extracted as described in the section 2.4.1 from embryos at several developing stages and adult organs was used as the template in a reverse transcription reaction using random primers and the AMW-Reverse Transcriptase (Roche). 1 µg of the cDNA was used in a PCR reaction (Taq DNA Polymerase, Eppendorf) performed at 25 cycles with the aim to not reach the reaction *plateau*, but to remain in the exponential reaction phase. In order to have a standard for the normalization of the data, the constitutively expressed *elongation factor 1 alpha* (EF1α) gene was also tested in a parallel PCR. The reaction program was the following: initial denaturation, 2 min at +94 C, followed by denaturation, 30 s at +94 C – annealing, 45 s at +60 C – elongation, 60 s at +72 C, for 25 cycles, and a final elongation of 7 min at +72 C.

The Ccdc80 amplicon was a sequence of 379 bp in size and spanning between the exon 3 and the exon 6 of the Ccdc80 transcript.

The oligonucleotides used as the primers were the following:

Ccdc80 amplicon: 5'- CCAGGATCTCATCATGGAGC -3',

and 5'- GACCAGCTTCAGCACGGACA -3'.

EF1 α amplicon: 5'- GGTACTTCTCAGGCTGACTGT -3',

and 5'- CAGACTTGACCTCAGTGGTTA -3'.

10 μ l of each PCR product were then electrophoresis run on an agarose gel and blotted on a nylon Zeta-Probe GT membrane (Biorad). The blots obtained were hybridized with the same PCR products as the probes, which were labeled with [α -³²P]dCTP, Amersham (Random Primed DNA Labeling Kit, Roche). After hybridization, blots were exposed to a T-MAT G/RA (Kodak) film for the detection of the PCR product bands, on which we performed a densitometric analysis with the Quantity One software program, BioRad.

5.2.3 Morpholino knocking-down

The antisense MO for the Ccdc80 knocking-down (Ccdc80-morpholino, MO Ccdc80) was obtained from Gene Tools, Philomath, Oregon, US. It is a translational-blocking morpholino having the following sequence: 5'-AACCAAGCATATACCGTGCCCTCAT-3'. A 5-mismatch morpholino designed against the same region was used as the control for unspecific effect:

5'-AAgCAAcCATATAgCGTGcCTgAT-3'.

Different doses of each MO were used for testing morphological effects on embryos and/or for possible effects on the expression of specific molecular markers. The final dose for all the subsequent tests was 1 pmol/embryo.

As the control for unspecific effects, each knocking-down experiment was performed in parallel with injection of the same amount of a standard control oligo morpholino with no target in zebrafish and obtained from Gene Tools, Philomath, Oregon, US.

Rescue experiments were performed to assess the specificity of the *CL*-morpholino knocking-down.

The specific action of *CL*-morpholino in blocking the Ccdc80 transcript was evaluated with the co-injection of MO Ccdc80 at the dose of 1 pmol/embryo, together with different doses of the

synthetic full-length *Ccdc80* mRNA. The full rescue was reached with the injection of 400 pg of *Ccdc80* mRNA, as it was evidenced by *in vivo* morphological and WISH analyses of injected embryos. *In vivo* observations were performed during somitogenesis, at 24 hpf, and 48 hpf, and the WISH analyses were performed to evaluate *myoD* and *cmc 2* expression patterns at the stage of 8-10 somites and 48 hpf, respectively.

5.2.4 Whole-Mount *In Situ* Hybridization (WISH)

With the aim to detect the mRNA transcript of genes of interest in morphologically conserved whole embryos, Whole-Mount *In Situ* Hybridization (WISH) reactions have been performed in embryos at different developing stages. In the WISH technique, antisense RNA labeled probes are used that can specifically bind a corresponding sequence of the transcript under investigation, thus allowing its spatial localization in the whole embryo. Sense RNA probes for the same transcript sequences were also tested for aspecific bindings.

All the probes were cloned in a plasmid containing the promoters for an *in vitro* reverse transcription reaction. They were synthesized from the linearized plasmid and were labeled with the digoxigenin molecule using the DIG RNA Labeling kit, Roche, according to manufacturer's instruction. Labeled probes were purified with the High Pure RNA Isolation kit, Roche, quantified on an agarose gel, and used in the WISH at a concentration of 1 µg/ml.

The probe used for the *Ccdc80* transcript detection corresponds to the first 1125 bp of the CDR. For its application in WISH, it has been previously cloned in the pcDNA3 plasmid, which has the suitable T7 and SP6 promoters for the DIG riboprobes synthesis. For the antisense probe synthesis, plasmid was linearized with *EcoRI* restriction endonuclease and the reverse transcription was made with T7 RNA polymerase. For the sense control probe synthesis, plasmid was linearized with *BamHI* restriction endonuclease and reverse transcribed with SP6 RNA polymerase.

The other probes were already present in our lab as markers commonly used for the analysis of embryonic specific regions.

Embryos were raised as described in section 2.1, fixed in 4 % paraformaldehyde (PFA), manually decorionated in Phosphate Buffer Saline (PBS) solution and moved through methanol/PBS graded series to 100 % methanol for permeabilization and possible long storage, at -20 C.

The hybridization protocols for the WISH reactions were optimized for each probe and/or developing stage.

After hybridization, probes were immunologically detected using anti-digoxigenin Fab fragments from sheep specific IgG, conjugated with alkaline phosphatase (Anti-Digoxigenin-AP, Fab fragments, Roche), and the NBT/BCIP (Roche) phosphatase substrates for a colorimetric detection. The phosphatase reaction gave a water insoluble dark blue precipitate, which could be observed in a variable time from few minutes to few days according to the developing stage and the expression level of the transcript under investigation. After detection embryos were post-fixed in 4 % PFA and stored in PBS/EDTA at +4 C in the dark.

Embryos were then observed under the Leica MZ16F stereomicroscope and images have been acquired with the Leica DFC 480 digital camera and the IM500 software program (Leica Microsystems).

WISH protocols used were the Patterson protocol [120] and an high resolution protocol [121].

Cardiac specific markers were evaluated by WISH in *Ccdc80*-silenced embryos, in particular *Nkx2.5* [122], *Cmlc 2* [123], *Amhc* [124], *HrT* [125].

5.2.5 Histological analysis

Embryos were dehydrated through an ethanol/PBS graded series to 75% ethanol and their yolks were gently mechanically dissected. Embryos cleared from yolk were then treated as follows:

- 5 min 90% ethanol;
- 5 min 95% ethanol;
- 5 min 100% ethanol (twice);

- 5 min 100% xylol;

After this, embryos were flat mounted over a microscope slide in a 50% xylol and 50% Eukitt (Bio-optica) mounting medium. After this, they were observed under the Olympus BH-2 polarizing microscope and image analyzed with the (Olympus C-35AD-4) camera.

Embryos were dehydrated through a PBS/ethanol graded series to 90% ethanol. Then washed again in 90% ethanol and washed twice for 15 minutes in xylol. After this they were washed in liquid paraffin over night at +40 C. After this, old paraffin was replaced with new one every hour for three times. Then embryos were placed in the moulds, oriented and let to get cold at room temperature for few hours, finally moved at +4 C over night. 0.8 μ m sections were cut under the microtome Microm HM360 and let to dry at +40 C over night. After this, slides were treated as follows:

Deparaffination

- 15 min in xylol;

- 5 min. in xylol;

Hydration

- 2 min. absolute ethanol, twice;

- 2 min 95% ethanol;

- 1 min 90% ethanol;

- 1 min 70% ethanol;

- 1 min 50% ethanol;

Staining

- 1 min eosin;

Wash

- 1 min distilled water;

- 1 min tap water;

- 1 min distilled water;

Dehydration

- 2 min 50% ethanol;
- 2 min 70% ethanol;
- 2 min 90% ethanol;
- 2 min 95% ethanol;
- 2 min absolute ethanol (twice);

Mounting pre-treatment

- 2 min xylol;
- 5 min xylol.

Slides were then mounted with the Eukitt (Bio-Optica) mounting medium, observed under the Leica DM6000 B microscope equipped with the Leica DCF480 digital camera, and analyzed with the software program LAS (Leica Application Suite).

5.3 Immunohistochemistry and immunofluorescence

Fluorescence and Chromogenic Immunohistochemistry and Confocal Analysis were made as follows:

Several antibodies (Abs) were used, alone or together, smooth muscle cells antibody (Dako, dil 1/200); Myosin antibody (alfa mouse slow muscle-myosin, Chemicon, dil: 1/200); Troponin I antibody (clone H-170, rabbit polyclonal, dil:1/100); Fibronectin (clone P5F3 mouse monoclonal, dil: 1/100), Tropomyosin (clone CH1, mouse monoclonal, Santa Cruz, dil:1/100). Was used polyclonal anti-Ccdc80 antibody produced in rabbit (Sigma-Aldrich, Milan, Italy) at dilution 1/20.

Briefly, slides were treated with 0.3% hydrogen peroxide in methanol to block endogenous peroxidase activity, then washed with phosphate-buffered saline and incubated in buffered normal horse serum to prevent nonspecific Ab binding. Sections were incubated with the

primary Abs for 1 hour at room temperature. After washing, a biotin-labeled secondary Ab was applied, followed by an avidin-peroxidase conjugate. Diaminobenzidine was used as a chromogen.

Immunostaining was done simultaneously with Ab against Ccdc80 coupled with other antibodies, visualizing the outcome with anti-mouse or anti-rabbit fluorescein isothiocyanate- or rhodamine-conjugated secondary Abs. Nuclei were stained with TO-PRO 3 (Invitrogen, Molecular Probes; distributed by Invitrogen, Milan, Italy). Microphotographs were taken using a TCS-SL laser scanner confocal microscope (Leica, Wetzlar, Germany).

The parameters of wavelength detected for each fluorophore is as following: for FITC/Spectrum Green fluorophore Ex 480/30, for Spectrum Orange fluorophore Ex 535/50.

A control positive section of tonsil or bone marrow biopsy from autopsies was included for each Ab in each immunostaining session.

5.4 Northern Blot

Total RNA and mRNA poli (A)⁺ were denatured by treatment with formamide, fractionated by electrophoresis through a denaturing agarose gel containing formaldehyde, then transferred on a nylon Zeta-Probe GT membrane (Biorad). As the negative control the total RNA from rat lung, in which no Ccdc80 expression has been previously detected (data not shown), was used.

The blot obtained was hybridized with a specific probe for the detection of the Ccdc80 gene transcripts.

The probe was 1140 bp and located between the 5'UTR region and the first exon of the gene. It was PCR amplified using the following oligonucleotides as the primers:

5'-TTAGAATCCGCCACCATGAGGGCACGGTA-3' and

5'- GGCTGGGATCCATTGAGGGGTAGTA – 3'. After purification the PCR product was radio labeled with [α - ³²P]dCTP, Amersham (Random Primed DNA Labeling Kit, Roche) and used as the probe. After hybridization the blot was exposed to a T-MAT G/RA (Kodak) film for the detection of the bands corresponding to the Ccdc80 transcripts.

5.5 Western Blot

Protein extraction from formalin-fixed and paraffin embedded (FFPE) tissues were made as follows:

4 μ m sections of atria and ventricle of each sample were cut and placed in 1.5 mL microcentrifuge tubes. Sections were deparaffinized through two changes of xylene, followed by dehydration in graded ethanol/xylene, vortexed and centrifugated.

Surnatant was collected and place in a 1.5mL microcentrifuge tubes containing sodium dodecyl sulfate (SDS) buffer with 5% β -mercaptoetanol and digested at 90°C.

Surnatants were collected and place at -20°C until use.

Polyclonal anti-Ccdc80 antibody produced in rabbit (Sigma-Aldrich, Milan, Italy) at dilution 1/20 was used.

Protein concentration was determined using The Qubit® Protein Assay Kit (Life Technologies, Milan, Italy) designed specifically for use with the Qubit® Fluorometer (Life Technologies, Milan, Italy), according to the manufacturer's instructions.

1-Dimensional (1-D) Gel Separation and western blot analysis of Ccdc80 were made as follows:

Twenty micrograms of protein lysate from each sample were run on 4–10% Criterion TGX Stain-Free Precast Gels (BioRad, Milan, Italy) and transferred to nitrocellulose membranes

(Applichem, Milano, Italy) following the manufacturer's instructions. Membranes were blocked in TBST buffer with 5% low fat-milk for two hours and incubated with anti- Ccdc80 antibody (1:250, Sigma-Aldrich, Milan, Italy) at 4°C, overnight and probed with Cy5-coniugate goat anti rabbit IgG (1:1000,KPL, Prodotti Gianni, Milan, Italy) 1 hour at room temperature.

All western blot were visualized using Alliance 2.7 gel analyzer (UVITEC Cambridge, Eppendorf, Italy) and CHROMA RED channel for fluorecence signals.

The percent distribution of the fluorecence signals was determined by a densitometric software (Alliance 2.7 1D software, UVITEC, Eppendorf, Italy) after image acquisition of the stained gels.

6. Results

6.1 Functional role in Zebrafish

Semi quantitative RT-PCR analysis on adult tissues (Figure 18) shows that Ccdc80 is expressed in all the analyzed tissues. In particular, it is expressed in heart at the highest level, and in liver and intestine at the lowest level. Intermediate levels are evident in brain, ovarian tissue and the surrounding fat tissue, mesonephric duct, swim bladder, pancreas.

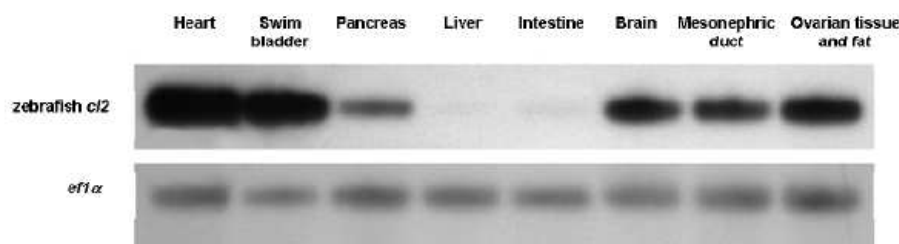


Figure 18
Zebrafish CL2 (Ccdc80) expression in adults

Semi-quantitative RT-PCR analysis was performed on embryos at different developing stages. Starting from 1-2 cells, and up to 106 hpf, Ccdc80 transcript is detectable in all the developing stages considered. It is present at high level since the one-cell stage and its

expression remains nearly constant during the cleavage and the blastula period. Then it decreases and remains at low level in the gastrulation period. During somitogenesis the *Ccdc80* mRNA level increases gradually, and reaches a peak at 22 somites.

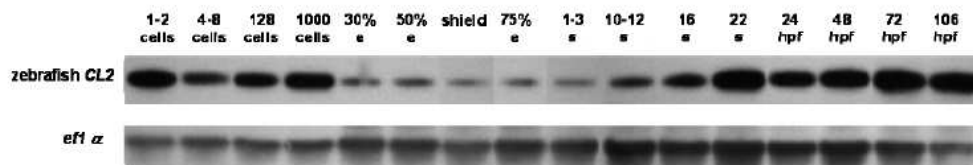


Figure 19
Zebrafish CL2 (CCDC80) expression analysis during embryonic development

WISH analysis was performed on embryos at the same developing stages as the quantitative PCR, with the aim to define the localization of the *Ccdc80* transcript in the whole embryos during development. The antisense *Ccdc80* ribo-probe used to detect the *Ccdc80* mRNA in the whole embryos demonstrates that during the cleavage and blastula periods it is homogeneously expressed in all the blastomers.

The same occurs in the gastrula period at lower level. In the segmentation period, starting from the stage of 7-8 somites up to late somitogenesis, *Ccdc80* transcript is localized in the notochord. After somitogenesis is completed, the signal begins to decrease in a rostral-to-caudal direction. At 24 hpf the transcript is still detectable in the caudal portion of the notochord, in the heart tube, dorsal aorta and its cephalic roots, in the caudal vein, and in the tail bud. At 48 hpf the *Ccdc80* transcript is still faintly detectable in the notochord, it is still present in aorta (including aortic arch) and caudal vein at a lower level and it appears in the inter-somitic caudal vessels. In the heart, is particularly evident in the atrio-ventricular junction and in bulbus arteriosus (Figure 20) Finally, it appears in the fin buds. At 72 hpf the *Ccdc80* transcript is still detectable in heart, dorsal aorta, and barely in the caudal vein and caudal inter-somitic vessels; a signal is present also in the cephalic region, in both the cranial cavity and musculature, and in the region surrounding the notochord. At 120 hpf the

expression is still evident in heart, appears in body muscles, in the swim bladder, and in the eye.

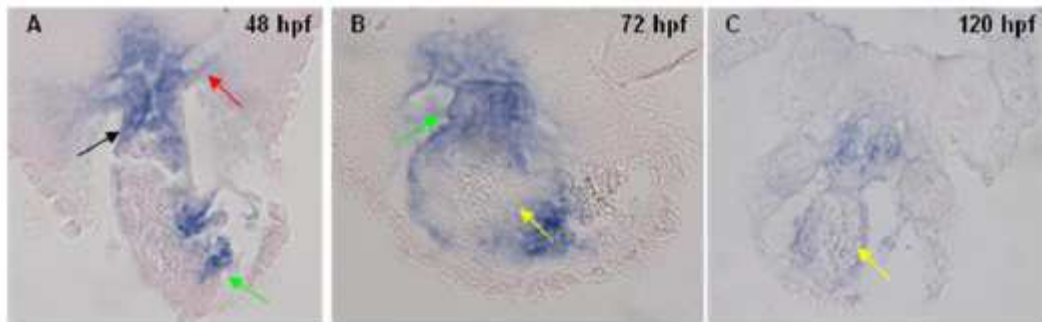


Figure 20

***In vivo* observation of developing embryos in the hatching at 48, 72 and 120 hpf**

A: embryo at 48 hpf. red arrow: aortic arch; green arrow: atrio-ventricular junction; black arrow: bulbus arteriosus. **B:** embryo at 72 hpf. Yellow arrow: atrium; green arrow: atrio-ventricular junction. **C:** embryo at 120 hpf. Yellow arrow: atrium.

The first phenotypical alteration can be observed in morphants during the segmentation period. In comparison to controls, at least 62% of the *Ccdc80*-morphants show multiple defects in the forming somites. Somites morphology is heterogeneously disorganized, with the loss of the proper shape. Somites can appear flat, “packed”, enlarged, with the presence of adjunctive boundaries (sub-segmentated), or without the proper boundaries. The second *in vivo* phenotypical alteration in *Ccdc80*-morphants can be observed in the pharyngula period of development, at 24-26 hpf. Although in *Ccdc80*-morphants the differentiated somites seem almost completely recovered and the embryos show proper motility, at this developing stage 65% of the *Ccdc80*-morphants show curved tails. In the hatching period, at 48 hpf, *Ccdc80*-morphants show defects in the developing heart, with a general enlargement of the atrium (figure 21). Moreover, edemas can be observed in the pericardial cavity, and in the cranial cavity. At 72 hpf, *Ccdc80*-morphants show similar, but more severe cardiac defects with respect to the previous developmental stage, with persistent edemas. Moreover, in the altered *Ccdc80*-morphants, blood stasis is evident in the sinus venosus region (Figure 22). Tails present an extremely heterogeneous morphology. They appear from nearly straight, to bent or curved, both convex and concave, also in the same injected batch of *Ccdc80*-morphants.

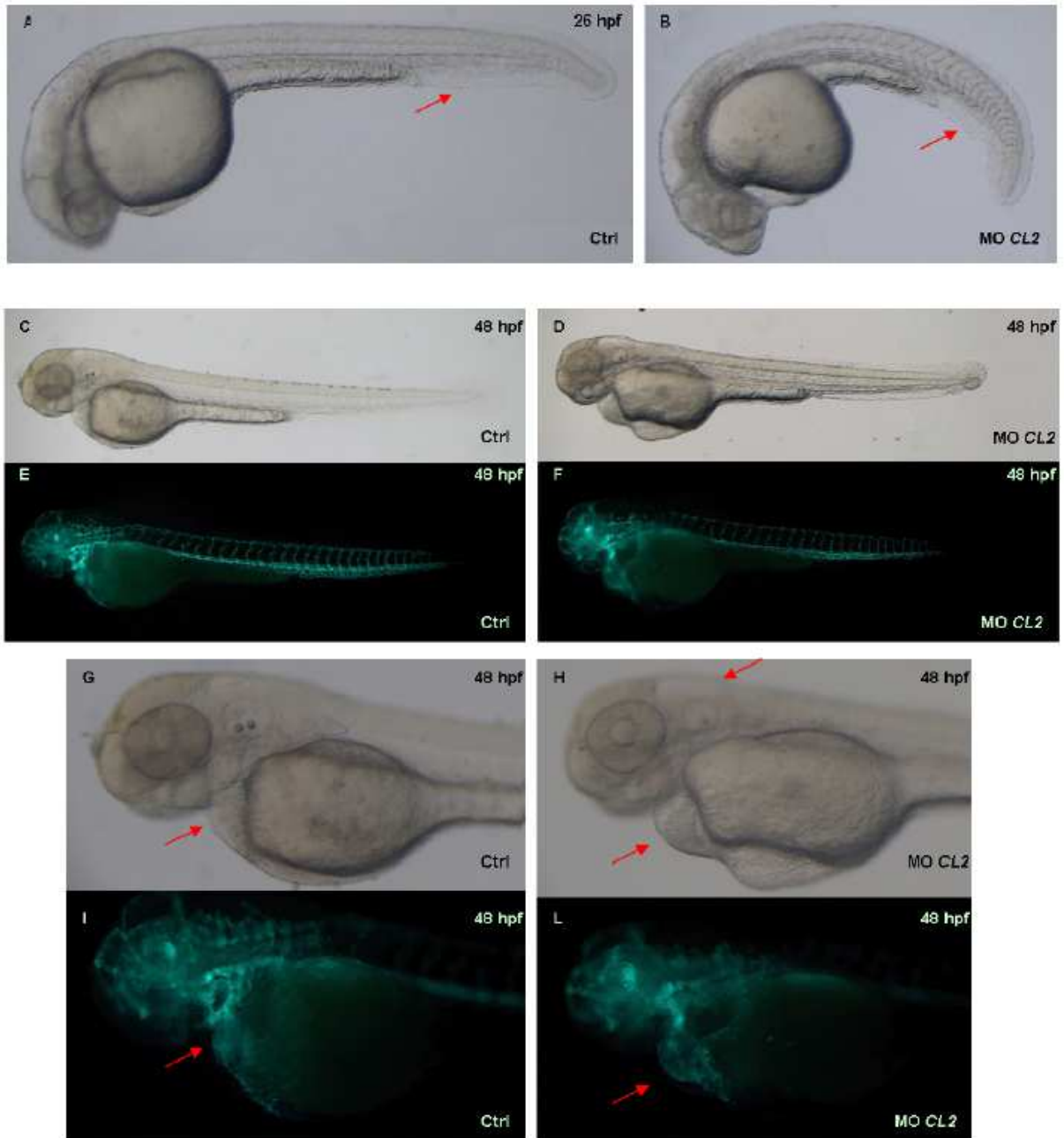


Figure 21

***In vivo* observation of developing embryos in the pharyngula (24 hpf) and hatching (48 hpf) periods**
In vivo images of embryos injected with 1 pmol of the *CL2* (*Ccdc80*) antisense morpholino and controls. Arrows indicate region of interest highlighting defects observed in morphants with respect to controls.
A-B: 24 hpf embryos. **C-L:** 48 hpf *tg(flk1):G-RCFP* embryos. **A, B, C, D, G, H:** bright-field. **E, F, I, L:** fluorescence. **A, C, E, G, I:** controls. **B, D, F, H, L:** morphants. **B:** curved tail. **G, H, I, L:** the same embryos as in **C, D, E, F**, at higher magnification. Morphants show edemas and the atrium enlargement

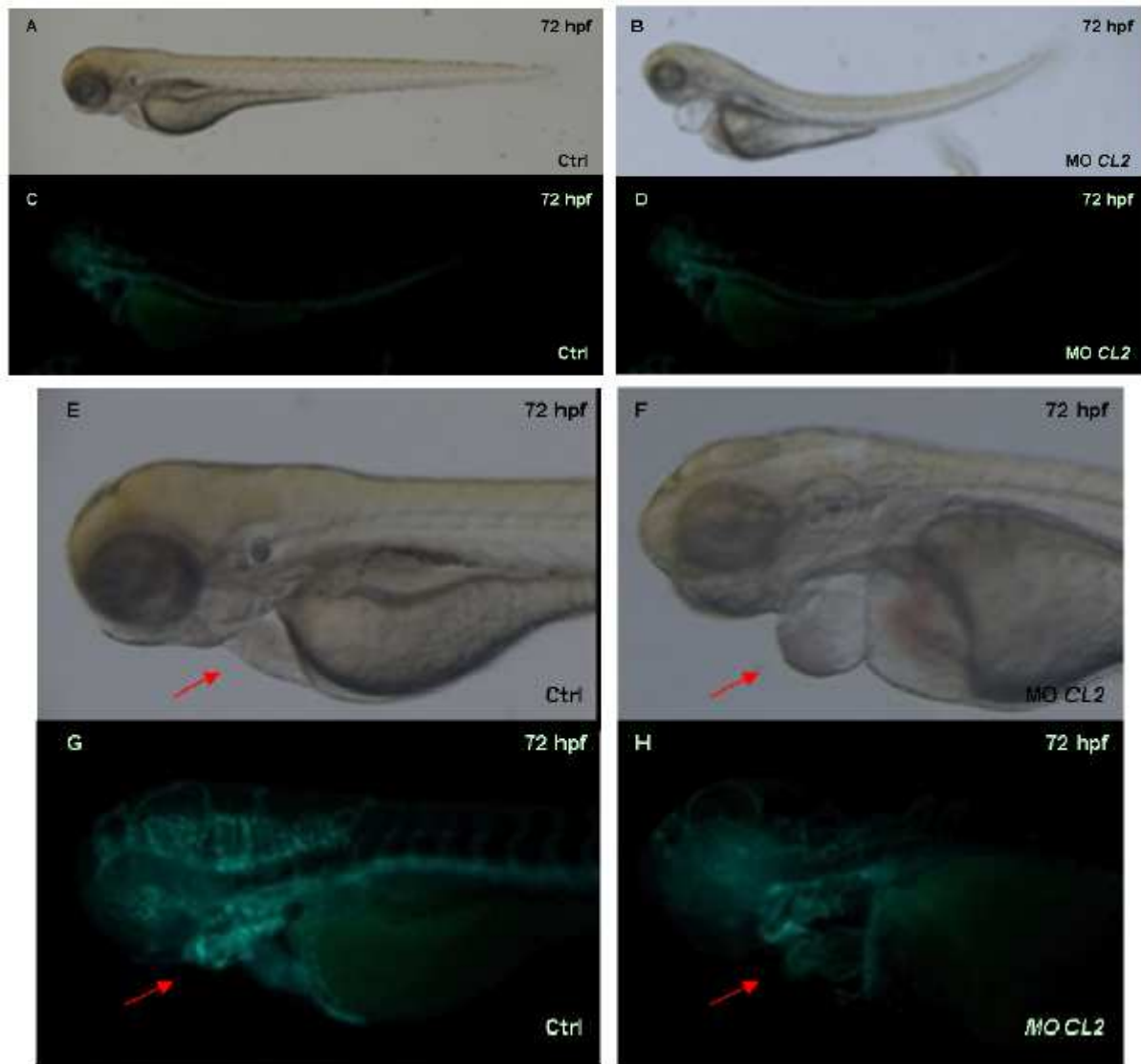


Figure 22

***In vivo* observation of developing embryos in hatching period (72 hpf)**

In vivo images of tg (*fli1*:EGFP)y1 embryos at 72 hpf, injected with 1 pmol of the CL2 (*Ccdc80*) antisense morpholino and controls. Arrows indicate region of interest highlighting defects observed in morphants with respect to controls. **A, B, E, F**: bright-field. **C, D, G, H**: fluorescence. **A, C, E, G**: controls. **B, D, F, H**: morphants. **E, F, G, H**: the same embryos as in **A, B, C, D**, at higher magnification. Morphants show high atrium enlargement with severe edemas, and the enlargement of pericardial chamber.

Cardiac specific markers were evaluated by WISH in *Ccdc80*-silenced embryos:

Nkx2.5 is normally expressed in the cardiac precursor cells at 8-10 somites, when the mesodermal cardiac field is committed. In most of the *Ccdc80*-silenced embryos its expression is properly patterned (Figure 23).

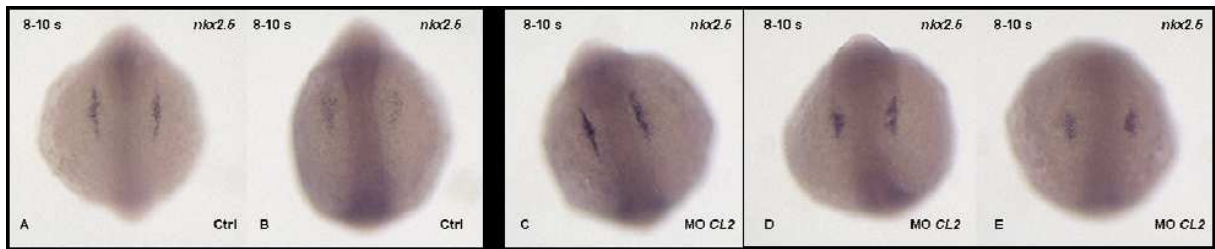


Figure 23

Nkx2.5 expression in silenced CL2 (CCDC80) embryos at 8-10 somites

A-E: *nkx2.5* expression pattern analyzed by Whole-Mount *in situ* hybridization. Embryos at 8-10 somites, injected with Ccdc80 morpholino (**C-E**), and controls (**A, B**) are shown. Dorsal view, anterior is up. **A:** controls with no alterations. **B:** controls with minimal alteration. **C:** morphants with no alterations. **D-E:** morphants with minimal alteration.

Cmlc 2 was investigated in Ccdc80-silenced embryos at 26 hpf, 48 hpf and 72 hpf, in order to evaluate the cardiac shape. At 26 hpf, 60% of the morphants show defects in heart tube morphology, while the same occurs in 9% of the controls (Figure 24). At 48 hpf, nearly 70% of the morphants show impaired cardiac looping or shape, while the same occurs in 8% of the controls (Figure 25). At 72 hpf, 41% of the morphants show heart defects in shape and / or looping, while the same occurs in 23% of the controls (Figure 26).



Figure 24

***Cmlc 2* expression in silenced CL2 (Ccdc80) embryos at 26 hpf**

A-D: *cmlc 2* expression pattern analyzed by Whole-Mount *in situ* hybridization. Embryos at 26 hpf, injected with Ccdc80 morpholino (**B-D**), and control (**A**) are shown. Dorsal view, ventral is down, left is right. **A:** controls with no alterations in heart tube. **B-D:** morphants with alteration in heart tube, which is not properly oriented or shaped.



Figure 25

***Cmlc 2* expression in silenced *Ccdc80* embryos at 48 hpf**

A-D: *cmlc 2* expression pattern analyzed by Whole-Mount *in situ* hybridization. Embryos at 48 hpf, injected with *Ccdc80* morpholino (**B-D**), and controls (**A**) are shown. Ventral view, head is up. **A:** 92 % of controls with no alterations. **B:** 33% of morphants with no alteration. **C, D:** 70% morphants showing enlarged atrium and / or impaired looping.

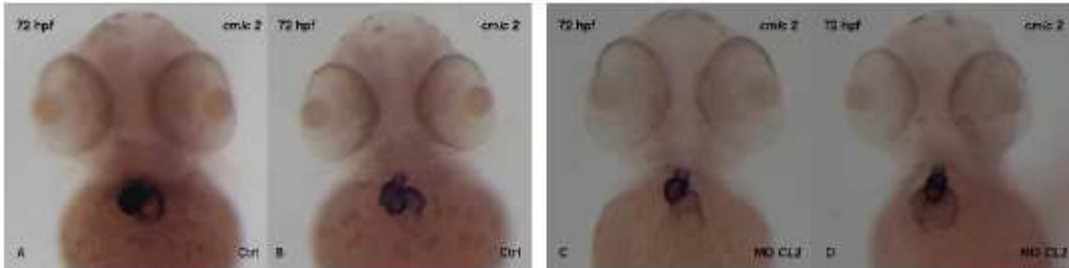


Figure 26

***Cmlc 2* expression in silenced CL2 (*Ccdc80*) embryos at 72 hpf**

A-D: *cmlc 2* expression pattern analyzed by Whole-Mount *in situ* hybridization. Embryos at 72 hpf, injected with *Ccdc80* morpholino (**B-D**), and controls (**A**) are shown. Ventral view, head is up. **A:** 77% controls showing no alterations. **B:** 23% controls showing minimal cardiac alterations. **C, D:** 41% morphants showing cardiac defects in shape and/or looping.

Amhc, was investigated in *CCDC80*-silenced embryos at 48 hpf. At this developing stage it is expressed in atrium. 21% of morphants show an enlarged atrium, while the same can be observed in 12.5% of the controls (Figure 27).

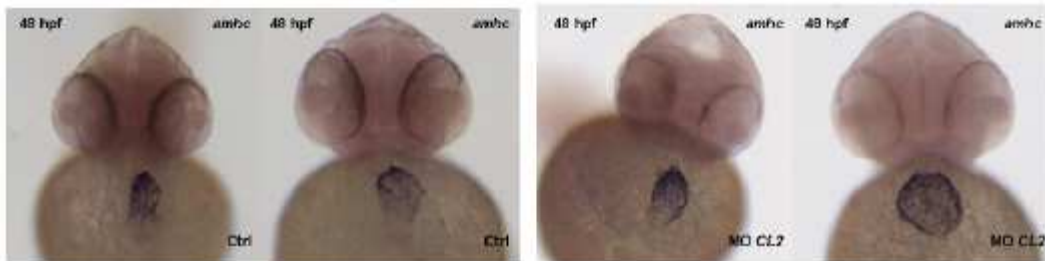


Figure 27

***Amhc* expression in silenced CL2 (*Ccdc80*) embryos at 48 hpf**

A-D: *amhc* expression pattern analyzed by Whole-Mount *in situ* hybridization. Embryos at 48 hpf, injected with *Ccdc80* morpholino (**C-D**), and controls (**A-B**) are shown. Ventral view, head is up. **A:** 87.5% of controls with no alterations. **B:** 12.5% of controls showing enlarged atrium. **C:** 79% of morphants showing no atrial defects. **D:** 21% of morphants showing enlarged atrium.

HrT, was investigated at 26 hpf. At this developmental stage, it is expressed in the aortic root and in heart. No defects are detectable in the aortic expression pattern, while the cardiac expression

pattern is impaired in 21% of the morphants. 100% of the controls show no defects in aorta and in the cardiac expression pattern (Figure 28).

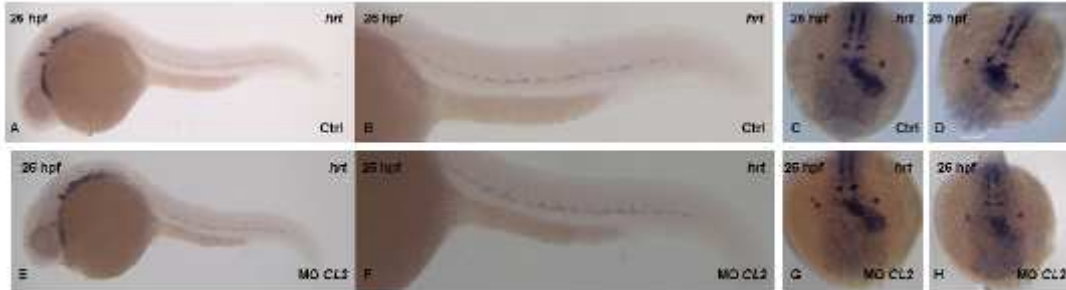


Figure 28

***HrT* expression in silenced *Ccdc80* embryos at 26 hpf**

A-H: *hrT* expression pattern analyzed by Whole-Mount *in situ* hybridization. Embryos at 26 hpf, injected with *Ccdc80* morpholino (**E-H**), and controls (**A-D**) are shown. **A, B, E, F:** lateral view, anterior is left. **C, D, G, H:** Dorsal view, ventral is down, left is right. **A-B:** 100% controls showing no alterations in dorsal aorta. **C:** 84% controls showing no heart alterations. **D:** 16% of controls showing impaired cardiac expression pattern. **E-F:** 100% morphants showing no alterations in dorsal aorta. **G:** 79 % of morphants showing no heart alterations. **H:** 21% of morphants showing impaired cardiac expression pattern.

Immunohistochemistry for *Ccdc80* in adult zebrafish heart appears slight positive in the ventricle with higher level of expression in atrium and atrio-ventricular junction (Figure 29).

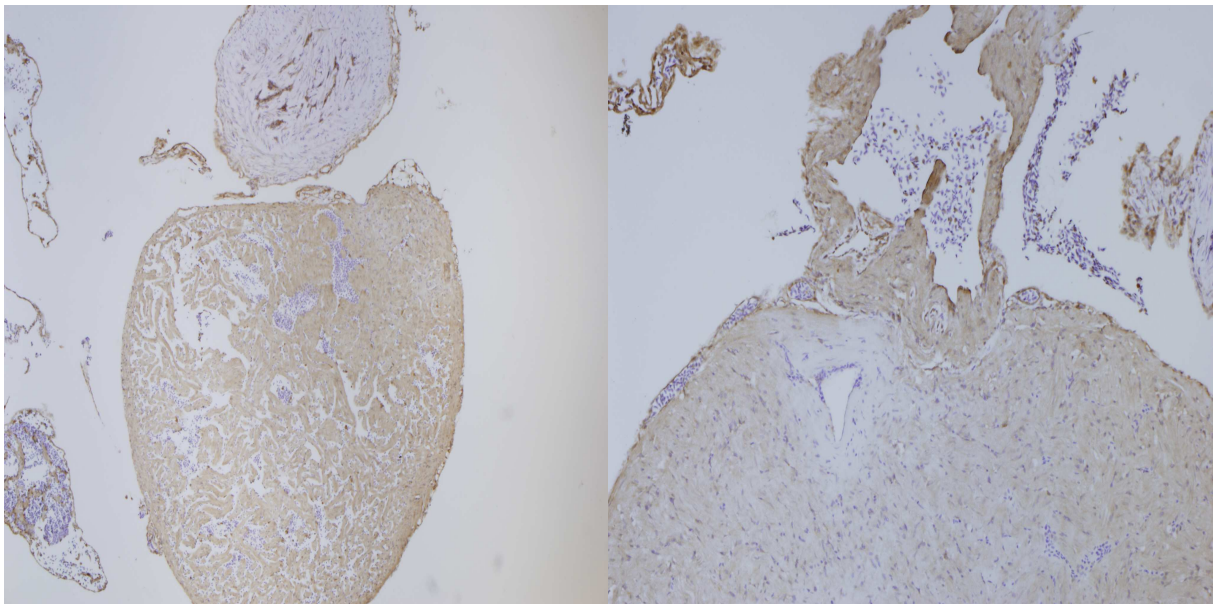


Figure 29

***Ccdc80* expression in zebrafish adult heart, immunohistochemistry.**

Left panel 80x, right panel 160x.

6.2 Expression in normal heart

The expression of Ccdc80 protein in normal hearts of rats (6 samples collected) is very low with a patchy cytoplasmic pattern both in atria and ventricles. Focal groups of cardiomyocytes appear heavy stained at the atrioventricular junction (Figure 30 and 31).

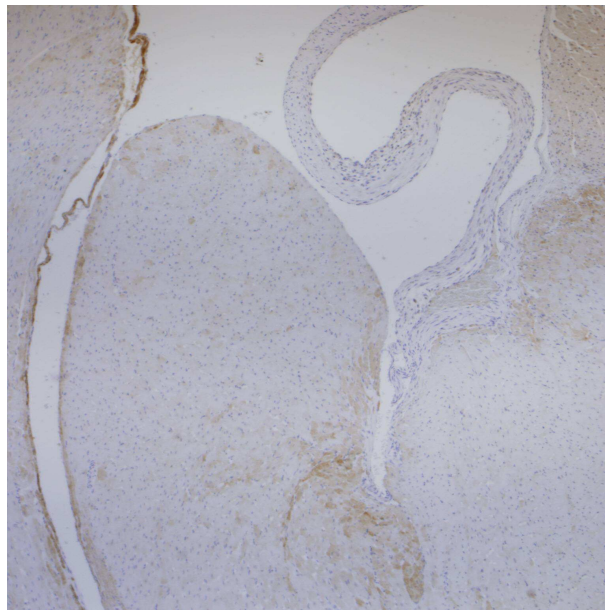


Figure 30
Ccdc80 expression in adult rat heart, immunohistochemistry, 80x.

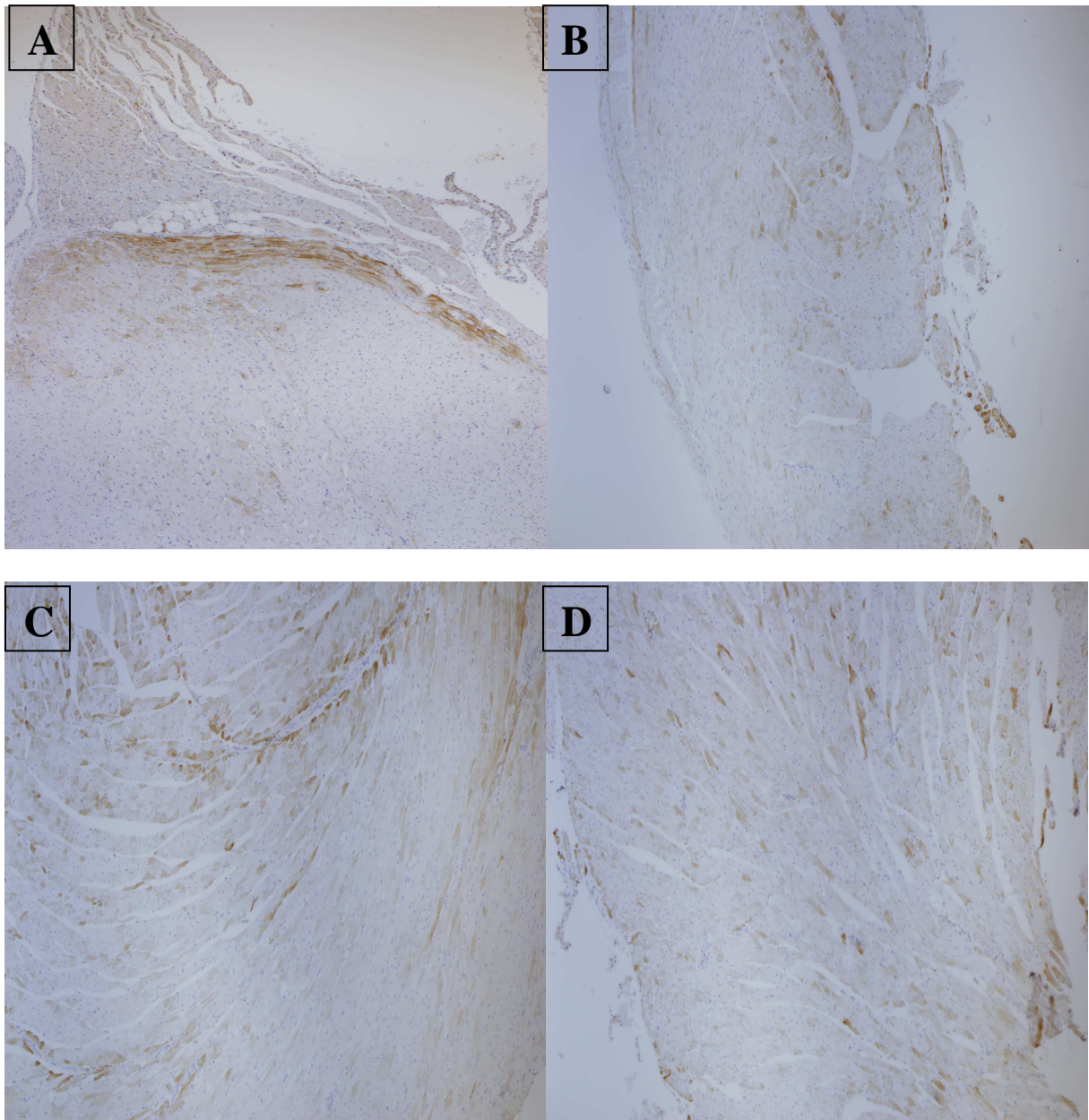


Figure 31
Ccdc80 expression in adult rat heart (80x), immunohistochemistry.
Panel A: atrioventricular junction; Panel B: right ventricle;
Panel C: septum; Panel D: left ventricle.

To evaluate the expression of Ccdc80 protein in normal human hearts we performed immunohistochemistry on 2 hearts from healthy donors, which were not transplanted for logistic problems.

Atria cardiomyocytes showed a cytoplasmic positivity with a patchy pattern: most of them exhibited a negative or mild staining, while only some of them showed strong positivity (Figure 32).

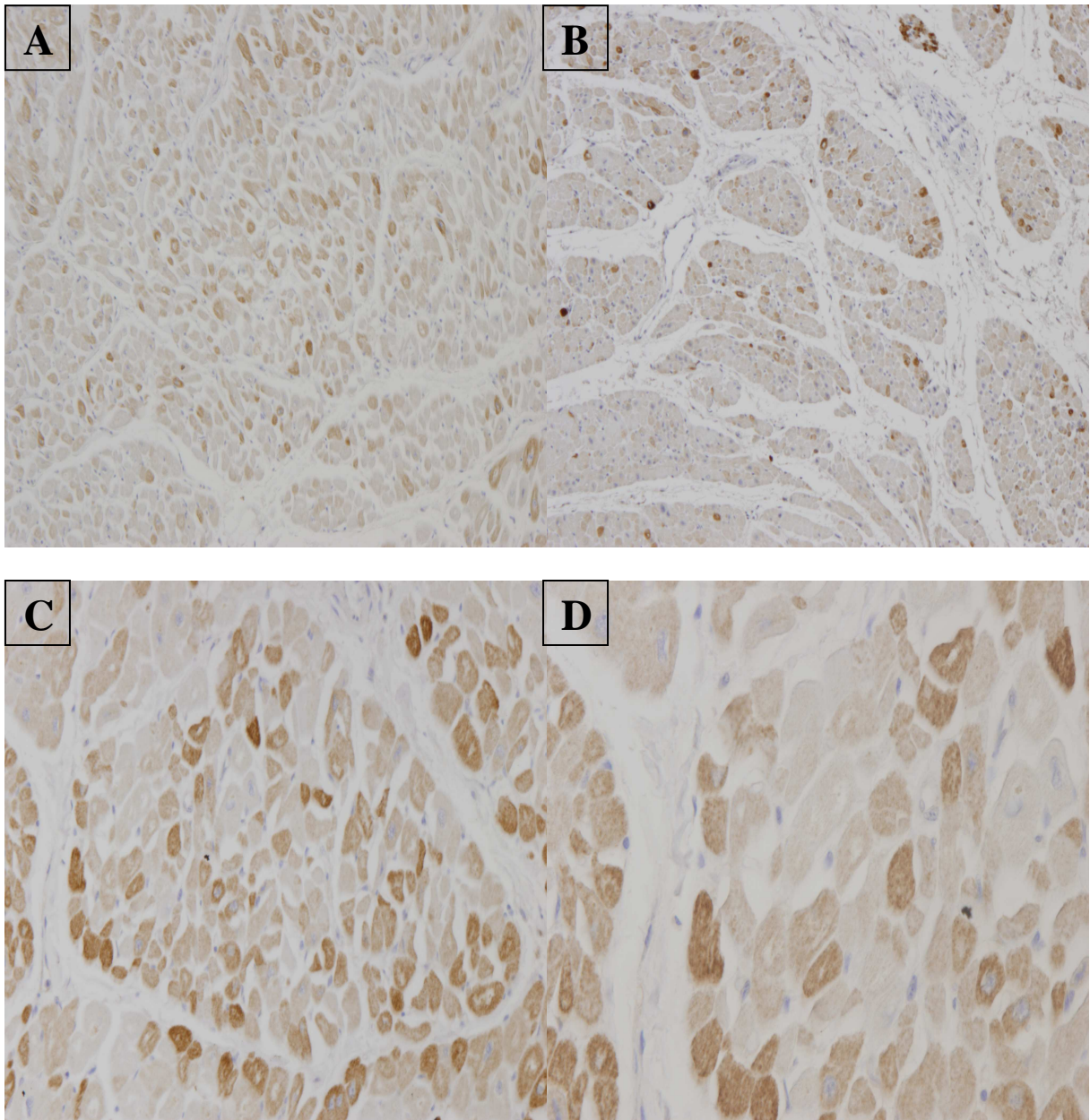


Figure 32
Ccdc80 expression in adult human atria, immunohistochemistry.
Panel A: left atrium, 80x; Panel B: right atrium, 80x
Panel C: left atrium, 160x; Panel D: left atrium, 320x.

Ventricles showed a homogeneous moderate staining, with cytoplasmic pattern and isolated myocytes that appeared negative (Figure 33 and 34).

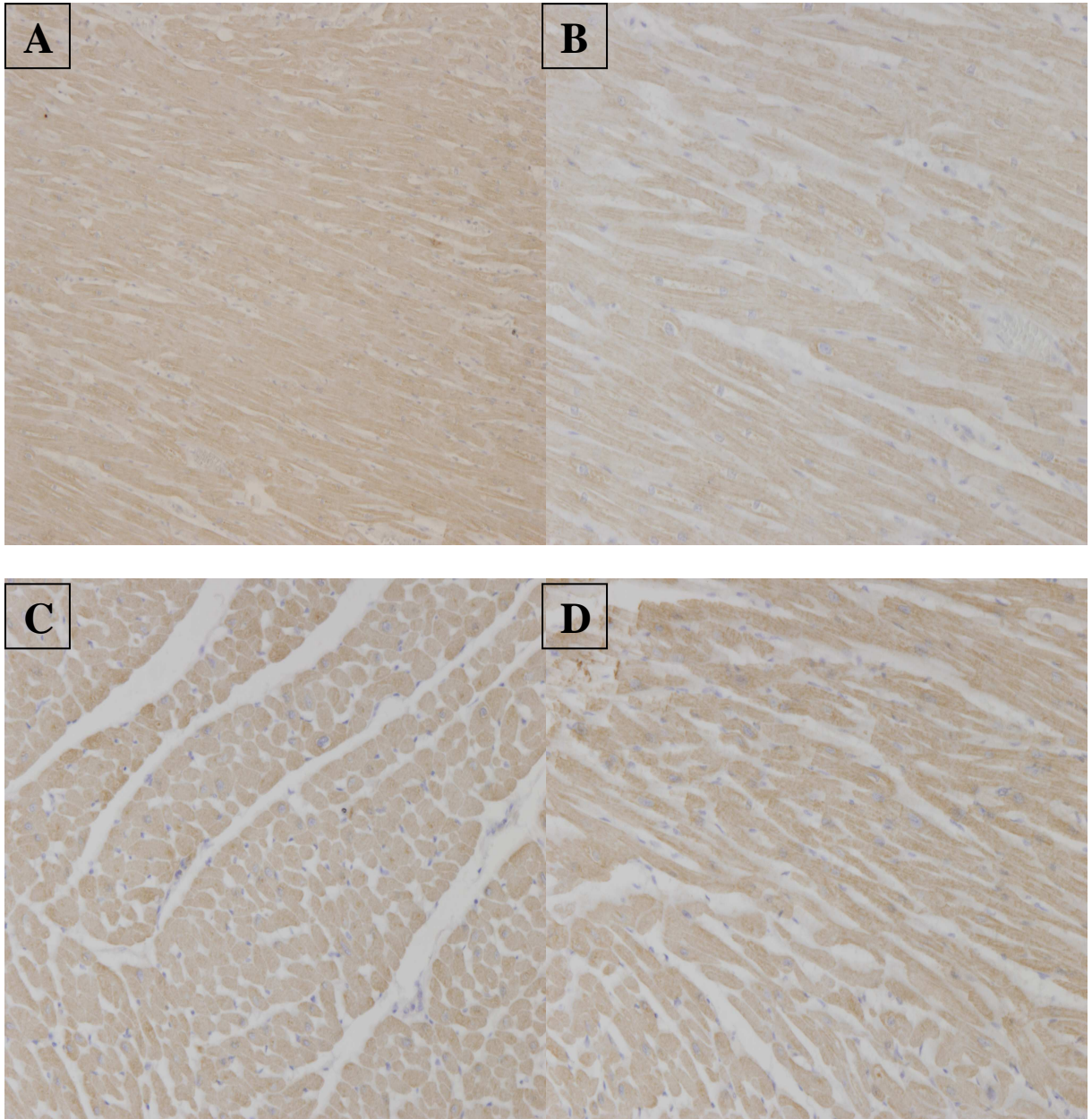


Figure 33
Cdc80 expression in adult human ventricles, immunohistochemistry.
Panel A: left ventricle, 80x; Panel B: left ventricle, 160x
Panel C and D: right ventricle, 160x.

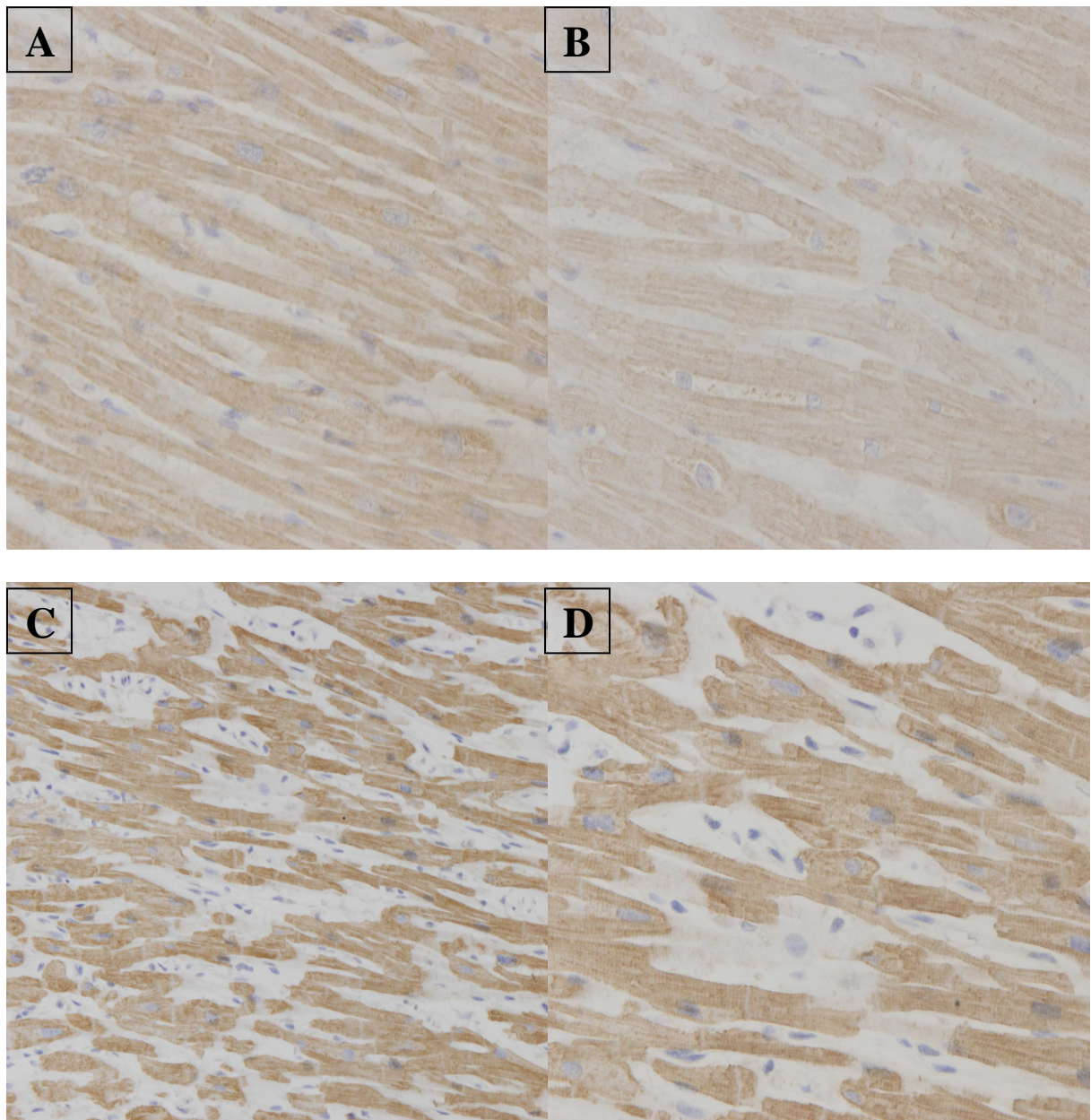


Figure 34
Ccdc80 protein expression in adult human ventricles.
High-power view of myocytes, with some of them negative to immunohistochemistry.
 Panel A: left ventricle, 320x; Panel B: right ventricle, 320x;
 Panel C: left ventricle, 160x. Panel D: left ventricle 320x.

Immunofluorescence analysis confirmed the cytoplasmic localization of the protein; no positivity was detected at nuclear level. Significant co-localization was found with sarcomeric proteins both in humans and rats, in particular with β -myosin, sarcomeric actin and troponin (Figure 35 - 37). Weaker co-localization was seen with tropomyosin (Figure 38) and desmin (data not shown).

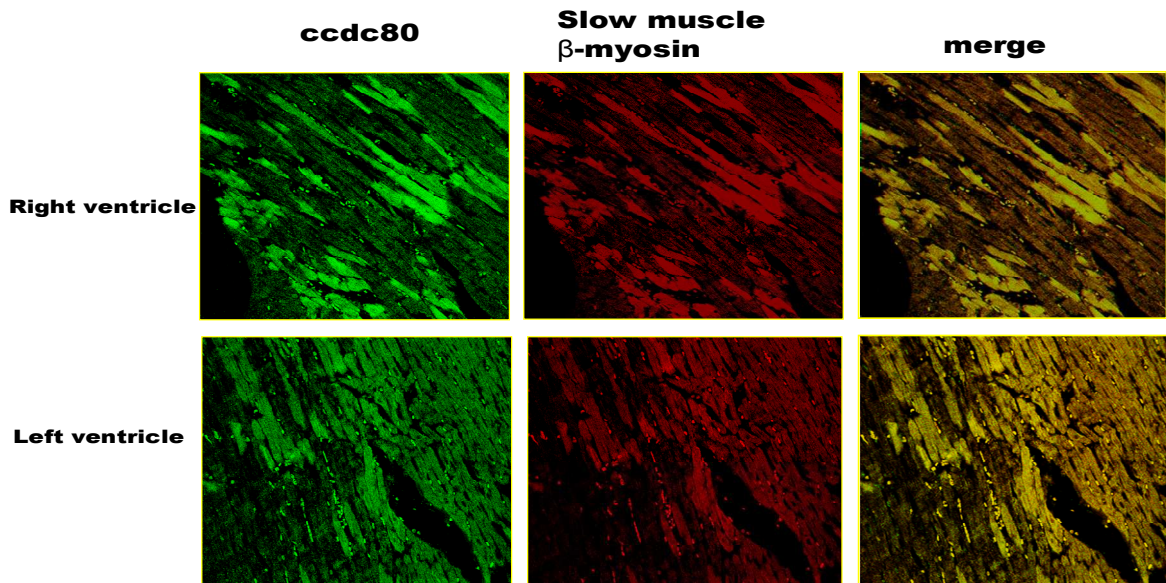


Figure 35
Immunofluorescence of Ccdc80 protein, co-localization with β-myosin, rat sample.

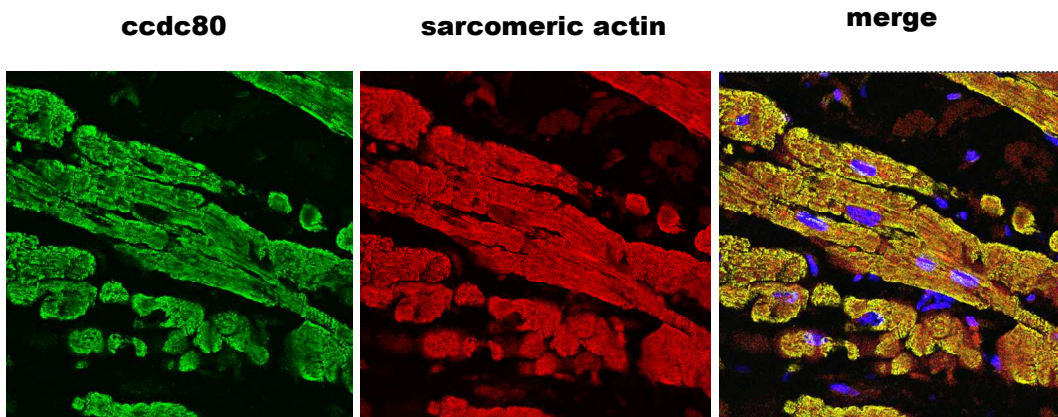


Figure 36
Immunofluorescence of Ccdc80 protein, co-localization with sarcomeric actin, left ventricle from human sample.

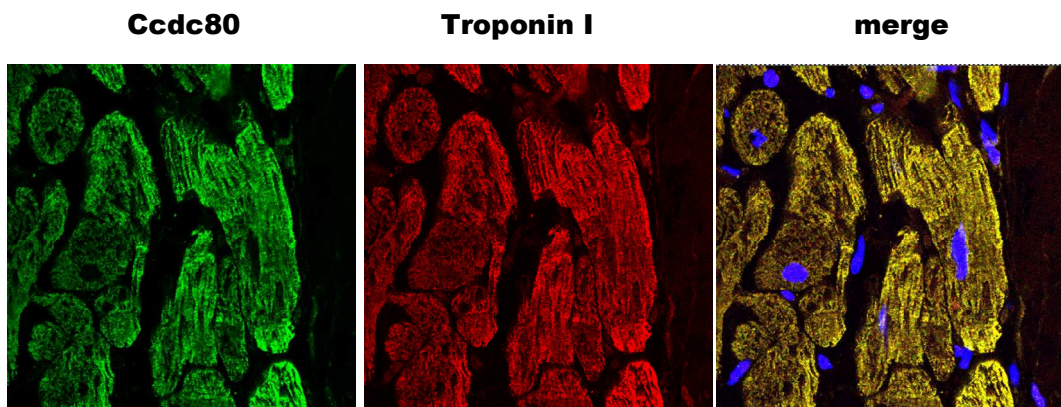


Figure 37
Immunofluorescence of Ccdc80 protein, co-localization with troponin I, left ventricle from human sample.

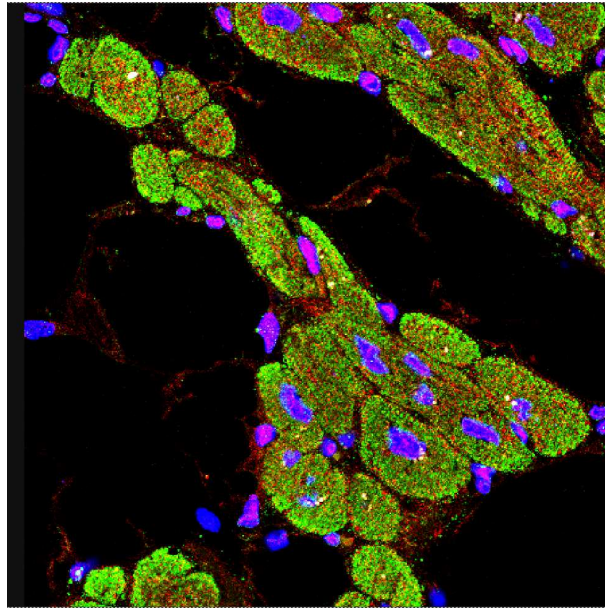


Figure 38

Merge image of immunofluorescence of Ccdc80 protein, co-localization with tropomyosin, human sample.

Northern blot analysis in normal human heart showed a greater expression of the Ccdc80-RNA in atria compared to ventricles (Figure 39).

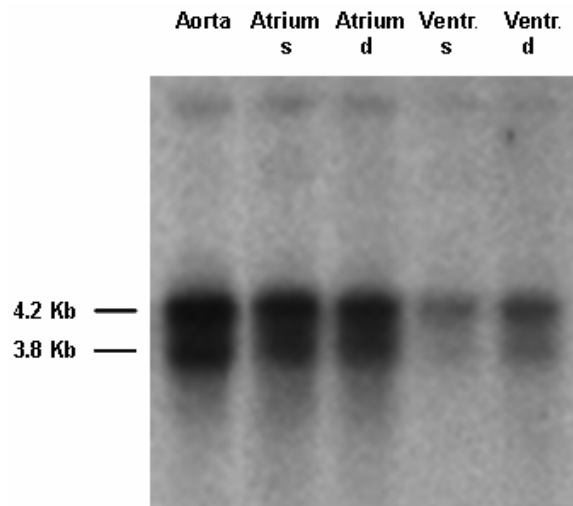


Figure 39

Northern Blot of Ccdc80 RNA expression.

Western blot analysis confirmed the presence of the Ccdc80 protein (108 Kd) in all specimens (atria and ventricles) with similar expression levels. We also found an isoform of 90 kd in the left atrium (Figure 40). Giving that Northern blot analysis showed a greater expression of

Ccdc80 RNA in atria compared to ventricles, its is possible to assume that an amount of the protein, produced by atria, could be secreted.

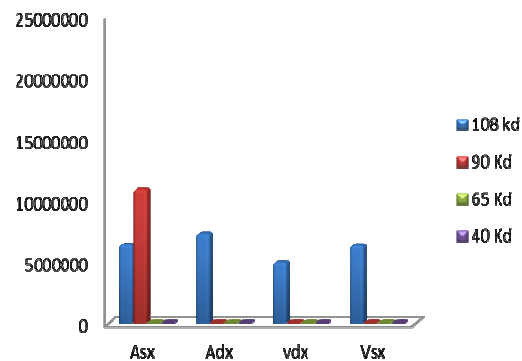


Figure 40
Western Blot of Ccdc80 protein expression (graphic representation).

6.3 Expression in failing heart

Compared to normal, MC-treated rats with right ventricle hypertrophy and failure showed an overexpression of Ccdc80 protein. Right ventricles of the 6 analysed rats showed a clear cut increase in numbers and expression of positive myocytes in comparison to controls (Figure 41). These findings appeared less evident in left ventricle and septum (Figure 42, see also Figure 47 and Table 1 for comparison).

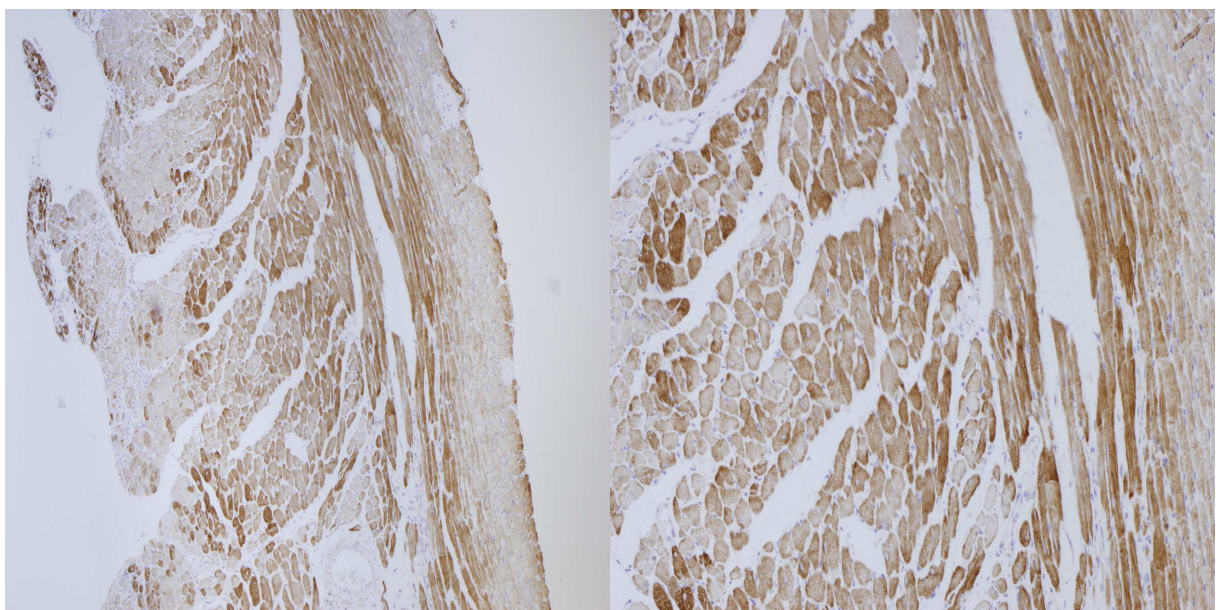


Figure 41
Ccdc80 protein expression in rat with heart failure induced by MCT, right ventricle, immunohistochemistry. Left panel: 80x; right panel: 160x.

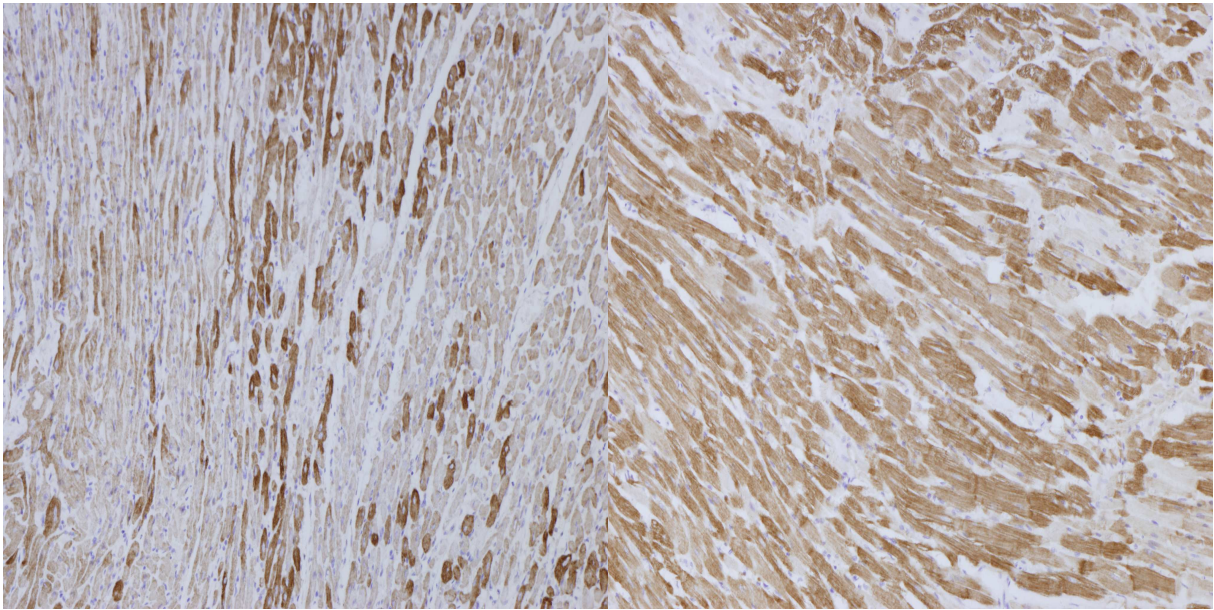


Figure 42
Ccdc80 protein expression in rat with heart failure induced by MCT,
immunohistochemistry, 160x.
 Left panel: septum; right panel: left ventricle.

Atria from 14 samples of human patients affected by DCM showed a homogenous increase of the Ccdc80 protein expression level in comparison to normal samples: almost all cardiomyocytes expressed the cytoplasmic protein from a moderate to strong level intensity (Figure 43 and 44, see also Figure 47 and Table 1 for comparison).

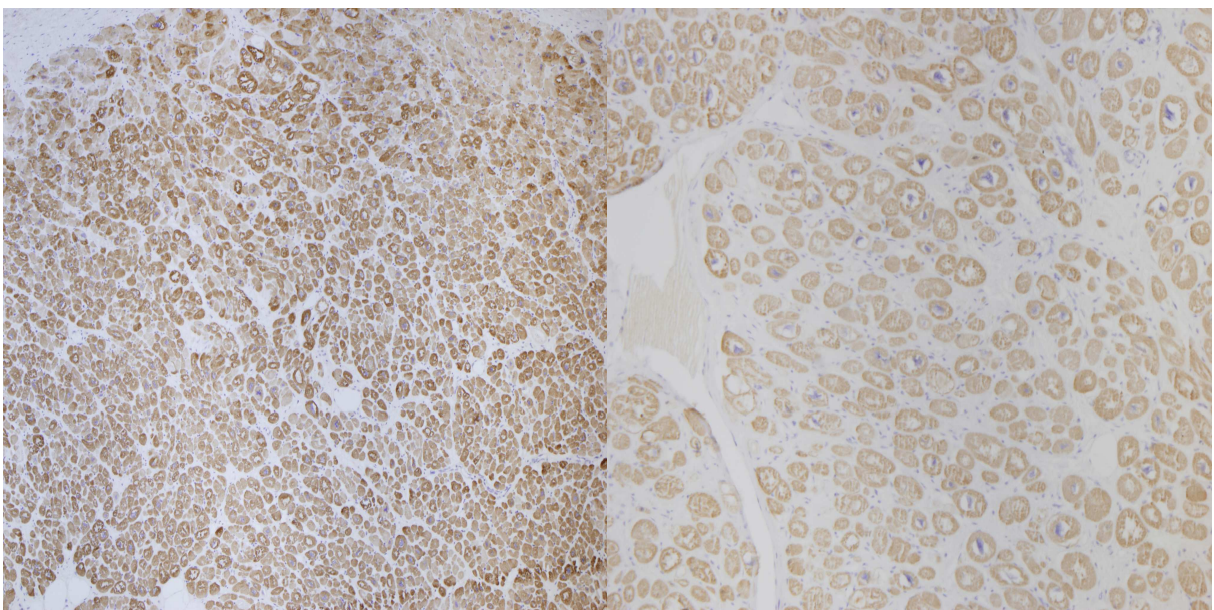


Figure 43
Ccdc80 protein expression in human sample of DCM,
immunohistochemistry, 80x.
 Left panel: left atrium; right panel: right atrium.

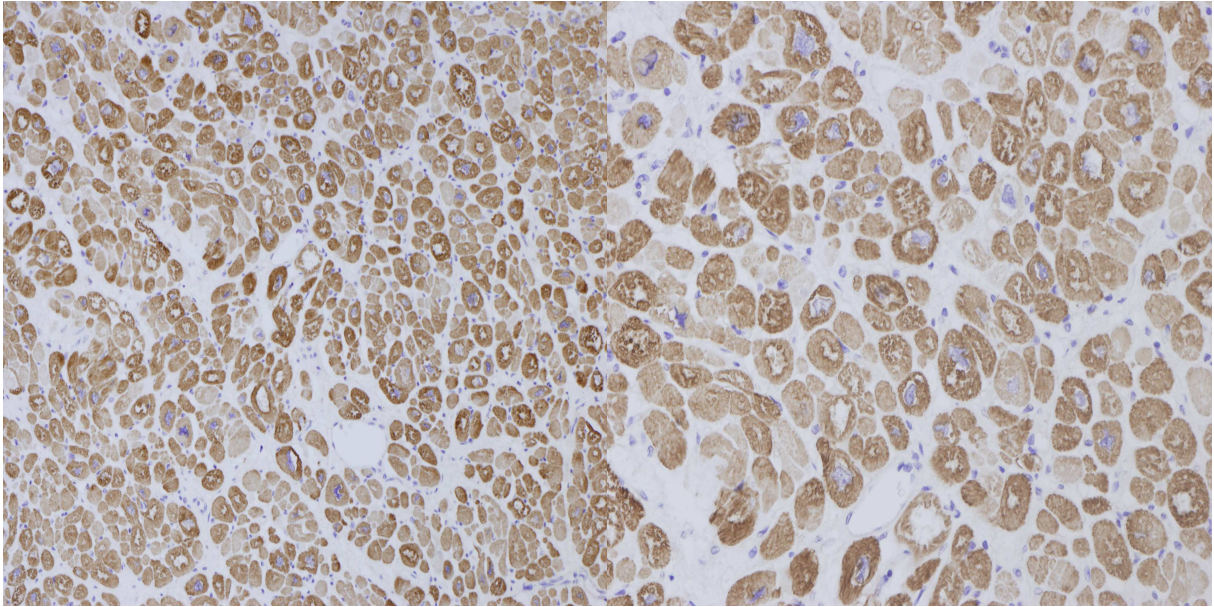


Figure 44
Ccdc80 protein expression in human sample of DCM,
immunohistochemistry, left atrium.
Left panel: 160x; right panel: 320x.

In ventricles less clear differences appeared when comparing normal to DCM samples: the pattern of positive staining remained homogeneous without increased expression of Ccdc80 protein. However, there was no evidence of negative cardiomyocytes as seen in normal ventricles (Figure 45 and 46, see also figure 47 and Table 1 for comparison).

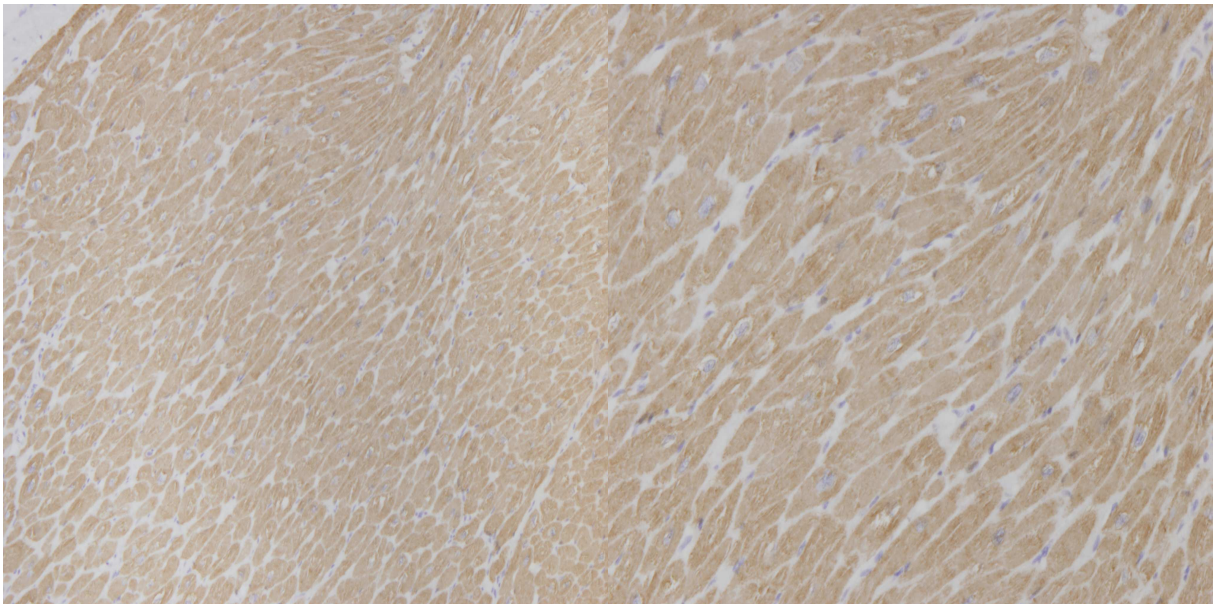


Figure 45
Ccdc80 protein expression in human sample of DCM,
immunohistochemistry, right ventricle.
Left panel: 80x; right panel: 160x.

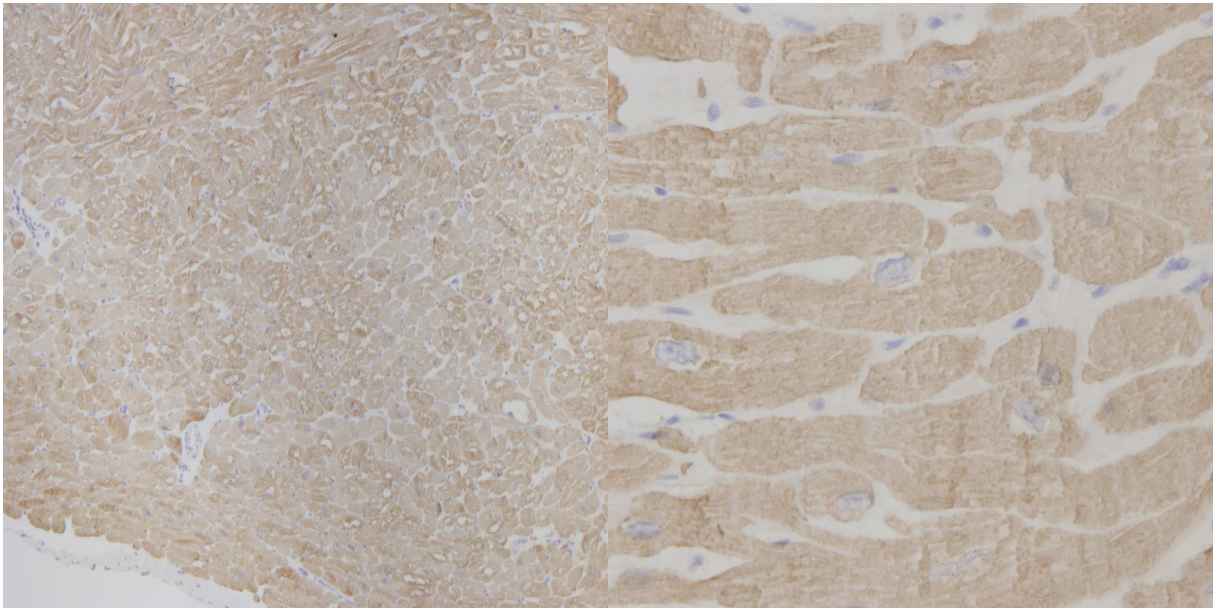


Figure 46
Ccdc80 expression in human sample of DCM,
immunohistochemistry, left ventricle.
 Left panel: 80x; right panel: 320x.

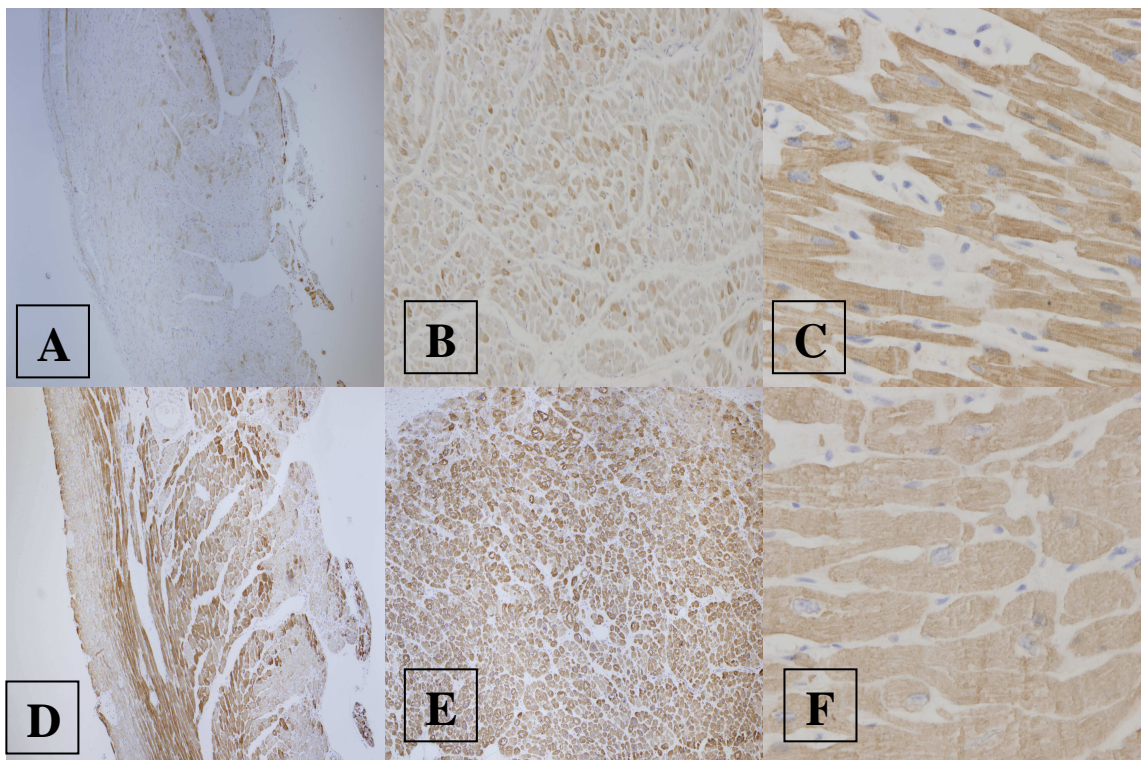


Figure 47
Summary of Ccdc80 protein expression in normal (upper panels) versus
pathological samples (lower panels); immunohistochemistry.
 Panel A, D : rat right ventricle, 80x; Panel B, E: Human left atrium, 80x;
 Panel C, F : human left ventricle, 320 x.

We also performed western blot analysis to quantify Ccdc80 protein expression in the pathological tissue. The blot showed a significant overexpression of Ccdc80 protein in both

atria and ventricles with a predominant expression in ventricles (Figure 48). It is important to underline here that, beyond the overexpression of the main isoform of the protein (108 Kd), the pathological samples also expressed different isoforms of the protein (40, 65 and 90 Kd), compared to normal samples. These isoforms are probably the results of intracellular post-transcriptional elaboration, such as cleavage or phosphorylation (65Kd).

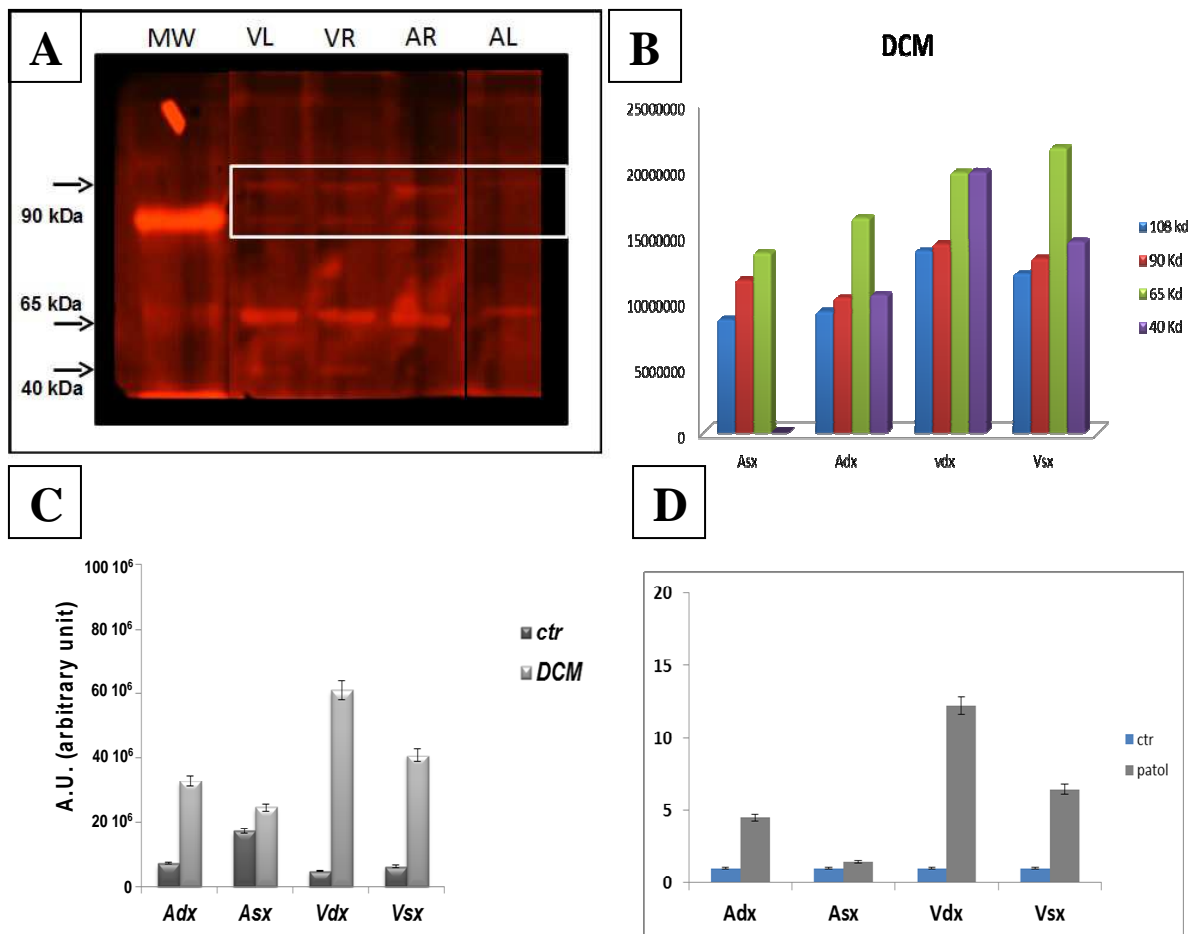


Figure 48

Western Blot of Cdc80 protein in DCM.

Panel A: different expression isoforms of the protein . MW, molecular weight; VL, left ventricle; VR, right ventricle; AR, right atrium; AL, left atrium. Arrows indicate 108, 65 and 40 Kd. The 90 Kd band coincide with marker of molecular weight.

Panel B: graphic representation of findings of panel A.

Panel C: comparison of protein expression in DCM vs normal samples. Absolute values, expressed in arbitrary units.

Panel D: expression levels compared to normal samples, normalized to 1.

6.4 Skeletal muscle

We also performed immunohistochemistry in samples of normal skeletal muscle and in pathological samples from patients affected by Duchenne muscular dystrophy.

Normal muscle showed positive cells with intense cytoplasmic positivity alternated to negative cells. In positive myocytes, staining is particularly strong in proximity of the cytoplasmic membrane (Figure 49). To rule out that this pattern could be linked to fibers properties, we also carried out immunohistochemistry for slow fibers (images not shown): no significant association between Ccdc80 positive fibers and either slow or fast myocytes was found.

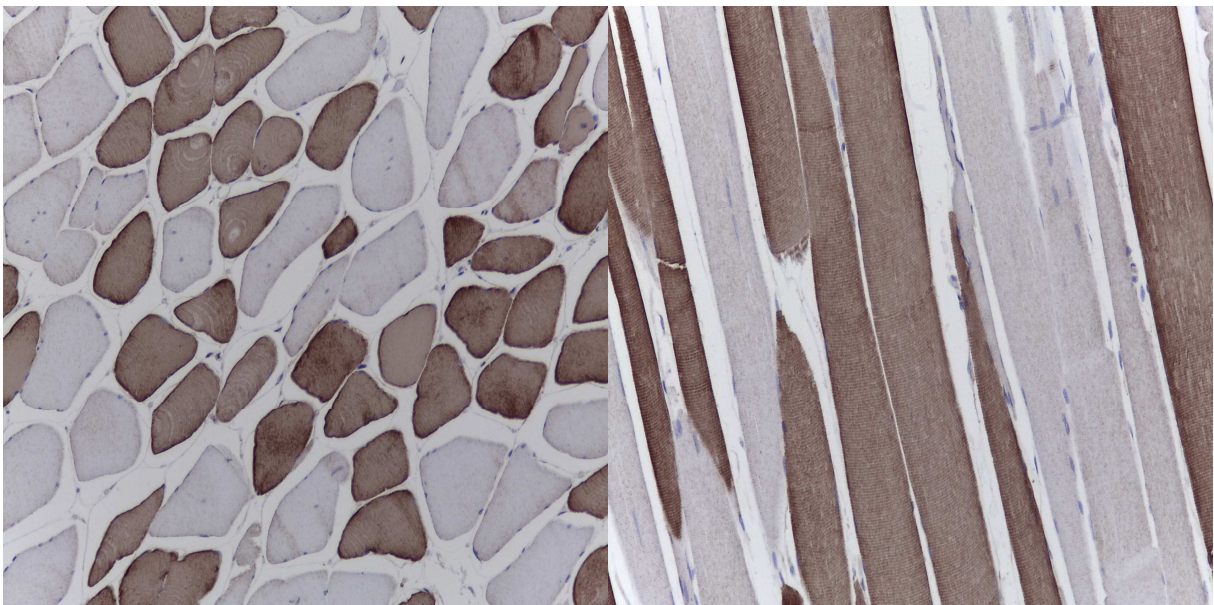


Figure 49

Ccdc80 protein expression in normal skeletal muscle; immunohistochemistry.
Left panel: transverse myocyte cut , 80x; right panel: longitudinal myocyte cut, 80x.

Immunofluorescence analysis on normal sample confirmed the cytoplasmic localization of the protein, particularly in proximity of the cytoplasmic membrane (Figure 50).

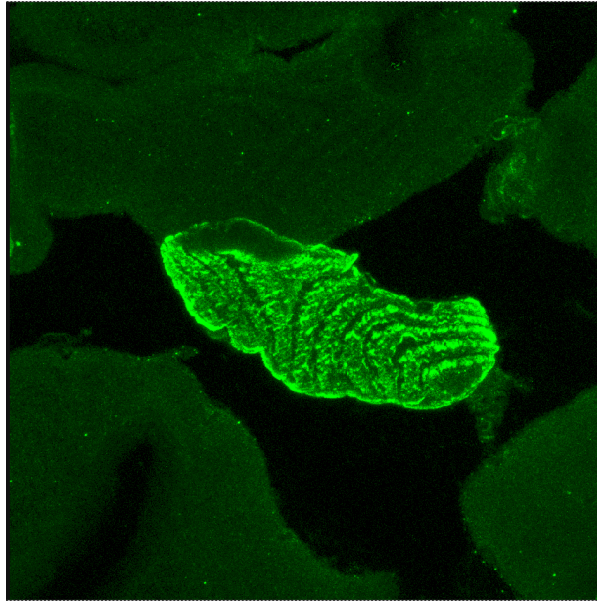


Figure 50
Ccdc80 protein expression in normal skeletal muscle; immunofluorescence.

The pathological skeletal muscles showed almost all myocytes expressing the protein with a moderate to strong positivity (Figure 51).

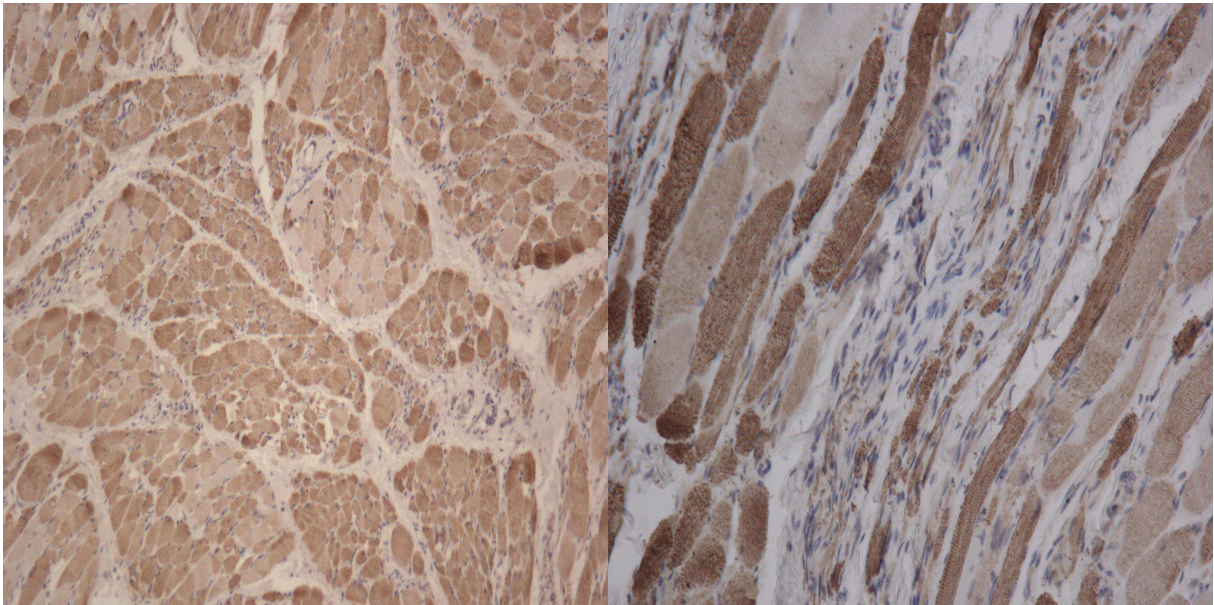


Figure 51
Ccdc80 protein expression in pathological skeletal muscle (Duchenne muscular dystrophy); immunohistochemistry; left panel: transverse myocyte cut, 20 x; right panel longitudinal myocyte cut, 40x.

Sample	Normal pattern	N	Pathological pattern	N
<i>Rat atria</i>	Negative staining, few myocytes with moderate/strong positivity	6	NA	
<i>Rat right ventricle</i>	Negative staining, few myocytes with moderate/strong positivity	6	Patchy, mild/moderate staining, few groups of myocytes with strong positivity	6
<i>Rat septum and left ventricle</i>	Negative staining, few myocytes with moderate/strong positivity	6	Patchy, mild/moderate staining, few groups of myocytes with strong positivity	6
<i>Human atria</i>	Patchy, negative or mild staining, few groups of myocytes with strong positivity	2	Homogeneous, moderate to strong staining	14
<i>Human ventricles</i>	Homogeneous moderate staining, isolated myocytes negative	2	Homogeneous moderate staining, no evidence of isolated negative myocytes	14
<i>Human skeletal muscle</i>	Positive myocytes with moderate/strong staining alternated to negative ones	2	Almost all myocytes with a moderate to strong staining	2

Table 1
Summary of Ccdc80 protein immunohistochemical expression
in normal versus pathological samples.

7. Discussion

Zebrafish heart is the first organ to form and function during embryonic development [126]. The cardiac field is located within the lateral plate mesoderm and is specified in the segmentation period. In early somitogenesis the cardiac precursors converge in the embryonic midline and are recognizable for the expression of the abovementioned transcription factor *nkx2.5* [122]. Endocardium and myocardium, with the specification of atrial and ventricular cell populations, are soon defined, and at 24 hpf the heart tube assembly is completed and shows regular contractions (Figure 52). Within the same developing stage, also axial vessels complete and, just after that, trunk circulation begins. At 48 hpf cardiac looping is completed and the formation of the cushions at the atrio-ventricular junction starts. These cushions will later differentiate into the atrio-ventricular valve.

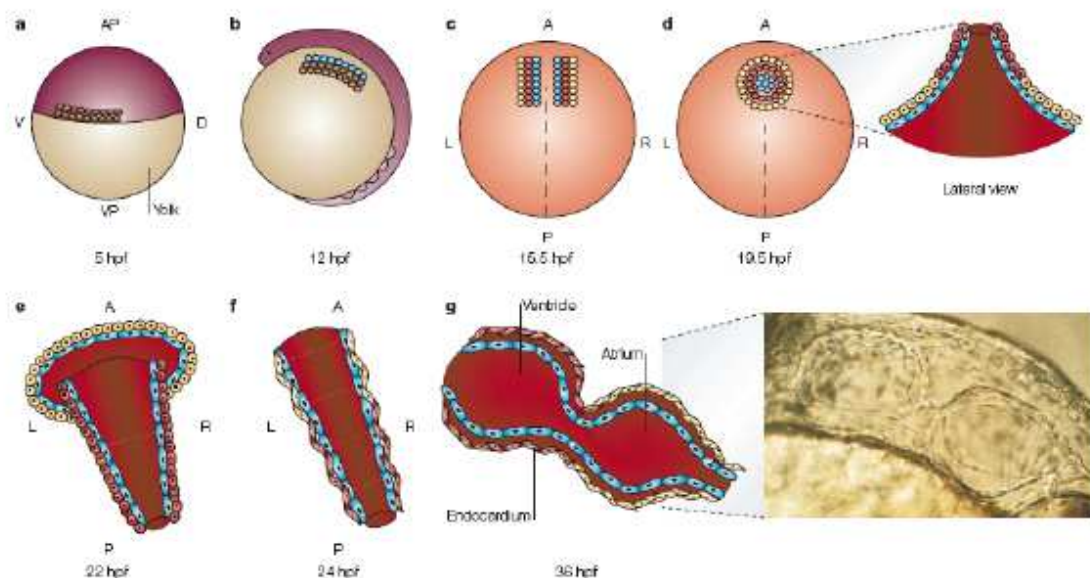


Figure 52

Zebrafish heart development

a | Just before gastrulation, 5 h post fertilization (hpf), the heart progenitor cells are located throughout the ventral and lateral regions of the embryo. **b** | After involution, these cells converge towards the embryonic axis and reach their destination at the level of the future hindbrain by the five-somite stage (~12 hpf). Three rows of cells are represented at this stage, the endocardial precursors (blue) lie most medially and the myocardial precursors most laterally. **c** | By the 13-somite stage (15.5 hpf), the myocardial precursors have segregated into preventricular (red) and preatrial (yellow) groups, although this segregation might well happen earlier. **d** | Starting at 19 hpf, the myocardial precursors merge posteriorly to form a horseshoe-shaped structure. By 19.5 hpf, as anterior cells migrate medially, the horseshoe transforms into a cone with the ventricular cells (red) at its centre and apex, and the atrial cells (yellow) at its base. The endocardial cells (blue) line the inside of the cone. **e** | Next, the cone telescopes out to form a tube. The ventricular end of the heart tube assembles first, followed by the atrial end. **f** | By 24 hpf, the tube lies along the anteroposterior axis with the atrial end to the left of the midline. Subsequently, by 30 hpf, visibly distinct ventricular and atrial chambers form. **g** | By 36 hpf, the heart

undergoes looping morphogenesis. and, by 48 hpf, functional valves are formed. (A, anterior; AP, animal pole; D, dorsal; P, posterior; V, ventral; VP, vegetal pole; L, left; R, right.).

In zebrafish, our findings showed that Ccdc80 protein is expressed in the forming heart, during all the developmental stages, and in particular in the atrio-ventricular boundary, in bulbus arteriosus and in the aortic arch at 48 hpf.

We also showed that Ccdc80-morphants showed defects in the developing heart, with a general enlargement of the atrium and impaired cardiac looping or shape, starting from the hatching period, at 48 hpf; moreover, at 72 hpf, the morphants showed more severe cardiac defects with blood stasis, evident in the sinus venosus region and peripheral congestion such as in heart failure; in addition they showed severe diffuse oedema, also in pericardial cavity and in the cranial cavity. It is important to underline that the defects in the heart of zebrafish morphants became evident only after pharyngula period of development (24-26 hpf): thus the phenotypical alterations were due to a disorder of the late phase of cardiac development, after the complete differentiation of myocytes.

Impaired cardiac looping and similar phenotypical alterations can be also produced by silencing of other genes, like bone morphogenetic protein (bmp)4, fibroblast growth factor (FGF) and notch1b, as well modifying wnt/ β -catenin pathway, that are involved in atrio-ventricular junction development [127-131]. In particular, in zebrafish notch1b and bmp4 are initially expressed throughout the anterior-posterior part of the heart and, subsequently, the expression of these genes is restricted to the area of the valve in formation (bmp4 in the myocardium and notch1b in the endocardium). About 48 hpf, there is the higher expression of notch1b and bmp4 respectively in the endocardium and myocardium of the atrio-ventricular junction (Figure 53) [131].

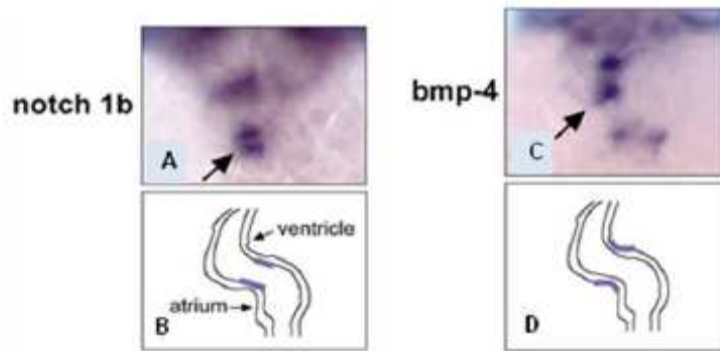


Figure 53

Notch1b and bpm4 expression in zebrafish heart at 48 hpf.

Localization of notch1b and bmp4 in the heart of zebrafish. A: expression of notch1b endocardium highlighted by in situ hybridization. B: Schematic representation of the expression pattern of notch1b. C: bmp4 expression in the myocardium as evidenced by in situ hybridization. D: schematic representation of the expression pattern of bmp4.

In summary, we demonstrated that Ccdc80 protein is indispensable for correct heart development in zebrafish model and that the phenotypical alterations are due to a disorder of the late phase of cardiac development, after the complete differentiation of myocytes. Given the known interactions of Ccdc80 protein with intracellular pathways, in particular with wnt/ β -catenin and bpm4, and given the similar phenotypical alterations, it is likely that Ccdc80 plays a similar key role in heart developing and morphology [91, 132].

Moreover, data obtained from immunohistochemistry showed that Ccdc80 protein exhibits a different pattern of expression in pathological conditions compared to normal hearts.

The atria of human patients affected by DCM showed a homogenous increase of the Ccdc80 expression level (moderate to strong staining) in comparison to normal samples (patchy pattern with negative or mild stain and only a few groups showing strong positivity).

In ventricles there is no evidence of spread negative cardiomyocytes, although the pattern remains homogeneous without evident increased expression of Ccdc80 protein.

Ventricles of MCT rats, compared to normal ones, also showed a clean-cut over-expression of Ccdc80 protein, particularly at right ventricular level, probably due to the higher pressure overload. Furthermore, skeletal muscle showed a similar modification of the pattern in pathological condition, with almost all myocytes expressing the protein with a moderate to

strong positivity. This pattern appeared very different from normal muscle, which show positive cells with intense positivity alternated to negative cells.

The western blot confirmed a significant over-expression of Ccdc80 protein in both atria and ventricles of DCM samples, with a 5-12 fold increased expression compared to normal samples. Among four different bands of Ccdc80 isoforms, normal samples express only the 108Kd form while DCM samples also showed different isoforms of the protein. Two of them were recognized as cleaved and phosphorylated isoform of 65Kd (SSG1) and as a probably secreted isoform, of 40Kd. Moreover, giving that in normal samples Northern blot analysis showed a greater expression of Ccdc80 RNA in atria compared to ventricles, its is possible to assume that an amount of the protein, produced by atria, could be secreted.

Taken together, these results suggest a possible role of Ccdc80 as a protein with an adaptive function, that is overexpressed in stress conditions, such as pressure/volume overload and myocytes dysfunction. It is well known indeed that Ccdc80 is up-regulated in stress related cardiac hypertrophy [110, 133].

Moreover, cultured muscle cells display reductive metabolic and muscle-system transcriptome adaptations, with particular increased expression of Ccdc80, as observed in muscle atrophy, activating tissue-remodeling and senescence processes [104]. This confirms a potential key role of Ccdc80 in stress related metabolic and intracellular adaptation.

Under pathological stress, the heart reactivates several signaling pathways that traditionally were thought to be operational only in the developing heart. One of these pathways is the WNT signaling pathway: Wnt controls heart development but is also modulated during adult heart remodelling and the interaction of Ccdc80 with this pathway is also well defined.

Besides wnt/ β -catenin pathway, also PKI-GMP dependent is constitutively expressed in adult heart with an important role.

In particular PKGI and cGMP inhibit left ventricular remodeling in response to pressure overload [108-109], and left ventricular pressure overload itself is known to modulate cardiac

SSG1 (orthologous of Ccdc80) expression [110]. The elevation of myocyte cyclic GMP levels by local actions of endogenous atrial natriuretic peptide (ANP) or by pharmacological inhibition of phosphodiesterase-5 was shown to counter-regulate pathological hypertrophy. Otherwise loss of cGKI in cardiac myocytes compromises the hypertrophic program to pathological stimulation, rendering the heart more susceptible to dysfunction [134]. Moreover, the overexpression of cGMP-dependent protein kinase type 1a (PKG1a) has been demonstrated to improve mesenchymal stem cells contributing to regeneration of the ischemic heart after myocardial infarction [135]. In addition, cGMP was shown to inactivates glycogensynthase kinase 3 β (GSK-3 β) via PKG by preventing the mitochondrial permeability transition pore (mPTP) opening. This leads to acute cardioprotection but also lead to prevention of hypertrophy and heart failure, by negatively regulating Akt activity (which, besides to critical for acute cardioprotection, can also lead to cardiac hypertrophy in case of excessive activation) [136]. Therefore, cGMP is a versatile signal with dual beneficial role in cardiac cell survival and Ccdc80 (in particular its ortologue SSG1), as PKGI phosphorylated substrate, could also protect myocardium from both hypertrophy and ischemia/reperfusion injury. Furthermore, Wnt inhibitors, which include also Ccdc80, could enhance the efficiency of BMP-4-directed cardiac differentiation of human pluripotent stem cells [137].

In experimental settings [138] frizzled-related proteins (sFRPs) can block Wnt activation signaling and sFRPs injected into the heart attenuated LV remodelling; depletion of a disheveled isoform (a signalling intermediate of both the canonical and noncanonical WNT pathway) attenuated LV remodelling while disheveled activation led to progressive dilated cardiomyopathy. Inhibition of nuclear β -catenin signaling downstream of the canonical WNT pathway significantly reduced postinfarct mortality and functional decline of LV function following chronic left anterior descending coronary artery ligation.

In summary, Wnt pathway plays a pivotal role in adult cardiac remodeling and may be suitable for therapeutic interventions (Figure 54). Currently, several molecular and cellular

mechanisms whereby WNT inhibition attenuates LV remodeling are proposed.

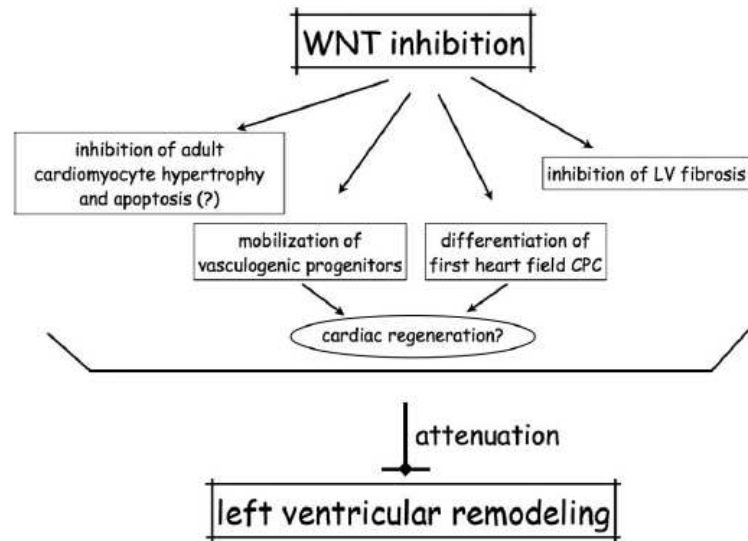


Figure 54
Schematic summary of cellular mechanisms contributing to the observed attenuation of LV remodeling on inhibition of WNT signaling at different levels.

Giving that Ccdc80 seems to have different roles in developing heart and in adult heart, likewise to other intracellular pathways, future studies will focus on two different directions. In particular, will be important to analyze the mutual relationship between Ccdc80 and notch1b, bmp4 and wnt pathway, with the aim to define their roles in the process of heart development, especially of the atrioventricular junction. Moreover, to clarify the functional role of Ccdc80 during heart failure and disease, future studies should examine specific models of zebrafish heart failure, with or without knocking down Ccdc80; similarly, could be interesting to analyze the response of Ccdc80 KO rats to monocrotaline infusion. In addition, further investigation are needed to explore the function of Ccdc80 and its relationship with other intracellular networks, both under normal conditions and during disease.

8. Conclusions

We demonstrated that Ccdc80 is expressed in the forming heart in zebrafish, during all the developmental stages, and that it is necessary for correct heart development. Ccdc80-morphants, indeed, showed defects in the developing heart, with impaired cardiac looping, atrium enlargement, blood stasis and peripheral congestion. These phenotypical alterations, which represent a proper heart failure, are due to a disorder of the late phase of cardiac development, after complete myocyte differentiation.

In normal human and rats, Ccdc80 mRNA, analyzed by Northern blot technique, showed a higher expression in atria compared to ventricles, while the Ccdc80 protein (108 Kd), analyzed by Western blot, showed similar expression levels in atria and ventricles. Ccdc80 protein showed a cytoplasmic localization with evident co-localization with sarcomeric proteins.

By immunohistochemistry, MCT rats, compared to normal ones, showed evident overexpression of Ccd80 protein especially in right ventricles, probably due to higher pressure overload. Also human atria of DCM patients showed evident overexpression of Ccdc80 with an homogenization of the expression pattern, compared to normal samples. Similar results are shown in stressed skeletal muscles. Although, there was no more evidence of spread negative cardiomyocytes in pathological heart, less clear difference are evident between normal and pathological ventricles. Interestingly, in western blot, beside a significant overexpression of Ccdc80 in both atria and ventricles, the pathological samples expressed different isoforms of the protein (40, 65 and 90 Kd) in comparison to normal samples, probably due to intracellular post-transcriptional processing of the protein.

In conclusion, our results demonstrated that Ccdc80 played a fundamental role for correct heart development and, in formed heart, shows a likely role as an adaptive protein to stress conditions such as pressure overload and myocytes dysfunction.

11. References

1. Maron BJ, Towbin JA, Thiene G. et al. Contemporary definitions and classification of the cardiomyopathies. An American Heart Association Scientific Statement from the Council on Clinical Cardiology, Heart Failure and Transplantation Committee; Quality of Care and Outcomes Research and Functional Genomics and Translational Biology Interdisciplinary Working Groups; and Council on Epidemiology and Prevention. *Circulation*. 2006; 113: 1807–1816.
2. Elliott P, Andersson B, Arbustini E et al. Classification of the cardiomyopathies: a position statement from the European Society of Cardiology Working Group on Myocardial and Pericardial Diseases. *European Heart Journal*. 2008; 29: 270–276.
3. Taylor MRG, Carniel E, Mestroni L. Cardiomyopathy, familial dilated. *Orphanet Journal of Rare Diseases*. 2006; 1: 27.
4. Towbin JA, Lowe AM, Colan SD et al. Incidence, causes, and outcomes of dilated cardiomyopathy in children. *Journal of the American Medical Association*. 2006; 296: 1867–1876.
5. Towbin JA and Bowles NE. The failing heart. *Nature*. 2002; 415: 227–233.
6. Richard P, Villard E, Charron P, Isnard R. The genetic bases of cardiomyopathies. *Journal of the American College of Cardiology*. 2006; 48: A79–A89.
7. Hibbard JU, Lindheimer M, Lang RM. A modified definition for peripartum cardiomyopathy and prognosis based on echocardiography. *Obstetrics and Gynecology*. 1999; 94: 311–316.
8. Johnson-Coyle L, Jensen L, Sobey A. Peripartum cardiomyopathy: review and practice guidelines. *American Journal of Critical Care*. 2012; 21: 89–99.
9. Elkayam U, Akhter MW., Singh H et al. Pregnancy associated cardiomyopathy: clinical characteristics and a comparison between early and late presentation. *Circulation*. 2005; 111: 2050–2055.
10. Sliwa K, Fett J, Elkayam U. Peripartum cardiomyopathy. *Lancet*. 2006; 368: 687–693.
11. Ansari AA, Fett JD, Carraway RE, Mayne AE, Onlamoon N, Sundstrom JB. Autoimmune mechanisms as the basis for human peripartum cardiomyopathy. *Clinical Reviews in Allergy and Immunology*. 2002; 23: 301–324.

12. Sliwa K, Forster O, Libhaber E et al. Peripartum cardiomyopathy: inflammatory markers as predictors of outcome in 100 prospectively studied patients. *European HeartJournal*. 2006; 27: 441–446.
13. Torre-Amione G, Kapadia S, Benedict C, Oral H, Young JB, and Mann DL. Proinflammatory cytokine levels in patients with depressed left ventricular ejection fraction: a report from the studies of left ventricular dysfunction (SOLVD). *Journal of the American College of Cardiology*. 1996; 27: 1201–1206.
14. Friedrich FW, Carrier L. Genetics of hypertrophic and dilated cardiomyopathy. *Curr. Pharm. Biotechnol*. 2012;13: 2467-76.
15. Lohrbus JA, Janzer RC, Kuntzer T, Matthieu JM, Pfend G, Goy JJ, Bogousslavsky J. Familial cardiomyopathy and distal myopathy with abnormal desmin accumulation and migration. *Neuromuscul. Disord*. 1998; 8: 77–86.
16. Ashrafian H, McKenna WJ, Watkins H. Disease pathways and novel therapeutic targets in hypertrophic cardiomyopathy. *Circ. Res*. 2011; 109: 86–96.
17. Ho CY. Genetics and clinical destiny: improving care in hypertrophic cardiomyopathy. *Circulation*. 2010; 122: 2430–2440.
18. Landstrom AP, Ackerman MJ. Mutation type is not clinically useful in predicting prognosis in hypertrophic cardiomyopathy. *Circulation*. 2010; 122: 2441–2449.
19. Saffitz JE. Arrhythmogenic cardiomyopathy: advances in diagnosis and disease pathogenesis. *Circulation*. 2011; 124: e390–e392.
20. Chien KR. Genotype, phenotype: upstairs, downstairs in the family of cardiomyopathies. *J. Clin. Invest*. 2003; 111: 175–178.
21. Kamisago M, Sharma SD, DePalma SR, Solomon S, Sharma P, McDonough B, Smoot L, Mullen MP, Woolf PK, Wigle ED, Seidman JG, Seidman CE. Mutations in sarcomere protein genes as a cause of dilated cardiomyopathy. *N. Engl. J. Med*. 2000; 343: 1688–1696.
22. Dellefave L, McNally EM. The genetics of dilated cardiomyopathy. *Curr. Opin. Cardiol*. 2010; 25: 198–204.
23. Villard E, Duboscq-Bidot L, Charron P, Benaiche A, Conraads V, Sylvius N, Komajda M. Mutation screening in dilated cardiomyopathy: prominent role of the beta myosin heavy chain gene. *Eur. Heart J*. 2005; 26: 794–803.
24. Mogensen J, Murphy RT, Shaw T, Bahl A, Redwood C, Watkins H, Burke M, Elliott PM, McKenna WJ. Severe disease expression of cardiac troponin C and T mutations

- in patients with idiopathic dilated cardiomyopathy. *J. Am. Coll. Cardiol.* 2004; 44: 2033–2040.
25. Hershberger RE, Siegfried JD. Update 2011: clinical and genetic issues in familial dilated cardiomyopathy. *J. Am. Coll. Cardiol.* 2011; 57: 1641–1649.
 26. Carballo S, Robinson P, Otway R, Fatkin D, Jongbloed JD, de Jonge N, Blair E, van Tintelen JP, Redwood C, Watkins H. Identification and functional characterization of cardiac troponin I as a novel disease gene in autosomal dominant dilated cardiomyopathy. *Circ. Res.* 2009; 105: 375–382.
 27. Murphy RT, Mogensen J, Shaw A, Kubo T, Hughes S, McKenna WJ. Novel mutation in cardiac troponin I in recessive idiopathic dilated cardiomyopathy. *Lancet.* 2004; 363: 371–372.
 28. Lakdawala NK, Dellefave L, Redwood CS, Sparks E, Cirino AL, Depalma S, Colan SD, Funke B, Zimmerman RS, Robinson P, Watkins H, Seidman CE, Seidman JG, McNally EM, Ho CY . Familial dilated cardiomyopathy caused by an alpha-tropomyosin mutation: the distinctive natural history of sarcomeric dilated cardiomyopathy. *J. Am. Coll. Cardiol.* 2010; 55: 320–329.
 29. Lakdawala NK, Givertz MM. Dilated cardiomyopathy with conduction disease and arrhythmia. *Circulation.* 2010; 122: 527–534.
 30. Olson TM, Kishimoto NY, Whitby FG, Michels VV. Mutations that alter the surface charge of alpha-tropomyosin are associated with dilated cardiomyopathy. *J. Mol. Cell. Cardiol.* 2001; 33: 723–732.
 31. Olson TM, Michels VV, Thibodeau SN, Tai YS, Keating MT. Actin mutations in dilated cardiomyopathy, a heritable form of heart failure. *Science.* 1998; 280: 750–752.
 32. Li D, Tapscoft T, Gonzalez O, Burch PE, Quiñones MA, Zoghbi WA, Hill R, Bachinski LL, Mann DL, Roberts R. Desmin mutation responsible for idiopathic dilated cardiomyopathy. *Circulation.* 1999; 100: 461–464.
 33. Goldfarb LG, Park KY, Cervenáková L, Gorokhova S, Lee HS, Vasconcelos O, Nagle JW, Semino-Mora C, Sivakumar K, Dalakas MC. Missense mutations in desmin associated with familial cardiac and skeletal myopathy. *Nat. Genet.* 1998; 19: 402–403.
 34. Muñoz-Mármol AM, Strasser G, Isamat M, Coulombe PA, Yang Y, Roca X, Vela E, Mate JL, Coll J, Fernández-Figueras MT, Navas- Palacios JJ, Ariza A, Fuchs E. A

- dysfunctional desmin mutation in a patient with severe generalized myopathy. *Proc. Natl. Acad. Sci. U.S.A.* 1998; 95: 11312–11317.
35. Petrof BJ. Molecular pathophysiology of myofiber injury in deficiencies of the dystrophin–glycoprotein complex. *Am. J. Phys. Med. Rehabil.* 2002; 81: S162–S174.
 36. Monaco AP. Dystrophin, the protein product of the Duchenne/Becker muscular dystrophy gene. *Trends Biochem. Sci.* 1989; 14: 412–415.
 37. Muntoni F, Melis MA, Ganau A, Dubowitz V. Transcription of the dystrophin gene in normal tissues and in skeletal muscle of a family with X-linked dilated cardiomyopathy. *Am. J. Hum. Genet.* 1995; 56: 151–157.
 38. Minetti C, Bonilla E. Mosaic expression of dystrophin in carriers of Becker’s muscular dystrophy and the X-linked syndrome of myalgia and cramps. *N. Engl. J. Med.* 1992; 327: 1100.
 39. Tsubata S, Bowles KR, Vatta M, Zintz C, Titus J, Muhonen L, Bowles NE, Towbin JA. Mutations in the human delta-sarcoglycan gene in familial and sporadic dilated cardiomyopathy. *J. Clin. Invest.* 2000, 106: 655–662.
 40. Schmitt JP, Kamisago M, Asahi M, Li GH, Ahmad F, Mende U, Kranias EG, MacLennan DH, Seidman JG, Seidman CE. Dilated cardiomyopathy and heart failure caused by a mutation in phospholamban. *Science.* 2003; 299: 1410–1413.
 41. Haghghi K, Kolokathis F, Gramolini AO, Waggoner JR, Pater L, Lynch RA, Fan GC, Tsiapras D, Parekh RR, Dorn GW 2nd, MacLennan DH, Kremastinos DT, Kranias EG. A mutation in the human phospholamban gene, deleting arginine 14, results in lethal, hereditary cardiomyopathy. *Proc. Natl. Acad. Sci. U.S.A.* 2006; 103: 1388–1393.
 42. Charron P, Komajda M. Molecular genetics in hypertrophic cardiomyopathy: towards individualized management of the disease. *Expert Review of Molecular Diagnostics*, 2006; 6: 65–78.
 43. Elliott P, McKenna W.J. Hypertrophic cardiomyopathy. *Lancet.* 2004; 363: 1881–1891.
 44. Maron B J. Hypertrophic cardiomyopathy. *Circulation.* 2002; 106: 2419–2421.
 45. Richard P, Fressart V, Charron P, Hainque B. Genetics of inherited cardiomyopathies. *Pathologie Biologie.* 2010; 58: 343–352.
 46. Richard P, Villard E, Charron P, Isnard R. The genetic bases of cardiomyopathies. *Journal of the American College of Cardiology.* 2006; 48: A79–A89.

47. Hershberger R E, Lindenfeld J, Mestroni L, Seidman C E, Taylor M R G, Towbin J A. Genetic evaluation of cardiomyopathy—a heart failure society of America practice guideline. *Journal of Cardiac Failure*. 2009; 15: 83–97.
48. Xu Q, Dewey S, Nguyen S, Gomes A V. Malignant and benign mutations in familial cardiomyopathies: insights into mutations linked to complex cardiovascular phenotypes. *Journal of Molecular and Cellular Cardiology*. 2010;48: 899–909.
49. Gimeno J R, Monserrat L, Perez-Sanchez I et al. Hypertrophic cardiomyopathy. A study of the troponin-T gene in 127 Spanish families. *Revista Espanola de Cardiologia*. 2009; 62: 1473–1477.
50. Oakley C M. Report of the WHO/ISFC task force on the definition and classification of cardiomyopathies. *British Heart Journal*. 1980; 44: 672–673.
51. Benotti J R, Grossman W, Cohn PF. Clinical profile of restrictive cardiomyopathy. *Circulation*. 1980; 61: 1206–1212.
52. Rajagopalan N, Garcia M J, Rodriguez L et al. Comparison of new Doppler echocardiographic methods to differentiate constrictive pericardial heart disease and restrictive cardiomyopathy. *American Journal of Cardiology*. 2001; 87: 86–94.
53. Kushwaha S S, Fallon J T, Fuster V. Medical progress—restrictive cardiomyopathy. *New England Journal of Medicine*. 1997; 336: 267–276.
54. Fitzpatrick A P, Shapiro L M, Rickards A F, Poole-Wilson P A. Familial restrictive cardiomyopathy with atrioventricular block and skeletal myopathy”. *British Heart Journal*. 1990; 63 114–118.
55. Thiene G, Corrado D, Basso C. Arrhythmogenic right ventricular cardiomyopathy/dysplasia. *Orphanet Journal of Rare Diseases*. 2007; 2: 45.
56. McKenna W J et al. Diagnosis of arrhythmogenic right ventricular dysplasia/cardiomyopathy. Task Force of the Working Group Myocardial and Pericardial Disease of the European Society of Cardiology and of the Scientific Council on Cardiomyopathies of the International Society and Federation of Cardiology. *British Heart Journal*, 1994; 71: 215–218.
57. Corrado D, Leoni L, Link M S et al. Implantable cardioverter-defibrillator therapy for prevention of sudden death in patients with arrhythmogenic right ventricular cardiomyopathy/dysplasia. *Circulation*. 2003; 108: 3084–3091.
58. Nava A, Thiene G, Canciani B et al. Familial occurrence of right ventricular dysplasia: a study involving nine families. *Journal of the American College of Cardiology*. 1988, 12: 1222–1228.

59. Rampazzo A, Nava A, Danieli G A et al. The gene for arrhythmogenic right ventricular cardiomyopathy maps to chromosome 14q23-q24. *Human Molecular Genetics*. 1994; 3: 959–962.
60. Gerull B, Heuser A, Wichter T et al. Mutations in the desmosomal protein plakophilin-2 are common in arrhythmogenic right ventricular cardiomyopathy. *Nature Genetics*. 2004; 36: 1162–1164.
61. Bonn´e S, Van Hengel J, Van Roy F. Chromosomal mapping of human armadillo genes belonging to the p120(ctn)/plakophilin subfamily. *Genomics*. 1998; 51: 452–454.
62. Syrris P, Ward D, Evans A et al. Arrhythmogenic right ventricular dysplasia/cardiomyopathy associated with mutations in the desmosomal gene desmocollin-2. *American Journal of Human Genetics*. 2006; 79: 978–984.
63. Pilichou K, Nava A, Basso C et al. Mutations in desmoglein-2 gene are associated with arrhythmogenic right ventricular cardiomyopathy. *Circulation*. 2006; 113: 171–1179.
64. Rampazzo A. Regulatory mutations in transforming growth factor-beta 3 gene cause arrhythmogenic right ventricular cardiomyopathy type 1. *Journal of the American College of Cardiology*. 2005; 45: 10A–11A.
65. Rampazzo A, Nava A, Malacrida S et al. Mutation in human desmoplakin domain binding to plakoglobin causes a dominant form of arrhythmogenic right ventricular Cardiomyopathy. *American Journal of Human Genetics*. 2002; 71: 1200–1206.
66. Tiso N, Stephan D A, Nava A et al. Identification of mutations in the cardiac ryanodine receptor gene in families affected with arrhythmogenic right ventricular cardiomyopathy type 2 (ARVD2). *HumanMolecular Genetics*. 2001; 10: 189–194
67. Marcantonio D, Chalifour LE, Alaoui-Jamali MA, Alpert L, Huynh HT. Cloning and characterization of a novel gene that is regulated by estrogen and is associated with mammary gland carcinogenesis. *Endocrinology*. 2001; 142:2409–2418.
68. Mu H, Ohta K, Kuriyama S, Shimada N, Tanihara H, Yasuda K, Tanaka H. Equarin, a novel soluble molecule expressed with polarity at chick embryonic lens equator, is involved in eye formation. *Mech Dev*. 2003; 120:143–155.
69. Aoki K, Sun YJ, Aoki S, Wada K, Wada E. Cloning, expression, and mapping of a gene that is upregulated in adipose tissue of mice deficient in bombesin receptor subtype-3. *Biochem Biophys Res Commun*. 2002; 290:1282–1288.

70. Bommer GT, Jager C, Durr EM, Baehs S, Eichhorst ST, Brabletz T, Hu G, Frohlich T, Arnold G, Kress DC, Goke B, Fearon ER, Kolligs FT. DRO1, a gene down-regulated by oncogenes, mediates growth inhibition in colon and pancreatic cancer cells. *J Biol Chem.* 2005; 280: 7962–7975.
71. Visconti R, Schepis F, Iuliano R, Pierantoni GM, Zhang L, Carlomagno F, Battaglia C, Martelli ML, Trapasso F, Santoro M, Fusco A. Cloning and molecular characterization of a novel gene strongly induced by the adenovirus E1A gene in rat thyroid cells *Oncogene.* 2003; 22: 1087-97.
72. Santoro M, Melillo RM, Grieco M, Berlingieri MT, Vecchio G and Fusco A. The TRK and RET tyrosine kinase oncogenes cooperate with ras in the neoplastic transformation of a rat thyroid epithelial cell line. *Cell Growth Differ.* 1993; 4: 77-84.
73. Pan J, Nakanishi K, Yutsudo M, Inoue H, Li Q, Oka K, Yoshioka N, Hakura A. Isolation of a novel gene down-regulated by v-src. *FEBS Lett.* 1996; 383: 21-25.
74. Dry KL, Aldred MA, Edgar AJ, Brown J, Manson FD, Ho MF, Prosser J, Hardwick LJ, Lennon AA, Thomson K et al. Identification of a novel gene, ETX1 from Xp21.1, a candidate gene for X-linked retinitis pigmentosa (RP3). *Hum Mol Genet.* 1995; 4: 2347-53.
75. Kurosawa H, Goi K, Inukai T, Inaba T, Cheng KS, Shinjyo T, Rakestraw KM, Naeve CW. Two candidate downstream target genes for E2A-HLF. *Blood.* 1999; 93: 321-32.
76. Liu Y, Monticone M, Tonachini L, Mastrogiacomo M, Marigo V, Cancedda R, Castagnola P. URB expression in human bone marrow stromal cells and during mouse development. *Biochem Biophys Res Commun.* 2004; 322(2): 497-507.
77. Pawłowski K, Muszewska A, Lenart A, Szczepińska T, Godzik A, Grynberg M. A widespread peroxiredoxin-like domain present in tumor suppression- and progression-implicated proteins. *BMC Genomics.* 2010; 11:590-608.
78. Brusegan C, Pistocchi A, Frassine A, Della Noce I, Schepis F, et al. Ccdc80-11 Is Involved in Axon Pathfinding of Zebrafish Motoneurons. *PLoS ONE.* 2012; 7(2): e31851.
79. Lewis KE, Eisen JS. Hedgehog signaling is required for primary motoneuron induction in zebrafish. *Development.* 2001; 128: 3485–3495.
80. Shimakage M, Kodama K, Kawahara K, Kim CJ, Ikeda Y, Yutsudo M, Inoue H: Downregulation of drs tumor suppressor gene in highly malignant human pulmonary neuroendocrine tumors. *Oncol Rep.* 2009; 21(6):1367-1372.
81. Tambe Y, Yoshioka-Yamashita A, Mukaiho K, Haraguchi S, Chano T, Isono T,

- Kawai T, Suzuki Y, Kushima R, Hattori T, et al. Tumor prone phenotype of mice deficient in a novel apoptosis-inducing gene, drs. *Carcinogenesis*. 2007, 28(4):777-784.
82. Tambe Y, Isono T, Haraguchi S, Yoshioka-Yamashita A, Yutsudo M, Inoue H. A novel apoptotic pathway induced by the drs tumor suppressor gene. *Oncogene*. 2004, 23(17):2977-2987.
 83. Tambe Y, Yamamoto A, Isono T, Chano T, Fukuda M, Inoue H. The drs tumor suppressor is involved in the maturation process of autophagy induced by low serum. *Cancer Lett*. 2009; 283(1):74-83.
 84. Manabe R, Tsutsui K, Yamada T, Kimura M, Nakano I, Shimono C, Sanzen N, Furutani Y, Fukuda T, Oguri Y, et al. Transcriptome-based systematic identification of extracellular matrix proteins. *Proc Natl Acad Sci USA*. 2008; 105(35):12849-12854.
 85. Ferraro A, Schepis F, Leone V, Federico A, Borbone E et al. Tumor Suppressor Role of the *CL2/DRO1/CCDC80* Gene in Thyroid Carcinogenesis. *J Clin Endocrinol Metab*. 2013; 98: 2834–2843.
 86. Ferragud J, Avivar-Valderas A, Pla A, De Las Rivas J, de Mora JF. Transcriptional repression of the tumor suppressor DRO1 by AIB1. *FEBS Lett*. 2011; 585: 3041–3046.
 87. Anzick SL, Kononen J, Walker RL, Azorsa DO, Tanner MM, Guan XY, Sauter G, Kallioniemi OP, Trent JM, Meltzer PS. AIB1, a steroid receptor coactivator amplified in breast and ovarian cancer. *Science*. 1997; 277: 965–968.
 88. Ferrero M, Avivar A, Garcia-Macias MC, de Mora JF. Phosphoinositide 3-kinase/AKT signaling can promote AIB1 stability independently of GSK3 phosphorylation. *Cancer Res*. 2008; 68: 5450–5459.
 88. Li H, Gomes PJ, Chen JD. RAC3, a steroid/nuclear receptor associated coactivator that is related to SRC-1 and TIF2. *Proc. Natl. Acad. Sci. USA*. 1997; 94: 8479–8484.
 89. Avivar A, Garcia-Macias MC, Ascaso E, Herrera G, O'Connor JE, de Mora, J.F. Moderate overexpression of AIB1 triggers pre-neoplastic changes in mammary epithelium. *FEBS Lett*. 2006; 580: 5222–5226.
 90. Okada T, Nishizawa H, Kurata A, Tamba S, Sonoda M, Yasui A, Kuroda Y, Hibuse T, Maeda N, Kihara S, Hadama T, Tobita K, et al. URB is abundantly expressed in adipose tissue and dysregulated in obesity. *Biochemical and Biophysical Research Communications*. 2008; 367: 370–376.

91. Tremblay F, Revett T, Huard C, Zhang Y, Tobin J F, Martinez R V, Gimeno R E. Bidirectional Modulation of Adipogenesis by the Secreted Protein Ccdc80/DRO1/URB. *The Journal of Biological Chemistry*. 2009; 284: 8136–8147.
92. Hu E, Liang P, Spiegelman B M. AdipoQ is a novel adipose-specific gene dysregulated in obesity. *J. Biol. Chem.* 1996; 271: 10697–10703.
93. MacDougald O A, Hwang C S, Fan H, Lane M D. Regulated expression of the obese gene product (leptin) in white adipose tissue and 3T3-L1 adipocytes. *Proc. Natl. Acad. Sci. U. S. A.* 1995; 92: 9034–9037.
94. Kaestner K H, Christy R J, McLenithan J C, Braiterman L T, Cornelius P, Pekala P H, Lane M D. Sequence, tissue distribution, and differential expression of mRNA for a putative insulin-responsive glucose transporter in mouse 3T3-L1 adipocytes. *Proc. Natl. Acad. Sci. U. S. A.* 1989; 86, 3150–3154.
95. Oishi Y, Manabe I, Tobe K, Tsushima K, Shindo T, Fujiu K, Nishimura G, Maemura K, Yamauchi T, Kubota N, Suzuki R, Kitamura T, Akira S, Kadowaki T, Nagai R. Krüppel-like transcription factor KLF5 is a key regulator of adipocyte differentiation *Cell Metab.* 2005; 1: 27–39.
96. Tontonoz P, Hu E, Spiegelman B M.. Stimulation of adipogenesis in fibroblasts by PPAR gamma 2, a lipid-activated transcription factor. *Cell.* 1994; 79: 1147–1156.
97. Longo K A, Wright W S, Kang S, Gerin I, Chiang S H, Lucas P C, Opp M R, MacDougald O A. Wnt10b inhibits development of white and brown adipose tissues. *J. Biol. Chem.* 2004; 279: 35503–35509.
98. Tremblay F, Huard C, Jessie D, Gareski T, Will S, Richard A-M, Syed J, Bailey S, Brenneman K A, Martinez R V, Perreault M, Lin Q, Gimeno R E. Loss of Coiled-Coil Domain Containing 80 Negatively Modulates Glucose Homeostasis in Diet-Induced Obese Mice. *Endocrinology.* 2012; 153(9):4290–4303.
99. O’Leary E E, Mazurkiewicz-Muñoz A M, Argetsinger L S, Maures T J, Huynh H T, Su C C. Identification of Steroid-Sensitive Gene-1/Ccdc80 as a JAK2-Binding Protein. *Molecular Endocrinology* 2013; 27:619-634.
100. Kralovics R, Passamonti F, Buser AS, et al. A gain-of-function mutation of JAK2 in myeloproliferative disorders. *N Engl J Med.* 2005; 352:1779–1790.
101. Baxter EJ, Scott LM, Campbell PJ, et al. Acquired mutation of the tyrosine kinase JAK2 in human myeloproliferative disorders. *Lancet.* 2005; 365:1054–1061.
102. Aaronson DS, Horvath CM. A road map for those who know JAK-STAT. *Science.* 2002; 296: 1653–1655.

103. Ohki-Hamazaki H, Watase K, Yamamoto K, et al. Mice lacking bombesin receptor subtype-3 develop metabolic defects and obesity. *Nature*. 1997; 390: 165–169.
104. Raymond F, Métairon S, Kussmann M, Colomer J, Nascimento A, Mormeneo E, García-Martínez C, Gómez-Foix A M. Comparative gene expression profiling between human cultured myotubes and skeletal muscle tissue. *BMC Genomics*. 2010; 11: 125-141.
105. Saenz A, Azpitarte M, Armananzas R, Leturcq F, Alzualde A, et al. Gene Expression Profiling in Limb-Girdle Muscular Dystrophy 2A. *PLoS One*. 2008; 3(11): e3750.
106. Wang G, Surks H K, Mary Tang K, Zhu Y, Mendelsohn M E, Blanton R M. Steroid-sensitive Gene 1 Is a Novel Cyclic GMP-dependent Protein Kinase I Substrate in Vascular Smooth Muscle Cells. *The Journal of biological Chemistry*. 2013; 288: 24972–24983.
107. Hofmann F, Ammendola A, Schlossmann J. Rising behind NO: cGMP-dependent protein kinases. *J. Cell Sci*. 2000; 113: 1671–1676.
108. Blanton R M, Takimoto E, Lane A M, Aronovitz M, Piotrowski R, Karas R H, Kass D A, Mendelsohn M E. Protein kinase GI α inhibits pressure overload-induced cardiac remodeling and is required for the cardioprotective effect of sildenafil *in vivo*. *J. Am. Heart Assoc*. 2012; 1: e003731.
109. Takimoto E, Champion H C, Li M, Belardi D, Ren S, Rodriguez E R, Bedja D, Gabrielson K L, Wang Y, Kass D A. Chronic inhibition of cyclic GMP phosphodiesterase 5A prevents and reverses cardiac hypertrophy. *Nat. Med*. 2005; 11: 214–222.
110. Mirotsov M, Dzau V J, Pratt R E, Weinberg E O. Physiological genomics of cardiac disease. Quantitative relationships between gene expression and left ventricular hypertrophy. *Physiol. Genomics*. 2006; 27: 86–94.
111. Vescovo G, Ceconi C, Bernocchi P, et al. Skeletal muscle myosin heavy chain expression in rats with monocrotaline-induced cardiac hypertrophy and failure. Relation to blood flow and degree of muscle atrophy. *Cardiovasc Res*. 1998; 39: 233-41.
112. Angelini A, Castellani C, Ravara B, Franzin C, Pozzobon M, Tavano R, Dalla Libera L, Papini E, Vettor R, De Coppi P, Thiene G, Vescovo G. Stem-cell therapy in an experimental model of pulmonary hypertension and right heart failure: Role of paracrine and neurohormonal milieu in the remodeling process. *The Journal of Heart and Lung Transplantation*. 2011; 30: 1281-1293.

113. Reindel J F, Roth RA. The Effects of Monocrotaline Pyrrole on Cultured Bovine Pulmonary Artery Endothelial and Smooth Muscle Cells. *American Journal of Pathology*. 1991; 138: 707-719.
114. Langleben D, Reid L M. Effect of methylprednisolone on monocrotaline-induced pulmonary vascular disease and right ventricular hypertrophy. *Lab Invest*. 1985; 52: 298-303.
115. Hilliker K S, Garcia C M, Roth R A. Effects of monocrotaline and monocrotaline pyrrole on 5-hydroxytryptamine and paraquat uptake by lung slices. *Res Commun Chem Pathol Pharmacol*. 1983; 40: 179-197.
116. Mattocks A R, White I N H. The conversion of pyrrolizidine alkaloids to N-oxides and to dihydropyrrolizidine derivatives by rat lung microsomes in vitro. *Chem-Biol Interact*. 1971; 3: 383-396.
117. Barnes J M, Magee P N, Schoental R. Lesions in the lungs and livers of rats poisoned with the pyrrolizidine alkaloid fulvine and its N-oxide. *J Pathol Bacteriol*. 1964; 88: 521-531.
118. Bruner L H, Hilliker K S, Roth R A. Pulmonary hypertension and ECG changes from monocrotaline pyrrole in the rat. *Am J Physiol*. 1983; 245: H300-H306.
119. Kimmel C B, Ballard W W, Kimmel S R, Ullmann B, Schilling T F. Stages of embryonic development of the zebrafish. *Dev Dyn*, 1995; 203(3): 253-31.
120. Patterson LJ, Gering M, Patient R. Scl is required for dorsal aorta as well as blood formation in zebrafish embryos. *Blood*. 2005; 105(9): 3502-11.
121. Thiss C, Thiss B. High-resolution in situ hybridization to whole-mount zebrafish embryos. *Nat Protoc*. 2008; 3(1):59-69.
122. Chen JN, Fishman MC. Zebrafish tinman homolog demarcates the heart field and initiates myocardial differentiation. *Development*. 1996; 122(12): 3809-16.
123. Yelon D, Horne SA, Stainier DY. Restricted expression of cardiac myosin genes reveals regulated aspects of heart tube assembly in zebrafish. *Dev Biol*. 1999; 214: 23-37.
124. Yutzey, KE, Rhee, JT, Bader, D. Expression of the atrial-specific myosin heavy chain AMHC1 and the establishment of anteroposterior polarity in the developing chicken heart. *Development* 1994; 120:871–883.
125. Szeto DP, Griffin KJ, Kimelman D. HrT is required for cardiovascular development in zebrafish. *Development*. 2002; 129(21):5093-101.

126. Stainier DY. Zebrafish genetics and vertebrate heart formation. *Nat Rev Genet*, 2001; 2(1): 39-48.
127. Tirosh-Finkel L, Zeisel A, Brodt-Ivenshitz M, Shamai A, Yao Z, Seger R, Domany E, Tzahor E. BMP-mediated inhibition of FGF signaling promotes cardiomyocyte differentiation of anterior heart field progenitors. *Development*. 2010; 137: 2989-3000.
128. Verhoeven M C, Haase C, Christoffels V M, Weidinger G, Bakkers J. Wnt Signaling Regulates Atrioventricular Canal Formation Upstream of BMP and Tbx2. *Birth Defects Research*. 2011; 91: 435-440.
129. Klaus A, Saga Y, Taketo M M, Tzahor E, Birchmeier W. Distinct roles of Wnt/ β -catenin and Bmp signalling during early cardiogenesis. *PNAS*. 2007; 104: 18531–18536.
130. Westin J, Lardelli M. Three novel Notch genes in zebrafish: implications for vertebrate Notch gene evolution and function. *Dev Genes Evol*. 1997; 207(1): 51-63.
131. Niessen K, Karsan A. Notch Signaling in Cardiac Development. *Circ Res*. 2008; 102: 1169-1181.
132. Rossol-Allison J, Stemmler L N, Swenson-Fields K I, Kelly P, Fields P E, McCalla S J, Casey P J, Fields T A. Rho GTPase activity modulates WNT3A/ β -catenin signalling. *Cell Signal*. 2009; 21(11): 1559–1568.
133. Galindo C L, Skinner M A, Errami M, Olson L D, Watson D A, Li J, McCormick J F, McIver L J, Kumar N M, Pham T Q, Garner H R. Transcriptional profile of isoproterenol-induced cardiomyopathy and comparison to exercise-induced cardiac hypertrophy and human cardiac failure. *BMC Physiology* 2009; 9: 23-45.
134. Frantz S, Klaiber M, Baba H A, Oberwinkler H, Volker K, Gabner B, Bayer B, Abeber M, Schuh K, Feil R, Hofmann F, Kuhn M. Stress-dependent dilated cardiomyopathy in mice with cardiomyocyte-restricted inactivation of cyclic GMP-dependent protein kinase I *European Heart Journal*. 2013; 34: 1233–1244.
135. Wang L, Pasha Z, Wang S, Li N, Feng Y, et al. Protein Kinase G1a Overexpression Increases Stem Cell Survival and Cardiac Function after Myocardial Infarction. *PLoS ONE*. 2013; 8(3): e60087.
136. Xua Z, Leeb SR, Hanb J. Dual role of cyclic GMP in cardiac cell survival. *The International Journal of Biochemistry & Cell Biology*. 2013; 45: 1577–1584.
137. Ren Y, Young Lee M, Schliffke S, Paavola J, Amos P J, Ge X, Ye M, Zhu S, Senyei G, Lum L, Ehrlich B E, Qyang Y. Small molecule Wnt inhibitors enhance the

efficiency of BMP-4-directed cardiac differentiation of human pluripotent stem cells. *Journal of Molecular and Cellular Cardiology*. 2011; 51: 280–287.

138. M W Bergmann. WNT Signaling in Adult Cardiac Hypertrophy and Remodeling. Lessons Learned From Cardiac Development. *Circulation Research* 2010; 107:1198-1208.

10. Acknowledgments

Il mio più grande ringraziamento non può non andare che al Prof. Thiene, per avermi dato la possibilità di frequentare la scuola di dottorato ed avermi regalato un'esperienza di altissimo valore professionale che porterò per sempre con me. Un ringraziamento particolare va alla Prof.ssa Angelini per la grandissima professionalità accompagnata da tanta fiducia e generosità nei miei confronti. A loro va la mia riconoscenza per avermi sempre sostenuto e dato sicurezza, specialmente in un momento di particolare difficoltà.

Vorrei inoltre esprimere gratitudine alle persone che hanno lavorato intensamente affinché le semplici idee si concretizzassero in questo lavoro, in particolare Marny Fedrigo e Chiara Castellani, oltre che tutto il personale dei laboratori.

Un forte ringraziamento va al Dott. Filippo Schepis, vero ideatore dello studio, che mi ha seguito, aiutato e consigliato con l'affetto di un vero fratello maggiore. A lui ed al personale che lavora e collabora con il laboratorio di Gastroenterologia del Policlinico di Modena, in particolare la Dott.ssa Dalla Noce ed il Prof. Cotelli, va la mia gratitudine per aver curato e svolto gli esperimenti sugli zebrafish.

In ultimo desidero ringraziare tutte le persone care che mi hanno supportato in questi anni.